

6-3-96

# SANDIA REPORT

SAND95-2017/2 • UC-721

Unlimited Release

Printed May 1996

## The Second Iteration of the Systems Prioritization Method: A Systems Prioritization and Decision-Aiding Tool for the Waste Isolation Pilot Plant

Volume II: Summary of Technical Input and Model Implementation

N. H. Prindle, F. T. Mendenhall, W. Beyeler, K. Trauth, S. Hora, D. Rudeen, D. M. Boak

Prepared by  
Sandia National Laboratories  
Albuquerque, New Mexico 87185 and Livermore, California 94550  
for the United States Department of Energy  
under Contract DE-AC04-94A185000

Approved for public release; distribution is unlimited.



**MASTER**

Issued by Sandia National Laboratories, operated for the United States Department of Energy by Sandia Corporation.

**NOTICE:** This report was prepared as an account of work sponsored by an agency of the United States Government. Neither the United States Government nor any agency thereof, nor any of their employees, nor any of their contractors, subcontractors, or their employees, makes any warranty, express or implied, or assumes any legal liability or responsibility for the accuracy, completeness, or usefulness of any information, apparatus, product, or process disclosed, or represents that its use would not infringe privately owned rights. Reference herein to any specific commercial product, process, or service by trade name, trademark, manufacturer, or otherwise, does not necessarily constitute or imply its endorsement, recommendation, or favoring by the United States Government, any agency thereof or any of their contractors or subcontractors. The views and opinions expressed herein do not necessarily state or reflect those of the United States Government, any agency thereof or any of their contractors.

Printed in the United States of America. This report has been reproduced directly from the best available copy.

Available to DOE and DOE contractors from  
Office of Scientific and Technical Information  
PO Box 62  
Oak Ridge, TN 37831

Prices available from (615) 576-8401, FTS 626-8401

Available to the public from  
National Technical Information Service  
US Department of Commerce  
5285 Port Royal Rd  
Springfield, VA 22161

NTIS price codes  
Printed copy: A08  
Microfiche copy: A01

# The Second Iteration of the Systems Prioritization Method: A Systems Prioritization and Decision-Aiding Tool for the Waste Isolation Pilot Plant

## Volume II: Summary of Technical Input and Model Implementation

N. H. Prindle,<sup>1</sup> F. T. Mendenhall,<sup>2</sup> W. Beyeler,<sup>3</sup>  
K. Trauth,<sup>4</sup> S. Hora,<sup>5</sup> D. Rudeen,<sup>6</sup> and D. M. Boak<sup>7</sup>  
Sandia National Laboratories  
Albuquerque, NM 87185

### ABSTRACT

Systems Prioritization Method (SPM) is a decision-aiding tool developed by Sandia National Laboratories for the U.S. Department of Energy Carlsbad Area Office to provide an analytical basis for programmatic decision making for the Waste Isolation Pilot Plant (WIPP). SPM integrates decision-analysis techniques, performance and risk-assessment tools, and advanced information technology. The results are presented in a decision matrix showing cost, duration, and maximum probability of demonstrating compliance (PDC) for all activities in a given cost and duration category. This is the second volume in the series *The Second Iteration of the Systems Prioritization Method: A Systems Prioritization and Decision-Aiding Tool for the Waste Isolation Pilot Plant*, a three-volume report on the second iteration of SPM (SPM-2). The scope of SPM-2 was restricted to evaluating the predicted performance of the disposal system with respect to selected portions of the applicable U.S. Environmental Protection Agency's long-term performance regulations, 40 CFR 191.13 (radionuclide containment requirements) and 40 CFR 268.6 (hazardous constituent concentration requirements). A technical baseline based on existing information on the disposal system was developed and evaluated with respect to its adequacy for demonstrating compliance. When the baseline proved to be inadequate, the PDC was calculated for potential future states of knowledge about the disposal system using elicited outcomes of proposed activities and combinations of activities (activity sets) that, if implemented, would potentially lead to compliance. SPM-2 defined the most viable combinations of scientific investigations, engineered alternatives, and waste acceptance criteria for supporting the final compliance application for WIPP. This volume provides a summary of the technical input for SPM-2. It

---

<sup>1</sup> Strategic Studies Department

<sup>2</sup> Physical Sciences Department

<sup>3</sup> Science Applications International Corp., Albuquerque, NM 87106

<sup>4</sup> Computer and Compliance Support Department

<sup>5</sup> University of Hawaii at Hilo, Hilo, HI 96720

<sup>6</sup> New Mexico Engineering Research Institute, Albuquerque, NM 87106

<sup>7</sup> WIPP Performance Assessment Code Development Department

describes the SPM-2 technical baseline and the activities, activity outcomes, outcome probabilities, and input parameters for SPM-2 analysis. The implementation of the SPM-2 conceptual models for the baseline and the activities in the computer codes is also discussed.

# CONTENTS

ACRONYMS.....	vii
CODES.....	viii
1. INTRODUCTION .....	1
2. SPM-2 BASELINE.....	3
2.1 Introduction .....	3
2.2 Scenario Screening.....	3
2.3 Gas Generation.....	3
2.4 Actinide and Colloid Source Terms .....	5
2.5 Seals.....	6
2.5.1 Seal Permeability .....	6
2.6 RCRA Source Term .....	9
2.6.1 Contaminant Screening .....	11
2.6.2 SPM-2 Data Input .....	12
2.7 Rock Mechanics .....	12
2.8 Disposal Room.....	14
2.9 Salado .....	15
2.9.1 SPM-2 Salado Baseline Model Overview .....	16
2.9.2 Position Paper Model.....	17
2.9.3 Necessary Efforts.....	20
2.9.4 Post-Processing Techniques for Comparison to Regulatory Criteria .....	22
2.9.5 Tie-in to the Conceptual Model Components .....	25
2.9.6 Parameter Values and Distributions for the SPM-2 Salado Baseline Model.....	27
2.9.7 SPM-2 Salado Baseline Model Two-Phase Relationships .....	29
2.10 Non-Salado .....	31
2.10.1 Release Paths.....	32
2.10.2 Culebra Flow and Physical Retardation .....	33
2.10.3 Chemical Retardation.....	33
2.10.4 Intrusion Holes and the Castile Brine Reservoir.....	34
2.10.5 Climate Change.....	34
2.10.6 Castile Brine Reservoirs .....	35
2.11 RH-TRU .....	35
2.12 EAs.....	35
3. ACTIVITIES, ACTIVITY OUTCOMES, OUTCOME PROBABILITIES, AND INPUT PARAMETERS FOR SPM-2 ANALYSIS .....	37
3.1 Introduction .....	37
3.2 Actinide Source Term.....	37
3.2.1 AST 1.1 – Dissolved Actinide Solubilities for Oxidation States +III – +VI.....	41
3.2.2 AST 1.2 – Dissolved Actinide Solubilities for Oxidation States +III – +V .....	42

3.3 Gas Generation.....	43
3.3.1 GG 1 – RPM and Supporting Data .....	43
3.4 Disposal Room.....	44
3.4.1 DR 1 – Decomposed Waste Properties .....	44
3.4.2 DR 2 – Blowout Releases .....	45
3.4.3 DR 3 – Non-Blowout Releases .....	48
3.5 Seals and Rock Mechanics.....	48
3.5.1 RM 1 – Rock Mechanics.....	48
3.5.2 SL 4 – Studies of Short and Long-Term Components .....	49
3.6 Salado .....	50
3.6.1 SAL 1 – Lab/Field Properties of Anhydrite .....	50
3.6.2 SAL 2 – Halite Far-Field Pore Pressure .....	55
3.6.3 SAL 3 – Halite Lab/Field Properties .....	56
3.6.4 SAL 4 – Contaminated Brine Outflow .....	57
3.7 Non-Salado .....	61
3.7.1 NS 1 – Dewey Lake - Paper and Low-Effort Field Studies.....	61
3.7.2 NS 2 – Culebra Fracture/Matrix/Flow - Lab.....	62
3.7.3 NS 3 – Culebra Fracture/Matrix/Flow - Field .....	63
3.7.4 NS 4 – Multi-Well Tracer Test .....	63
3.7.5 Parameters for the Combined Activities NS 2, NS 3, and NS 4.....	64
3.7.6 NS 5 – Sorbing Tracer Test .....	64
3.7.7 NS 6 – Chemical Retardation (U and Am) .....	65
3.7.8 NS 7 – Chemical Retardation for Th, Np, Pu, U, and Am.....	66
3.7.9 NS 8.1 – Concentrations and Transport of Colloid Carriers: High-Molecular Weight Organic Compounds (HMWOCs) and Microbes.....	68
3.7.10 NS 8.2 – Enhanced Colloid Experimental Program .....	69
3.8 EAs.....	71
3.8.1 EA 1 – Backfill with pH Buffer .....	72
3.8.2 EA 2 – Backfill with pH Buffer and Waste Form Modification .....	73
3.8.3 EA 3 – Passive Markers.....	74
3.9 WAC.....	75
3.9.1 WAC 1 – Non-Corroding Waste Containers .....	75
3.9.2 WAC 2 – Elimination of Humic-Containing Waste Drums .....	76
4. COMPUTATIONAL IMPLEMENTATION OF THE SPM-2 CONCEPTUAL MODELS...	77
5. REFERENCES .....	79
APPENDIX: MEMORANDA AND LETTERS REGARDING REFERENCE DATA.....	A-1

## Tables

2-1. FEP-Related Assumptions for SPM-2 Scenario Screening.....	4
2-2. SPM-2 Baseline Concentrations for Mobile Actinides .....	6
2-3. Concentrations of Mobile Actinide Bearing Colloidal Particles in M/dm <sup>3</sup> .....	7
2-4. Weighted Head Space Concentrations of RCRA-Regulated Hazardous VOC Constituents .....	13
2-5. Modeling Parameters for a Hypothetical Brine Reservoir in the Castile Formation .....	36
3-1. SPM-2 Final Activity List.....	38
3-2. Probability Distributions for Actinide Concentration for the oxidation states +III, +IV, +V, and +VI for SPM-2 Analysis for Activity AST 1.1 .....	41
3-3. Probability Distribution for Actinide Concentrations for the Oxidation States +III, +IV, and +V for SPM-2 Analysis for Activity AST 1.1 .....	43
3-4. DR 2 Elicited Outcomes and Their Probabilities.....	47
3-5. Reduction Factors and Their Probabilities Used in the SPM-2 Analysis for the Successful Outcome of Activity DR 2.....	47
3-6. Probability Distribution for the Reduction Release Factors for SPM-2 Analysis for Activity DR 3 .....	49
3-7. Short-Term and Long-Term Component Seal Permeability for Activities SL 4 + RM 1, Short-Term and Long-Term Component Studies.....	50
3-8. Parameter Distribution for Anhydrite Porosity for Activity SAL 1.....	52
3-9. Parameters for Anhydrite Permeability for Activity SAL 1 .....	52
3-10. Parameter Distribution for Critical Gas Saturation in Anhydrite for Activity SAL 1 .....	53
3-11. Parameter Distribution for Critical Brine Saturation in Anhydrite for Activity SAL 1 .....	53
3-12. Parameter M for Calculating Threshold Pressure for Activity SAL 1 .....	54
3-13. Probability Distribution for C <sub>min</sub> Values for Activity SAL 1, Without Alterations to the Interbed.....	54
3-14. Probability Distribution for C <sub>min</sub> Values for Activity SAL 1, With Alterations to the Interbed.....	55
3-15. Distribution of Far-Field Pore Pressure Values for Activity SAL 2.....	56
3-16. Distribution of Far-Field Halite Permeability Values for Activity SAL 2.....	56
3-17. Values for Gas Threshold Pressure of Halite for Activity SAL 3 .....	57
3-18. Probability Intervals for the Brine Mass Storage Parameter for Activity SAL 4.1.....	58
3-19. Probability Intervals for the Brine Mass Storage Parameter for Activity SAL 4.2.....	59
3-20. Probability Intervals for the Brine Mass Storage Parameter for Activity SAL 4.3.....	60
3-21. Outcomes, Probabilities, and Parameter Values for Activities NS 2, NS 3, and NS 4 .....	61
3-22. Parameter Determination for Activities NS 2, NS 3, and NS 4.....	62
3-23. Matrix K <sub>d</sub> Values for Modeling Dissolved Actinide Transport in the Culebra for Activity NS 6 .....	66
3-24. K <sub>d</sub> Values for Modeling Dissolved Actinide Transport in the Culebra for Activity NS 7... 68	
3-25. Concentrations of Actinides for Activity NS 8.1 .....	69
3-26. Parameters and Distributions for Actinide Colloid Carriers – Mineral Fragments and Actinide Macromolecules for Activity NS 8.2.....	71
3-27. Actinide Solubilities with EA 1 in Log.....	73

## Figures

2-1. SPM-2 baseline permeabilities for shaft model elements.....	8
2-2. Schematic of DRZ and TZ definitions.....	19
3-1. Probabilities for blowout releases for Activity DR 2.....	46

## ACRONYMS

BMR	Baseline Meeting Record
CAO	Carlsbad Area Office
CCDF	Complementary Cumulative Distribution Function
CI	Compliance Indicator
DOE	U.S. Department of Energy
DRZ	Disturbed Rock Zone
EA	Engineered Alternative
EATF	Engineered Alternatives Task Force
EEG	Environmental Evaluation Group
EPA	U.S. Environmental Protection Agency
FEP	Features, Events, and Processes
HMWOC	High-Molecular Weight Organic Compound
INEL	Idaho National Engineering Laboratory
IRIS-2	Integrated Risk Information System
LHS	Latin Hypercube Sampling
LWB	Land Withdrawal Boundary
MB	Marker Bed
MD	Multimechanism Deformation
MDCF	Multimechanism Deformation Coupled Fracture
PA	Performance Assessment
PDC	Probability of Demonstrating Compliance
PDF	Probability Density Function
QA	Quality Assurance
RCRA	Resource Conservation and Recovery Act
RH-TRU	Remotely Handled Transuranic Waste
RFP	Rocky Flats Plant
RPM	Reaction-Path Model
SNL	Sandia National Laboratories
SPM	Systems Prioritization Method
SPM-1	Systems Prioritization Method - First Iteration
SPM-2	Systems Prioritization Method - Second Iteration
SQL	Sample Quantitation Limit
TRU	Transuranic
TRUPACT-II	Transuranic Package Transporter-II
TRUCON	TRUPACT-II content
TZ	Transition Zone
VOC	Volatile Organic Compound
WAC	Waste Acceptance Criteria
WID	Westinghouse Waste Isolation Division
WIPP	Waste Isolation Pilot Plant

## CODES

BRAGFLO BRine And Gas FLOW

# 1. INTRODUCTION

The Systems Prioritization Method (SPM) is a decision-aiding tool developed by Sandia National Laboratories (SNL) for the U.S. Department of Energy Carlsbad Area Office (DOE/CAO). SPM provides an analytical basis for supporting programmatic decisions for the Waste Isolation Pilot Plant (WIPP) to meet selected portions of the applicable U.S. Environmental Protection Agency (EPA) long-term performance regulations (40 CFR 191.13(a), the radionuclide containment requirements, and 40 CFR 268.6, the hazardous constituent concentration requirements promulgated under the Resource Conservation and Recovery Act (RCRA)). The first iteration of SPM (SPM-1), the prototype for SPM, was completed in September 1994. It served as a benchmark and a test bed for developing the tools needed for the second iteration of SPM (SPM-2). SPM-2, completed in March 1995, is intended for programmatic decision making.

This is Volume II of the three-volume final report of the second iteration of the SPM (SPM-2). It describes the technical input and model implementation for SPM-2 and presents the SPM-2 technical baseline and the activities, activity outcomes, outcome probabilities, and the input parameters for SPM-2 analysis. Volume I of this report provides a synopsis of the method and the SPM-2 results. Volume III described the analysis of the SPM-2 results to determine recommended programmatic paths for meeting DOE/CAO objectives.

The SPM-2 conceptual models were identified through the position paper process, Sandia's SPM-2 baseline process, SPM-2 activity set process, the DOE/CAO guidance for SPM-2, and the SNL management and DOE/CAO SPM steering team review processes. The process of defining the SPM-2 technical baseline involved compiling technical position papers, attending stakeholder meetings, reviewing stakeholder input, and holding multiple baseline definition and management review meetings. The SPM-2 baseline process is described in Sections 3.3 and 3.4 of Volume I. The elicitation process used to define the activities and their outcomes is described in Section 3.5 of Volume I.

Section 2 of this volume summarizes the conceptual models and data defined for the SPM-2 technical baseline. Section 3 of Volume II summarizes the SPM-2 activities, the potential outcomes of each activity (hereafter referred to simply as "potential outcomes"), the probabilities of each outcome, and the parameter distributions used to model each activity outcome. Section 4 discusses how the baseline and activities were implemented in the computer codes for the SPM-2 analysis. While every effort was made to model the conceptual approaches identified in the position papers, several concerns were not adequately addressed by the computer models. These issues are to be addressed by the side investigations (see Volume I, Sections 3.4.2 and 3.4.3).

**Intentionally Left Blank**

## **2. SPM-2 BASELINE**

### **2.1 Introduction**

This section summarizes the final recommendations for the SPM-2 technical baseline. The process of defining this baseline involved compiling technical position papers, attending stakeholder meetings, reviewing stakeholder input, and holding multiple interdisciplinary baseline definition and management review meetings. A discussion of this process can be found in Sections 3.3 and 3.4 of Volume I of this report. This section is organized by position paper topic.

### **2.2 Scenario Screening**

SPM-2 scenario screening examined features, events, and processes (FEPs) for inclusion in the SPM-2 analysis. Table 2-1, developed at the Scenario Screening baseline meeting, lists the FEPs included directly in the analysis (indicated by a "yes") and FEPs to be considered in side investigations (indicated by a "no"). Several other modeling assumptions, identified at the scenario screening baseline meeting, were as follows:

Borehole Closure - Assume silty sand.

Borehole Permeability - Assume  $10^{-11}$  to  $10^{-14}/m^2$  variability across boreholes.

Borehole Number - Assume 25 boreholes/km<sup>2</sup>/10,000 years (from M. H. McFadden, "Systems Prioritization Method Information Needs and Product Requirements," Sandia National Laboratories memorandum to R. Lincoln, December 19, 1994, in Appendix).

General Assumption - Assume use of data already in the WIPP Performance Assessment (PA) database for the baseline unless otherwise specified.

Near-Miss Assumptions - Treat near-miss calculations the same as the human-intrusion hole scenarios. For example: (a) undisturbed for compliance with RCRA and 40 CFR 191 - no new holes inside the land withdrawal area; (b) nearest near-miss - holes just outside the boundary analyzed as a pressure sink; (c) disturbed requirements - holes within the boundary.

### **2.3 Gas Generation**

For purposes of the SPM-2 baseline, the model for gas generation consisted of the average-stoichiometric gas generation model (WIPP PA Division, 1991; Sandia WIPP Project, 1992) to which gas generation from brine radiolysis was added. Plastic/rubber degradation was sampled from 0 to 100% (i.e., from all to none of the plastics/rubber materials may degrade, sampled on a uniform distribution). Data for the model were obtained from L. H. Brush, "Likely Gas-

Table 2-1. FEP-Related Assumptions for SPM-2 Scenario Screening (from Scenario Development Baseline Meeting Record (BMR) Revision 3, December 18, 1994)

FEP Issues	Included Directly in SPM-2 Calculations	Notes, Comments, Issues
<b>Near Field Issues</b>		
Enhanced communication with marker beds as a result of caving	Yes	None
Thermal effects on fluid flow	No	Side investigations are needed.
Contaminant transport in near field	Yes	None
<b>Intrusion-Related Issues</b>		
Near misses	No	Side investigations are needed. Should include Castile Brine hits for repository misses.
Fluid injection	No	Side investigations are needed (injecting brine from Castile into the Culebra).
Long-term brine flow	Yes	Degraded plugs
Brine flow to the surface during drilling (controlled and blowout)	No	Side investigations are needed.
Borehole connections to units below the repository	No	Issue raised by the Non-Salado group; further discussion and possible side investigations needed.
Borehole connections to units above other than the Culebra	Yes	None
Creep closure of boreholes in the Salado	No	Westinghouse Waste Isolation Division (WID) position is that salt will creep closed; however, it may be difficult to demonstrate that at least some boreholes do not remain propped open.
Brine slurries	No	Issue raised by the Environmental Evaluation Group (EEG). This issue needs to be addressed by the Disposal Room Group.

Table 2-1. FEP-Related Assumptions for Scenario Screening (Continued)

FEP Issues	Included Directly in SPM-2 Calculations	Notes, Comments, Issues
<b>Groundwater Flow Issues</b>		
Creation of "short circuit flowpaths" (e.g., withdrawal wells)	No	Side investigations are needed.
Shallow drilling for all purposes	No	Side investigations are needed
Groundwater withdrawal effect on regional flow	No	Side investigations are needed.
Potash mining/subsidence	No	Side investigations are needed.
Time-varying rock properties in Non-Salado	No	Side investigations are needed.
Fluid injection	No	Side investigations are needed.
Brine density effects	No	Side investigations are needed.
Miscellaneous things that could affect recharge; climate change, irrigation, damming, vegetational changes	No	Side investigations are needed.
<b>Other Issues</b>		
Dissolution around borehole	No	Creation of sinkholes. Side investigations are needed.
Nuclear criticality in near- and far- field	No	Side investigations are needed.
Uncertainty in inventory	No	Should be treated as a Waste Acceptance Criteria (WAC) issue, not a scenario construction issue.

Generation Reactions and Current Estimates of Gas-Generation Rates for the Long-Term WIPP Performance Assessment," Sandia National Laboratories memorandum to M. S. Tierney, June 18, 1993 (see Appendix).

## 2.4 Actinide and Colloid Source Terms

The concentrations assumed for mobile actinides for the SPM-2 baseline appear in Table 2-2. Note that the concentrations shown in Table 2-2 assume there is sufficient material present to

Table 2-2. SPM-2 Baseline Concentrations for Mobile Actinides

Actinide	Concentration	
	log(Molar)	Molar
Thorium	-5.6	$2.5 \times 10^{-6}$
Uranium	0.0	1.0
Neptunium	-2.0	$1.0 \times 10^{-2}$
Plutonium	-3.4	$4.0 \times 10^{-4}$
Americium	0.0	1.0

reach the specified concentrations. If the actinides were insufficient to reach the concentrations in Table 2-2, the available actinides were used to determine inventory-limited concentrations.

Table 2-3 defines the colloidal concentrations for the SPM-2 baseline.

## 2.5 Seals

The SPM-2 main shaft seal system was simplified for the baseline as: 1) a short-term seal, and 2) a long-term seal. The short-term seal modeled all of the short-term components, both those at the Salado/Rustler contact designed to keep brine out of the shafts and those nearer the base of the shaft seal designed to keep gas out of the shafts.

The conceptual main shaft seal model for the baseline consisted of short-term and long-term permeabilities for shaft model elements. No long-term function was assigned to panel seals, in keeping with DOE's position. The role of panel seals was based in part on the analyses discussed in Section 4.3 of *Systems Prioritization Method – Iteration 2 Baseline Position Paper: Repository Seals Program*. Baseline parameters for the main shaft seals were modeled in SPM-2 as described below.

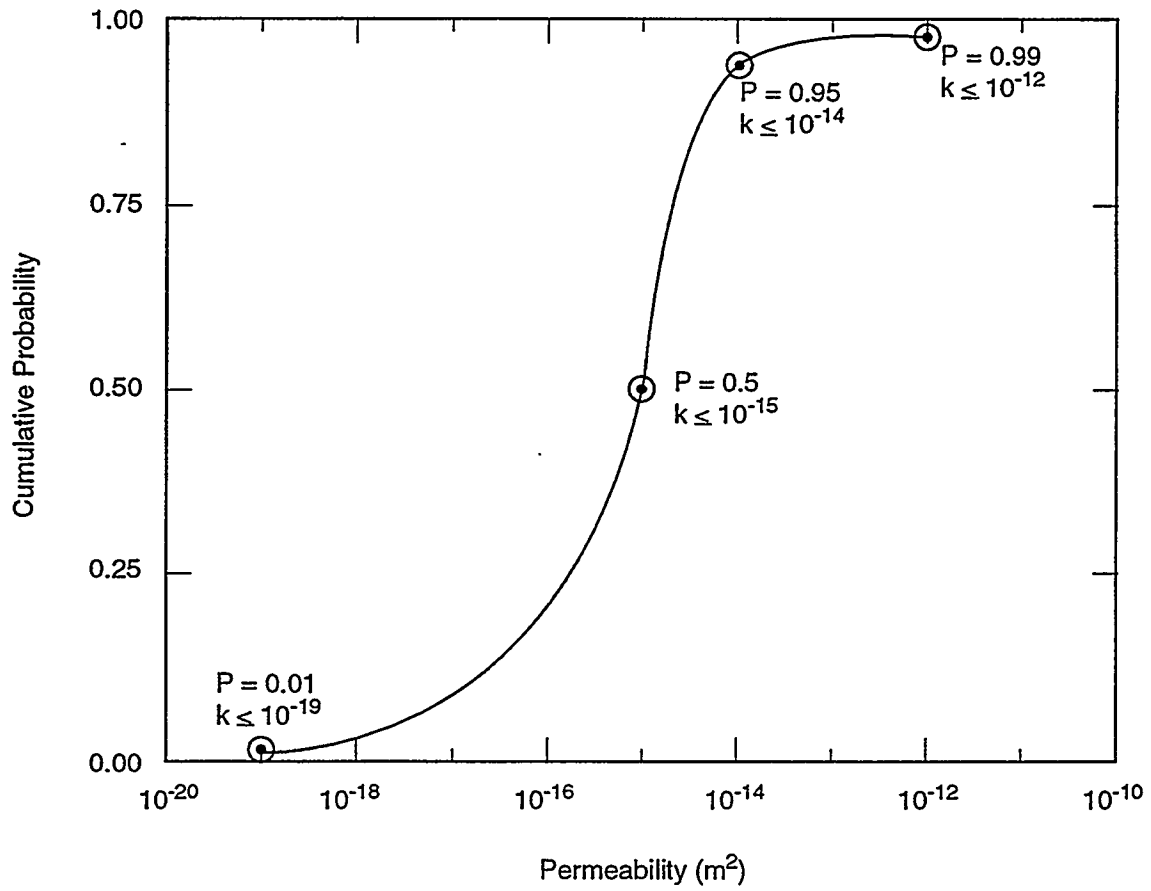
### 2.5.1 Seal Permeability

Calculations sampled on a value for seal permeability with a distribution between  $10^{-12} \text{ m}^2$  and  $10^{-20} \text{ m}^2$ . The baseline sample distribution curve is shown in Figure 2-1. It has the following characteristics:

Table 2-3. Concentrations of Mobile Actinide-Bearing Colloidal Particles in M/dm<sup>3</sup>

Colloidal Particle	Colloid Type	Plutonium	Uranium	Thorium	Neptunium	Americium	Diameter (μm)	Diffusion Constant Reduction Factor <sup>a</sup>
Mineral fragments	"Hard-sphere" carrier	0.0E+00	0.0E+00	0.0E+00	0.0E+00	0.0E+00	0.001 to 1	Not required
Microbacteria	Sterically-stabilized carrier	1.0E-04	1.0E-04	1.0E-04	1.0E-04	1.0E-04	2	Not applicable
High-Molecular-Weight Organic Matter	"Soft-sphere" carrier	2.0E-04	2.0E-04	2.0E-04	2.0E-04	2.0E-04	0.01	100
Actinide Macro-molecules	Actinide-intrinsic	0.0E+00	0.0E+00	0.0E+00	0.0E+00	0.0E+00	0.002	Not required

<sup>a</sup> The diffusion constant reduction factor is used to reduce the free water diffusion constants used in the WTPP 1992 PA calculations (i.e., divide the free water diffusion constants by the reduction factor shown).



Baseline Parameters	
	• Sample Distribution
<100 yr	• Set Short-Term Seal to Sampled Permeability
	• Set Long-Term Seal to $10^{-12}$ m <sup>2</sup>
>100 yr	• Set Short-Term Seal to $10^{-12}$ m <sup>2</sup>
	• Set Long-Term Seal to Sampled Permeability

TRI-6121-276-0

Figure 2-1. SPM-2 baseline permeabilities for shaft model elements.

- 1) A 0.01 quantile at a permeability of  $10^{-19} \text{ m}^2$ .
- 2) A 0.50 quantile (median) at a permeability of  $10^{-15} \text{ m}^2$ .
- 3) A 0.99 quantile at a permeability of  $10^{-12} \text{ m}^2$ .

For the first 100 years:

- 1) The short-term shaft seal permeability was sampled from the seals permeability distribution curve in Figure 2-1.
- 2) The long-term shaft seal permeability was assumed to be  $10^{-12} \text{ m}^2$ .

After 100 years:

- 1) The short-term shaft seal permeability was assumed to be  $10^{-12} \text{ m}^2$ .
- 2) The long-term shaft seal permeability was set at the value sampled for the short-term component for the first 100 years.

Length of the shaft seals were set as follows:

- 1) The long-term salt seal length was fixed at 60 m.
- 2) The short-term seal length was fixed at 49 m.

Note the change in parameters at 100 years. This was based on the assumption that if the short-term seal component is able to keep brine out of the long-term seal for the first 100 years, the long-term seal component will consolidate as planned, and perform well. Accordingly, if the short-term seal component is not able to keep brine out of the long-term seal for the first 100 years, the long-term seal will not perform well.

The model grid shown in Figure 4-2 of *Systems Prioritization Method – Iteration 2 Baseline Position Paper: Repository Seals Program* does not include a lower short-term seal component located between Marker Bed (MB) 136 and MB 134. This particular short-term component would become important if significant gas is generated and if no long-term seal is placed in the panels upon closure of the facility. Gas transmission to the shaft was modeled to be insignificant in the first 100 years, during which time the lower shaft salt seal would become effective, as discussed in Section 4.3 of *Systems Prioritization Method – Iteration 2 Baseline Position Paper: Repository Seals Program*. Therefore, to be completely consistent with shaft seal designs and the baseline parameter sampling, the lower short-term component was included.

## 2.6 RCRA Source Term

SPM-2 used the headspace-concentration limited model to assess hazardous organic chemicals in the gas phase under undisturbed conditions. As described in detail in the March 17th, 1995,

(Revision 3) draft of the *Hazardous Constituent Source Term Position Paper*, the model used weighted headspace gas analytical data from 536 drums of TRU-mixed waste to derive the volatile organic compound (VOC) source term. In this model, saturated vapor concentrations are assumed for semi-VOCs. For SPM-2, concentration limits corrected for gas available porosity for each VOC and semi-VOC in the gas phase were compared to health-based soil levels derived from the EPA's Integrated Risk Information System (IRIS-2) database.

The assumptions used for modeling the heavy metal constituents were:

- 1) Lead is the only heavy metal present in large quantity; and
- 2) All heavy metal constituents are saturated at their respective solubility limits in the brine.

Where the solubility limits for metals were not known for WIPP brines, a RCRA violation was assumed if WIPP disposal room brines crossed the regulatory boundary. This assumption accounts for any RCRA heavy metals that may be in the waste, and is consistent with the base-case scenario for 40 CFR 191.15.

Concentrations at the disposal unit boundary for gas/vapor phase VOCs and semi-VOCs were corrected for gas available porosity in the marker beds at the lateral disposal unit boundary and in shaft materials at the top of the Salado. Compliance with RCRA was assumed when the concentration calculated at the unit boundary was less than the health-based level for soil. As modeled for SPM-2, performance assumptions included the following:

- No credit was taken for chemical and physical attenuation (e.g., organic degradation, sorption and immobilization, storativity along transport pathways) within the repository or along transport pathways.
- It was assumed that sufficient gas is generated to elevate the (repository) pressure to sufficient levels to drive gas-phase hazardous constituents to the disposal unit boundary.
- No credit was taken for dilution of the hazardous constituents concentrations by the presence of waste-generated gas.
- Minimum brine saturation and maximum gas saturation were assumed, which maximized soil-based concentrations of hazardous constituents.
- Maximum anhydrite porosity was assumed to be 3%, which maximized soil-based concentrations of hazardous constituents.
- Maximum pressure in the gas phase was assumed to be lithostatic pressure (14.8 mPa), which maximized soil-based concentrations of hazardous constituents.
- MB 138, a combination of anhydrites "a" and "b," and MB 139 were considered to be anhydrite marker bed pathways. The four shafts comprising the shaft pathways were represented as a single shaft.

Parameter values are listed in M. Fewell and P. E. Sanchez, "Soil-Based VOC and Semi-VOC Concentration in the Gas Phase for SPM-2," March 29, 1995, Sandia National Laboratories memorandum, to F. Mendenhall and N. Prindle (see Appendix). Note that the volume parameter cancels out, making thickness of the pathway an inconsequential parameter.

Assumptions inherent in using weighted headspace measurements, detailed in Attachment Q to the Waste Analysis Plan of the *No-Migration Variance Petition*, Revision 1 (U.S. DOE, 1990, Appendix B), included the following:

- TRUPACT-II (Transuranic Package Transporter-II) content (TRUCON) code waste volumes in the WIPP Waste Analysis Plan are representative of waste to be emplaced in WIPP;
- Headspace data being collected at Idaho National Engineering Laboratory (INEL) and Rocky Flats Plant (RFP) are representative of data for all waste destined for the WIPP; and
- Uncertainty in the potential for post-closure release mechanisms to elevate concentrations of VOCs in the gas phase above those measured in drums is captured by conservative performance assumptions defined for SPM-2.

Revision 3 (March 17, 1995) of the *Hazardous Constituent Source Term Paper* suggests using one-half the sample quantitation limit (SQL) as an assumed input parameter for VOC constituents for which there are no data or that were undetected in sampling. SPM-2 did not use this approach. This assumption affected the following VOCs:

Carbon disulfide  
Cyclohexanone  
2-Ethoxyethanol  
Ethyl acetate  
Isobutanol  
2-Nitropropane  
1,1,2-Trichloroethane  
Trichlorofluoroethane  
Vinyl chloride  
Formaldehyde  
Hydrazine

### 2.6.1 Contaminant Screening

To the extent the information was available for a particular constituent, SPM-2 applied the health-based soil comparison to all hazardous VOCs and semi-VOCs listed in the Resource

Conservation and Recovery Act Part B Permit Application Waste Analysis Plan (U.S. DOE, 1993). SPM-2 took no credit for 40 CFR 268.6 regulatory assumptions that require only consideration of hazardous constituents listed in Appendix VIII of 40 CFR 261. By definition of the health-based soil standard, SPM-2 was intended to result in the screening of organic constituents for further modeling on the basis of toxicity. The SPM-2 screening technique is consistent with that used for the operational phase of WIPP, which uses headspace concentration and toxicity values to identify indicator chemicals for modeling.

No health-based limits were provided by the EPA for carcinogenicity or systemic toxicity for the following constituents:

- 2-Ethoxyethanol
- 2-Nitropropane
- Vinyl chloride
- 1,2,4-Trimethylbenzene
- 1,3,5-Trimethylbenzene
- Z 1,2 Dichloroethylene
- 1,1-Dichloroethane
- Cyclohexane

## 2.6.2 SPM-2 Data Input

Table 2-4 identifies input parameters and health-based soil standards for the SPM-2 analysis of VOCs. The average of the existing sample population of weighted headspace concentrations was used in cases where data were available. Cases where the data were not available, or where the VOCs were undetected in sampling, are noted in the table as NA. Detailed explanation of the weighted headspace method is provided in the March 17th, 1995, *Hazardous Constituent Source Term Paper*, and the operational-phase *Draft No-Migration Variance Petition* completed in May 1995 (U.S. DOE, 1995b).

## 2.7 Rock Mechanics

For the SPM-2 baseline, creep closure was modeled using the Multimechanism Deformation (MD) Creep Constructive model approach, which includes:

- Tresca (flow potential);
- Large strain codes;
- Parameters based on material property input (defined in Sandia WIPP Project, 1992);
- Stratigraphy, as defined in Munson et al., 1989; and
- Initial stress, as presented in Wawersik and Stone, 1989.

Table 2-4. Weighted Head Space Concentrations of RCRA-Regulated Hazardous VOC Constituents

Chemical	Concentration (average ppmv)
Acetone	92.6
Benzene	9.18
Bromoform	9.09
1-Butanol	101
2-Butanone	76.2
Carbon tetrachloride	560
Chlorobenzene	12.1
Chloroform	15.5
Cyclohexane	15.4
1,1-Dichloroethane	9.26
1,2-Dichloroethane	9.07
1,1-Dichloroethene	11.1
cis-1,2-Dichloroethene	9.05
Ethyl benzene	10.1
Ethyl ether	12.1
Methanol	261
Methylene chloride	739
4-Methyl-2-pentanone	97.9
1,1,2,2-Tetrachloroethane	9.11
Tetrachloroethene	9.09
Toluene	25.1
1,1,1-Trichloroethane	492
Trichloroethene	21.2
1,1,2-Trichloro-1,2,2-trifluoroethane	52.4
1,2,4-Trimethylbenzene	12.1
1,3,5-Trimethylbenzene	8.96
p/m-Xylene	12.6
o-Xylene	15.3

## 2.8 Disposal Room

Over 30 separate Disposal Room and Cuttings Models with numerous assumptions were used for the SPM-2 baseline. These are summarized in Section 2 of *Systems Prioritization Method – Iteration 2 Baseline Position Paper: Disposal Room and Cuttings Models*, with the changes discussed below.

Two important components in the SPM-2 Disposal Room Model were the consolidation of waste and backfill, and the room response to gas generation over time. These processes were included in SPM-2 baseline as a room porosity surface value. The porosity surface defined room porosity as a function of time and the number of moles of gas present in the room.

One change to the models described in the position paper was that, in the SPM-2 baseline, the repository was assumed to contain no backfill of any kind (M. H. McFadden, “Systems Prioritization Method Information Needs and Product Requirements,” Department of Energy memorandum to R. Lincoln, December 19, 1994, in Appendix). In agreement with the position paper modeling assumptions, room porosity surfaces for both the waste-containing rooms and the empty north end of the repository were calculated and supplied for the SPM-2 baseline.

Several additional changes were made to the assumptions regarding the Waste Flow Model described in Section 3.3 of *Systems Prioritization Method – Iteration 2 Baseline Position Paper: Disposal Room and Cuttings Models*. The first change was in the flow model discussed in Section 3.3.1 of that document. In order to address room heterogeneity issues, an additional parameter was added to allow a variable fraction of the brine in the waste to be mobile. During the management review of the SPM-2 technical baseline, the value of this parameter was fixed at 0.5.

Another important change was in the permeability of the waste (Section 3.3.2 of *Systems Prioritization Method – Iteration 2: Baseline Position Paper: Disposal Room and Cuttings Models*). According to the most recent version of the spalling component of the cuttings model, waste released into the borehole is determined by the waste permeability, and by the difference in pore pressure between the waste prior to the intrusion and the borehole drilling fluid pressure during the intrusion. A variable permeability for the waste, however, is different than the waste permeability assumption used in the 1992 WIPP PA, in which the permeability of the waste was a constant value of  $1.73 \times 10^{-13} \text{ m}^2$ . The waste permeability was redefined for SPM-2 as follows. Compatibility with the cuttings model is assured by computing a permeability  $k$  associated with that porosity using the following equation:

$$k = a\eta^n$$

where  $a = 10^{-11} \text{ m}^2$ ,  $n = 4.6$ , and  $k$  is in units of  $\text{m}^2$ . This relationship is linear when the logarithm of permeability is plotted against the logarithm of porosity, and is an approximation of the

Kozeny-Carmen equation frequently used in soil mechanics (Freeze and Cherry, 1979, p. 357). The constants in this equation require one point on the straight line to be coincident with the permeability value  $10^{-13} \text{ m}^2$ , representing the waste permeability value assumed for the 1992 WIPP PA (Section 3.3.2.1 of *Systems Prioritization Method – Iteration 2 Baseline Position Paper: Disposal Room and Cuttings Models*). This permeability value corresponds to a porosity value of 0.37. The permeability of the second point on the curve was assumed to be  $10^{-17} \text{ m}^2$ , corresponding to a waste porosity of 0.05, and represents the lower bound states of most very highly consolidated geological materials (Freeze and Cherry, 1979, pp. 29 and 37). These two points defined the permeability-porosity relationship. As mentioned in Section 3.3.2.1 of Volume I of the *Systems Prioritization Method – Iteration 2 Baseline Position Paper: Disposal Room and Cuttings Models*, measurements on simulated unprocessed waste have shown compacted material permeabilities on the order of  $10^{-12}$  to  $10^{-16} \text{ m}^2$  (Luker et al., 1991). These material permeabilities are consistent with this relationship, but are insufficient to define a more exact relationship, particularly in the absence of information about the changes in waste state caused by decomposition.

Finally, because of uncertainty in the two-phase characteristic curves, sampling on the Brooks and Corey and the van Genuchten curve sets had the same range of parameters for SPM-2 calculations as proposed for the Salado curve set, with the capillary pressure correlated with the waste permeability through the Davies' correlation (Sandia WIPP Project, 1992, pp. 2-12 to 2-16). Whereas the change in the flow model (which defined the fraction of mobile brine in the disposal room as fixed at 0.5 for SPM-2) determines the active flowing fluid volume in the room, this model enhancement specified the two-phase characteristic curves for this flowing region.

The assumptions and parameters used to model cuttings release in SPM-2 were identical to those described in Section 4 of Volume I of the *Systems Prioritization Method – Iteration 2 Position Paper: Disposal Room and Cuttings Models*.

## 2.9 Salado

The SPM-2 Salado baseline model for Salado Formation fluid flow and transport containment (Salado baseline model) is described in this section. The SPM-2 Salado baseline model was based on the numerical models used in the 1992 WIPP PA with extensive modifications both in technique and interpretation. The modifications accounted for uncertainty known to exist but that had not been incorporated into previous PA analyses.

The SPM-2 Salado baseline model made use of, and was supported by, existing data and knowledge, as well as high-probability expected results from a limited suite of incomplete work. The Salado baseline model honored available data and supporting information and certain projected results, and attempted to encompass the potential impact of known uncertainty (i.e., known lack of understanding or characterization) of processes likely to occur. No factors were

introduced to account for “unknown” uncertainty, or the possibility of acquiring new knowledge in the future.

All known flow interactions of the Salado Formation were captured either explicitly or by assumption in the Salado baseline model. The model, however, was developed with primary emphasis on the three fundamental regulatory-related questions of fluid flow in the Salado Formation: 1) “How much brine will enter the repository?”; 2) “How far will gas move from the repository?”; and 3) “How far will brine move from the repository?” Brine contributes to gas generation in the repository, and thus brine inflow was characterized by the Salado baseline model because it provided vital parameters to the Disposal Room model.

Existing data supported the use of the computational model BRine And Gas FLOW (BRAGFLO) and associated numerical models for brine inflow calculations, as described more completely in the *Systems Prioritization Method – Iteration 2 Baseline Position Paper: Salado Formation Fluid Flow and Transport Containment Group (Salado Position Paper)*. However, it was believed that the present data and characterization did not support explicit calculation of brine movement distances or gas movement distances, as described below. Therefore, an exceedingly conservative alternative method based on post-processing of BRAGFLO calculations was specified for comparison of brine and gas outflow to regulatory criteria, for the purposes of SPM-2 calculations. Post-processing was defined as the analysis of numerical data created by a completed simulation to develop conclusions that are not based on the algorithms in the computer code.

### **2.9.1 SPM-2 Salado Baseline Model Overview**

The Salado baseline model was based on BRAGFLO and associated numerical models described in WIPP PA 1992 (WIPP PA, 1992a and b; WIPP PA, 1993a and b; Sandia WIPP Project, 1992), and modified by Appendix B, Section 2, and Section 3, of the *Salado Position Paper*. A fundamental modification to the WIPP PA 1992 (WIPP PA, 1992a and b; WIPP PA, 1993a and b; Sandia WIPP Project, 1992) model was the altered anhydrite modification, which was retained for use in the Salado baseline model. Certain enhancements and revised performance measures for the Salado baseline model were made, which appear below; however, the basic BRAGFLO model, nodalization, layering, and panel and repository representations were retained.

BRAGFLO was used as the basis of the SPM-2 baseline model because it was the best model for Salado fluid flow available. It demonstrated capabilities for modeling multiphase flow in the context of both 1) specific process interactions (room closure, gas generation, brine consumption, human intrusion, etc.) and 2) project-related demands (e.g., stochastic framework), that are necessary for a PA of the WIPP repository. Modifications to the configuration of BRAGFLO, specified in the following section, assured that the uncertainty associated with the BRAGFLO characterization of the repository and formation was captured by the model outputs. These

modifications can be grouped into three categories: 1) model enhancements by use of newly-added or newly-enabled governing equations; 2) change of parameter ranges from historical (i.e., WIPP PA 1992) values to updated values (reflecting new data and/or better characterization of uncertainty); and 3) the use of post-processing techniques where BRAGFLO in this Salado baseline model configuration was incapable of capturing the range of uncertainty.

To summarize, the Salado baseline model emphasized the three fundamental questions of Salado fluid flow: brine inflow, brine outflow, and gas outflow. The Salado baseline model numerically estimated brine inflow using BRAGFLO in a configuration modified from, but still similar to, those used in previous WIPP PAs. The Salado baseline model also numerically estimated the quantity of brine and gas outflow using BRAGFLO. However, the configuration of BRAGFLO used for the Salado baseline model was not considered adequate for estimating movement of brine and gas away from the repository. Therefore, the quantity of brine and gas reaching the boundary was calculated by analyzing BRAGFLO results.

## **2.9.2 Position Paper Model**

It was specified that a 1-degree formation dip be incorporated into the SPM-2 baseline. However, because the BRAGFLO code could not readily incorporate this change with verified results, the evaluation will be done as a side investigation. The SPM-2 baseline thus did not include 1-degree dip.<sup>1</sup>

The following model enhancements to the BRAGFLO model were specified as part of the Salado baseline model.

### **2.9.2.1 THE RELATIVE PERMEABILITY OF BOTH PHASES IN THE DISTURBED ROCK ZONE (DRZ) AND TRANSITION ZONE (TZ)=1**

The DRZ and TZ region definitions are depicted in Figure 2-2. These regions have time-varying properties due to DRZ formation and shrinkage, room consolidation, possible room expansion, and fracturing due to high gas pressure. These time-varying properties had not been quantified in a model usable by Performance Assessment, nor could the effects of these time-varying properties on fluid flow be predicted accurately. The DRZ and the TZ were modeled with a constant, high permeability relative to intact units of the Salado Formation. The saturation of this region with brine is expected to vary over time as brine inflow, gas exsolution, brine outflow, and gas outflow occurs. Relative permeability is sensitive to saturation, so it was possible that the relative permeability might be very low. Low relative permeability in the DRZ and TZ is generally thought to be less conservative than high relative permeability, because low relative permeability restricts brine flow to the repository. Relative permeabilities in the

---

<sup>1</sup> A 1-degree formation dip was also not included in the SPM-2 activity calculations.

deforming time-varying DRZ and TZ are unknown. Therefore, use of a constant high relative permeability was specified for the Salado baseline model.

The DRZ and the TZ are expected to fracture in response to possible high gas-generated pressure. Although the effective permeability (relative permeability times intrinsic permeability) of the DRZ and the TZ is assumed to be higher than intact far-field permeabilities of the Salado Formation, the possibility exists that fractured DRZ may have even higher effective permeability. Higher DRZ and TZ permeability favors gas and brine outflow into the far-field Salado Formation. Thus, there is uncertainty whether the assumption used for DRZ and TZ permeabilities is conservative with respect to gas and brine outflow. To address this uncertainty, as part of the Salado baseline model, a side investigation on the possible effects of fracturing in the DRZ is specified. It is expected that the study will confirm the Salado baseline model assumption; it may even allow a less conservative assumption to be implemented.

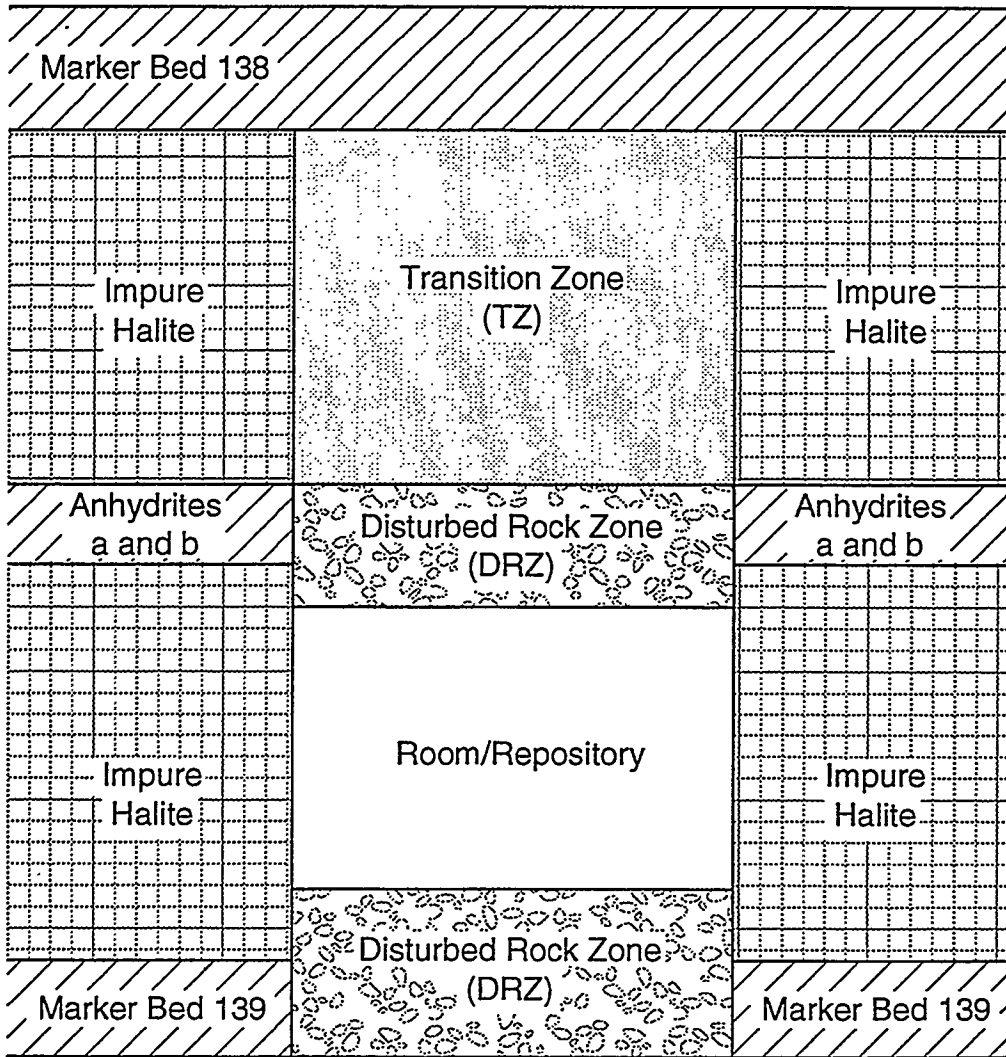
#### 2.9.2.2 ADD A 1 DEGREE DIP TO THE BRAGFLO MODEL

Webb and Larson (1996) investigated the impact of dip on brine inflow and gas migration, and found that dip affects gas migration distance and brine inflow under conditions of elevated (i.e., above natural) interbed permeability. In one case, brine inflow was calculated to increase 75% into the disposal region after interbeds were altered using the 1992 WIPP PA model of interbed fracture. Elevated interbed permeability will occur if interbeds fracture or dilate in response to high gas pressure in the repository. Because interbed fracture appears a likely response to high repository pressure, and because interbed fracture with dip may increase brine inflow, dip was included in defining the Salado baseline model.

The general layout specified for the Salado baseline model for the repository and the Salado Formation requires the use of two repository discretizations – one with the modeled panel region higher than the rest-of-repository region, and one with the panel region lower. The interbed fracturing model will need to be modified due to the inclusion of dip. A recommended modification is to make the fracture parameters specific to each element or node, not a constant value. This model enhancement should allow the possibility of countercurrent flow in the interbed and increased brine inflow to the room when interbed alteration occurs.

#### 2.9.2.3 CORRELATE THE THRESHOLD DISPLACEMENT PRESSURE WITH PERMEABILITY

The threshold displacement pressure of the interbeds, the DRZ, and the TZ were correlated with their respective permeability through the Davies' correlation (Davies, 1991), including uncertainty. This was done both prior to and after fracturing in every element composing these



Not to Scale

TRI-6115-

Figure 2-2. Schematic of DRZ and TZ definitions.

regions. Previously with the interbed alteration model, zero capillary pressure was assumed in the interbeds for all time to accommodate the anticipated threshold displacement pressure in fractured interbeds. Use of the Davies' correlation was based on the best available information on the expected behavior of threshold displacement pressure in the Salado Formation.

### **2.9.3 Necessary Efforts**

In some instances, positions in the Salado baseline model were justified based on expected outcomes of side investigations. The nature of the side investigations is such that they can potentially be completed within about a year from initiation, and their outcomes are certain, but not yet demonstrated. Four such side investigations have been identified for the Salado baseline model; one was described above, in Section 2.9.2.1, for the DRZ and TZ permeability assumptions. The other three are discussed below.

#### **2.9.3.1 2-D/3-D COMPARISON STUDY OF SALADO FLUID FLOW**

When the SPM-2 Salado baseline model was derived, the hybrid 2-D/3-D BRAGFLO configuration had not been numerically compared with more conventional 3-D nodalizations. Therefore, it was not known whether the configuration of BRAGFLO effectively simulated 3-D flow, which is required for a realistic estimate of brine inflow. The BRAGFLO configuration was a 2-D model in which the volumes of elements and their connection areas have been altered, in an approach thought to be consistent with the assumption of radial flow. Although this approach is standard for modeling radial flow to a borehole, features in the repository configuration specified for the Salado baseline model caused concern that the model might behave more like a 2-D model than a 3-D model. In a limited study on the effect of dip, brine inflow in a 3-D single-room model was found to be two to three times higher than in a 2-D single-room model. Because the BRAGFLO geometry had not been shown to accurately simulate 3-D brine flow to the repository, there was concern that it might generally underestimate brine inflow by a factor of 2 or 3.

For SPM-2, a side investigation will model an explicit comparison of 2-D to 3-D repository geometry. This study is solely for verifying the BRAGFLO geometry, and is independent of adding dip to the BRAGFLO model. This study will, however, yield insight into the 3-D mechanics of brine outflow which may favorably impact other assumptions contained in the Salado baseline model.

### 2.9.3.2 DISCRETE FRACTURE/MATRIX STUDY OF BRINE FLOW IN INTERBEDS

It is expected that some of the contaminated brine that can potentially flow out of the repository will flow through the matrix of interbeds, or adjacent halite-rich units, rather than through fractures. This conclusion, however, depends upon the nature of fractures in the anhydrite and the two-phase characteristics of the fractures, matrix, and adjacent halite units. The minimum value for the range of brine storage (discussed below, in Subsection 2.9.4.1) within the disposal system took into account that some contaminated brine will flow in the matrix of the interbeds or adjacent halite units and will not be available for transport to lateral boundaries in fractures. This conclusion was both uncertain and possibly nonconservative. To examine this issue, a side investigation consisting of a discrete fracture/matrix study of brine and gas transport in fractured interbeds has been specified. Because the actual fracture geometry and two-phase flow relations that might result from fractures caused by high gas pressure are uncertain, the modeling effort used a wide variety of possible fracture geometries and two-phase flow relations in order to span the range of possible conditions. Even though there was uncertainty in the model parameters in the specified study, it is extremely likely that at least some contaminated brine will flow into anhydrite matrix and adjacent halite regardless of the assumptions used, as long as the assumptions are bound by known facts. It was therefore highly probable that the Salado baseline model assumptions would be verified by the modeling effort.

### 2.9.3.3 EVALUATION OF DISSOLVED GAS EXSOLUTION EFFECTS

[Note: It was requested that the evaluation of dissolved gas exsolution effects be incorporated into the SPM-2 baseline. This could not be done for SPM-2. These effects are to be evaluated in a side investigation (see Section 3.4.2 in Volume I of this report).]

The WIPP 1992 PA BRAGFLO model did not include gas dissolved in high-pressure formation brine. In reality, as formation brine depressurizes near the repository, dissolved gas exsolves, providing additional impetus for brine inflow. Webb (1992) studied this effect on brine inflow to a constant pressure borehole. Dissolved gas exsolution increased the rate of brine inflow sufficient to introduce uncertainty about the BRAGFLO assumption. The impact on the repository is probably less than predicted by Webb for an open borehole, because the repository pressurization due to gas generation and creep closure makes flow to the repository more difficult than flow to an open borehole. For numerical reasons the Salado baseline model was not to incorporate gas exsolution. In the Salado baseline model, it was assumed that the effects of gas-phase exsolution will be negligible. This assumption will be verified through side investigations of a repository-scale model that incorporates gas exsolution as one of the processes occurring in the Salado Formation. This effort could likely be conducted in close cooperation with the 2-D/3-D model effort described above.

In this effort, the gas solubility will be modeled with a Henry's constant of  $4 \times 10^{10}$  Pa as suggested in Webb (1992), based on the study of Cygan (1991). The calculation should be started with brine fully saturated with dissolved gas, and no free gas phase (Beauheim et al., 1993). The effect of dissolved gas on the brine density and viscosity can be neglected because it is considered to be minor. The dissolved gas can be assumed to be pure nitrogen because this is the predominant naturally-occurring gas observed in the Salado Formation.

#### **2.9.4 Post-Processing Techniques for Comparison to Regulatory Criteria**

The Salado baseline model configuration did not allow direct comparison of calculated gas and brine movement in the Salado to regulatory criteria. The primary issues preventing direct comparison were: 1) the radial-flaring discretization of the repository and the Salado formation did not allow for accurate representation of buoyant force vectors in a dipping formation; 2) the panel/rest-of-repository representation of the disposal areas may not have allowed accurate resolution of the points of brine and gas outflow; 3) lack of verified Salado-specific two-phase curves yielded uncertainty in flow dynamics that was not entirely captured by varying between Brooks-Corey and van Genuchten/Parker; 4) the dynamics of fracture formation (or dilation) were poorly characterized; 5) the dynamics of WIPP fracture flow dynamics were poorly characterized; 6) the Salado baseline model configuration was unable to capture channeling and fingering dynamics; and 7) the porous-medium representation of multiphase fracture flow in the Salado baseline model was not realistic and, more importantly, had not been verified as adequate for regulatory purposes. Uncertainty in the response of the formation to high gas pressure in the repository (fracture characterization) was important because if migration of gas and especially brine to the lateral boundary occurs, it will almost certainly be through interbeds (or in other layers in the formation) whose permeability has been increased by dilation of existing, or the formation of new, fractures.

Because the Salado baseline model could not be used for direct comparison of contaminant movement distances and/or rates to regulatory standards, assumptions were made about how contaminants are transported to the boundary. For the Salado baseline model, these assumptions take the form of post-processing of BRAGFLO results to estimate the quantities of gas and brine that reach the boundary, the time they reach the boundary, and their concentration. Although the methods for both gas and brine are similar, the post-processing methods prescribed for quantifying transport of each phase are discussed separately in the following sections.

##### **2.9.4.1 BRINE OUTFLOW POST-PROCESSING**

While brine may flow out of the repository and into the surrounding formation due to local formation depressurization, it will not reach the far-field until the pressure exceeds the far-field pore pressure. For post-processing, the far-field pore pressure was called the brine containment pressure,  $P_{bc}$ . If brine flows towards the accessible environment, fluid storage within the Salado

Formation will delay and possibly prevent its arrival. Brine storage may occur in fractures, the surrounding matrix, and/or adjoining lithologic layers (e.g., the halite-rich rock adjoining an anhydrite interbed). Brine storage was included in the Salado baseline model. Its method of calculation is described below.

As a part of the BRAGFLO simulation, brine flux out of the repository was recorded on a frequent interval, so that the record of brine flow could be recreated by a post-processor. For maximum flexibility in post-processing and for use in SPM-2 activity sets, the fluxes between repository and adjacent regions were recorded, as was the flux between adjacent regions, the TZ, and all interbed layers. The concentration of contaminants in brine was also recorded, so that a detailed history of mass flux, concentration, and time could be recorded. This was necessary for calculating integrated releases, as detailed below.

The amount of brine that can be stored between the repository and the Land Withdrawal Boundary (LWB) is uncertain but bounded. It was assumed that all brine outflow from the repository moves into MB 139, because the likely stratification of brine under gas in the repository makes assuming brine outflow to other, above-repository interbeds not defensible at this time. It was also assumed that the known uncertainty in how brine flows within MB 139, and between MB 139 and adjacent halite-rich rock, could be addressed with a sampled parameter,  $C_b$ .

If  $P_{\text{repository}} > P_{bc}$  at any time, the total fluid mass reaching the boundary in 10,000 years is given by

$$M_{\text{brine at boundary}} = M_{\text{leaving repository}} - M_{\text{brine storage}}$$

where

$$M_{\text{brine storage}} = C_b \rho_b \phi \pi r^2 h_b$$

and  $C_b = 10^{-3}$  to 2; log uniform distribution  
 $\phi = 0.01$  (MB 139 porosity)  
 $r =$  distance to regulatory boundary  
 $h_b =$  MB 139 thickness  
 $b =$  density of brine

$M_{\text{brine storage}}$ , although cast in radially symmetric terms, was intended to account for several uncertainties, all of which were incorporated in the term  $C_b$ . The rationale behind the minimum value selected for  $C_b$  was based on the assumption that brine, if it is to reach the boundary, will flow through fractures. Fractures will likely a) propagate up-dip in a limited arc from the repository, b) be of small aperture, and c) channelize brine flow. A factor of  $10^{-2}$  was assigned

due to directional propagation (a wedge-shaped fracture 150 m wide at the LWB); a factor was not assigned for brine flow confined to the fracture aperture based on the expected results of the discrete fracture/matrix modeling study, and a factor of  $10^{-1}$  was assigned to account for likely channeling of brine that does flow within the fracture. Thus, the minimum storage volume for brine was estimated to be  $10^{-3}$  times the intact pore volume of MB 139 between the repository and LWB. The maximum value of  $C_b$ , 2, was based on the possibility of significant flow of brine in the interbed matrix (or old, undilated fractures), some flow into adjacent units, and dilation of the fractures creating new pore volume. The distribution for  $C_b$  was lognormal between  $10^{-3}$  and 2, giving a mean/median value of approximately  $4 \times 10^{-2}$ .

A hand calculation for the median brine storage using this post-processing technique provided the value of approximately  $9 \times 10^6$  kg, or 7,500 m<sup>3</sup> of brine. Due to the sampling method and large range about the median value, some realizations had storage volumes as low as about 180 m<sup>3</sup>, and some as much as about 360,000 m<sup>3</sup>.

#### 2.9.4.2 GAS OUTFLOW POST-PROCESSING

Gas, like brine, cannot reach the far field without first exceeding the resident pressure of far-field fluids. Additionally, gas must overcome the threshold displacement pressure to displace brine from pores. A defensible range for interbed threshold displacement pressure is 0 to 2 MPa greater than the far-field pore pressure (Beauheim et al., 1994). Therefore, for gas flow to the lateral boundary, the Salado baseline model, as a precondition, required repository pressures to exceed the far-field brine pore pressure at the repository horizon (a sampled value), plus a normally-distributed threshold displacement pressure of between 0 and 2 MPa. This pressure is called the gas containment pressure,  $P_{gc}$ . Unless the pressure in the repository exceeds this pressure, no gas will reach the lateral boundary.

If  $P_{repository} > P_{gc}$  at any time, a post-processing step to calculate gas reaching the boundary must be performed. Similarly to brine, the mass of gas reaching the boundary is calculated using the following equation:

$$M_{gas\ at\ boundary} = M_{leaving\ repository} - M_{gas\ storage}$$

where

$$M_{gas\ storage} = C_g \rho_g \phi \pi r^2 h_g$$

and

$C_g = 10^{-1}$  to  $10^{-6}$  (fractured interbeds);  $1/3$  to  $10^{-3}$  (unfractured interbeds)

$\phi = 0.01$

$r$  = distance to regulatory boundary

$h_g$  = composite thickness of anhydrites a, b, and MB 138

$\rho_g$  = density of gas (at  $P_{gc}$ )

The uncertainty associated with lateral gas flow to the LWB begins with all of the uncertainty associated with brine flow (because gas is also a fluid), but is greater due to the greater mobility of gas (lower viscosity), the reduced ability of gas to enter the matrix and adjacent units (high or uncharacterized and assumed high threshold pressure), the buoyant drive for gas flow directed up-dip, and the likely dominance of fracture flow for gas movement. Gas flow in fractures remains uncharacterized for the WIPP. These uncertainties are significantly greater than those associated with brine flow. Because of these uncertainties, the range of gas storage within the accessible environment boundaries is assumed to be uniformly lower than for brine. It was decided to evaluate the gas-storage parameter in terms of fractured (high pressure) interbeds, and unfractured interbeds. For fractured interbeds, the maximum (most favorable) value was determined by assigning a factor of 1 for flow direction (assuming radial fractures), a factor of 0.5 based on the relation between marker bed thickness and likely fracture aperture, and factor of 0.3 for fingering/channeling effects. The resulting factor of 1/15 was rounded to 1/10 for numerical simplicity. For fractured interbeds, the minimum (least favorable) value was determined by assigning a factor of  $10^{-2}$  for directed fractures, a factor of 1/5 for fracture aperture, a factor of  $10^{-2}$  fingering and channeling, and a factor of  $10^{-2}$  to account for uncertainty in two-phase flow properties. The resulting minimum value is  $10^{-6}$ . The sampled values on this range were lognormally distributed. For unfractured interbeds, the maximum value of 1/3 was assigned assuming radial flow through porous media with viscous fingering and channeling. The minimum value of  $10^{-3}$  was determined by assigning 0.1 factor for two-phase flow property uncertainty (no fractures means less uncertainty), a factor of 0.1 to account for the possibility of increased fingering and channeling, and a factor of 0.1 to account for likely up-dip flow due to buoyancy.

## 2.9.5 Tie-in to the Conceptual Model Components

This section provides additional links between the conceptual model and the Salado baseline model. A description of the components of the conceptual model appears in the *Salado Position Paper*.

### 2.9.5.1 STRATIGRAPHY

The Salado baseline model utilizes stratigraphy similar to that described in Section 3 of the *Salado Position Paper* for the process model. Based on a detailed study on this subject, this

stratigraphic representation is defensible for brine inflow and for calculating the flux of brine and gas out of the repository. It may not be defensible for calculating brine and gas movement in the interbeds away from the repository, because it does not allow channeling. This concern contributed to the implementation of post-processing techniques.

#### 2.9.5.2 SALT CREEP

The Salado baseline model did not account for the effects of salt creep in response to changes in pore-fluid pressure on fluid flow other than those accommodated by the effects of elastic compressibility of the rock matrix on porosity. The dramatic effects of salt creep on Salado fluid flow in the DRZ and regions near the repository were accounted for in the DRZ assumptions. The salt-creep fluid flow response to far-field pore pressure changes is less significant than fracturing, channeling, fingering, buoyancy, and fluid pressure gradients on the 10,000-year time scale. Due to the many assumptions and post-processing techniques adopted for far-field flow, this effect was neglected in the Salado baseline model.

#### 2.9.5.3 CONTAMINANT TRANSPORT

All aspects of uncertainty in contaminant transport and all processes described in the conceptual model, were accounted for in post-processing. In post-processing, there was no credit taken for sorption, decay, or other path, exposure, and/or travel-time dependent processes. The effects of dispersion, diffusion, and colloid transport, which modify contaminant movement, were accounted for in the  $C_b$  and  $C_g$  sampled parameters. The development of a method for incorporating the favorable effects of radionuclide decay along the flow path within the brine outflow post-processing technique is under consideration.

#### 2.9.5.4 THERMALLY DRIVEN FLUID FLOW

The Salado baseline model retained the assumption of isothermal conditions for the Salado Formation. Thus, thermally driven fluid flow was not included in the physics of the model. The uncertainty introduced by not considering thermally-driven fluid flow was considered to be captured within the range of brine inflow as calculated by the model, consistent with the observed differences between thermally-driven and isothermal brine inflow experiments in the WIPP underground (Nowak et al., 1988).

#### 2.9.5.5 MODEL INITIAL CONDITIONS

Uncertainty in initial conditions was associated with long-term movement of contaminants. Because of the post-processing assumptions implemented in the Salado baseline model, the uncertainty associated with initial conditions is considered to have been addressed.

#### 2.9.5.6 DRZ

The Salado baseline model altered the description of the DRZ and TZ so that the effective permeability of these regions will remain high regardless of their respective saturation levels. This new assumption is to be verified by an additional modeling effort in a side investigation.

#### 2.9.5.7 HYDROGEN DIFFUSION

Diffusion of hydrogen through the crystalline structure of minerals in the Salado Formation would decrease the repository pressure and the saturation of gas along VOC transport pathways. This will decrease gas migration, increasing confidence in compliance. It was thus conservatively ignored in the Salado baseline model.

#### 2.9.5.8 CHEMICAL REACTIONS

Concern about the effects of chemical reactions stems primarily from a lack of understanding about their effects on flow pathways for contaminants. Because post-processing assumptions were used to determine brine and gas storage (and, hence, contaminant storage), chemical reaction between repository fluids and the host rock were neglected in the Salado baseline model.

### 2.9.6 Parameter Values and Distributions for the SPM-2 Salado Baseline Model

The parameter values necessary for the Salado baseline model and their distributions are summarized below.

#### 2.9.6.1 IMPURE HALITE

Threshold Pressure	50 MPa; fixed
Permeability	$10^{-20}$ to $10^{-24}$ m <sup>2</sup> ; median $10^{-21}$ m <sup>2</sup>
Porosity	0.001 to 0.03; median 0.01

Specific Storage	$10^{-7}$ to $10^{-5}$ m <sup>-1</sup> ; median $10^{-6}$ m <sup>-1</sup>
Initial Pore Pressure	Hydrostatic; datum at MB 139 relative to shaft

### 2.9.6.2 ANHYDRITE

The interbed alteration model was applied using the following parameters:

Threshold Pressure	Correlated with local permeability according to Davies' correlation (Davies, 1991) with uncertainty
Initial Permeability	$10^{-17}$ to $10^{-20}$ m <sup>2</sup> ; median $10^{-19}$ m <sup>2</sup>
Maximum Fractured Permeability	$10^{-9}$ m <sup>2</sup>
Initial Porosity	0.001 to 0.03; median 0.01
Maximum Fractured Porosity	Initial Porosity + 0.01
Specific Storage	$10^{-7}$ to $10^{-5}$ m <sup>-1</sup> ; median $10^{-6}$ m <sup>-1</sup>
Initial Pore Pressure (MB 139)	12.0 to 13.0 MPa; median 12.5 MPa at repository elevation, adjusted hydrostatically for dip
Fracture Initiation Pressure	1 MPa lower than lithostatic to lithostatic, uniform distribution
Full Fracture Pressure	Initiation pressure + 2.5 MPa

### 2.9.6.3 DRZ

Threshold Pressure	Correlated with local permeability with uncertainty
Initial Permeability	$10^{-15}$ m <sup>2</sup>
Initial Porosity	Impure halite value
Maximum Fractured Porosity	Initial porosity + 0.01
Specific Storage	$10^{-5}$ m <sup>-1</sup>
Relative Permeability (gas)	1.0
Relative Permeability (brine)	1.0

#### 2.9.6.4 TZ

Threshold Pressure	Correlated with local permeability with uncertainty
Initial Permeability	$10^{-15} \text{ m}^2$
Initial Porosity	Impure Halite value
Maximum Fractured Porosity	Initial Porosity + 0.01
Specific Storage	$10^{-5} \text{ m}^{-1}$
Relative Permeability (gas)	1.0
Relative Permeability (brine)	1.0

#### 2.9.6.5 ALL REGIONS AND MATERIALS

Calculations sampled on the two-phase characteristic curves. All regions had the same curve set with region-specific values.

- mixed Brooks and Corey; 1/3 mixed van Genuchten/Parker.
- van Genuchten/Parker saturation definition changed from 1992 WIPP PA.
- appropriate equations summarized in Section 5.7 of the *Salado Position Paper*.

Gas Residual Saturation	0. to 0.4 - Uniform; median 0.2
Brine Residual Saturation	0. to 0.6 - Uniform; median 0.3
Brooks and Corey Parameter ( $\lambda$ )	0.2 to 10. - Median 0.7
van Genuchten/Parker m	$m = \lambda/(1 + \lambda)$

#### 2.9.7 SPM-2 Salado Baseline Model Two-Phase Relationships

The mixed Brooks and Corey and the mixed van Genuchten/Parker two-phase characteristic curves were recommended, as detailed below.

##### Brooks and Corey.

The original definition of effective saturation is

$$S_e = \frac{S - S_r}{1 - S_r},$$

where  $S_r$  is the residual wetting phase saturation.

The modified Brooks and Corey model redefines the effective saturation as

$$S'_e = \frac{S - S_r}{S_c - S_r},$$

where  $S_c$  is  $1 - S_{gr}$ .

The mixed approach uses both effective saturation definitions as follows:

$$P_c = \frac{P_d}{S_e^{1/\lambda}}$$

$$k_{r,w} = S_e^{(2+3\lambda)/\lambda}$$

$$k_{r,mw} = (1 - S'_e)^2 (1 - S_e^{(2+\lambda)/\lambda})$$

The mixed Brooks and Corey model was recommended over the original and modified approaches.

### Van Genuchten/Parker.

The effective saturation used by van Genuchten is

$$S_e = \frac{S - S_r}{S_s - S_r},$$

where  $S$ ,  $S_r$ , and  $S_s$ , are the saturation, residual liquid saturation, and full saturation value, respectively.

In the original implementation, the value of  $S_s$  is set equal to 1.0, so

$$S_e = \frac{S - S_r}{1 - S_r}.$$

Similar to Brooks and Corey, a modified saturation definition can be defined as

$$S'_e = \frac{S - S_r}{S_c - S_r}$$

where  $S_c$  is as defined above.

The mixed van Genuchten/Parker model is similar to mixed Brooks and Corey, because both effective saturation values are used.

The restricted form of the van Genuchten water retention equation ( $m = 1-1/n$ ) gives the capillary pressure equation

$$P_c = \frac{1}{\alpha} (S_e^{-1/m} - 1)^{1-m}.$$

Van Genuchten used the Mualem (1976) wetting phase relative permeability expression to get

$$k_{r,w} = S_e^{1/2} \left( 1 - \left( 1 - S_e^{1/m} \right)^m \right)^2.$$

Van Genuchten (1978, 1980) did not address nonwetting phase relative permeabilities. The Parker extension was recommended with the modified saturation definition similar to Brooks and Corey, or

$$k_{r,nw} = (1 - S_e')^{1/2} \left( 1 - S_e'^{1/m} \right)^{2m}.$$

## 2.10 Non-Salado

This section describes the Non-Salado component of the WIPP system that was developed in November and December of 1994 as input for SPM-2. This baseline was developed by a working group composed of staff from the SNL Geohydrology Department, the WIPP PA Computational Support Department, and the WIPP Compliance Support Department. An important driving objective of the Non-Salado baseline model development was that the model assumptions be based on information available as of December 1994.

In the specification of parameters to be sampled for the baseline SPM-2 analysis, an effort was made to focus on parameters for which radionuclide release at the accessible environment boundary was known to be sensitive to calculations made in previous PAs and other sensitivity studies (WIPP PA Department, 1993a; Reeves et al., 1991). The general format for the following description of the Non-Salado baseline model is a description of what has been specified and/or assumed for a particular model component, followed by comments on the rationale for that particular specification and/or assumption.

## 2.10.1 Release Paths

The PA code BRAGFLO was used to model partition flow in an intrusion borehole to three locations: the Culebra, the Magenta, and the top surface of the Rustler. Other members of the Rustler Formation are relatively tight rock lithologies with low hydraulic conductivities, and very little transport of radionuclides is expected to occur within these units. Twenty-five percent of the radionuclides that reach the top of the Rustler were *assumed* to be regulatory releases. Radionuclides that enter the Magenta were assumed not to reach the accessible environment during 10,000 years. Releases from the Culebra were calculated using a model of solute transport, SECO/TP.

For the BRAGFLO calculation that partitions flow to different hydrologic units, the value of transmissivity chosen for the Culebra was the highest value in the portion of the calibrated transmissivity fields that overlies the panels. In order to streamline the calculation process, this transmissivity was taken as the highest value sampled from the Culebra region directly overlying the waste-disposal panels in any of the 70 realizations of the Culebra transmissivity field (LaVenue and RamaRao, 1992).

The value of transmissivity for the Magenta was the lowest measured value for that unit over or near the panels,  $1 \times 10^{-8}$  m<sup>2</sup>/s (from borehole H-2a, Mercer, 1983). The thickness of the Magenta was specified as 8.5 m (from borehole H-2, Mercer, 1983, Table 1). The specified Magenta freshwater head was 961 m (Lappin et al., 1989, Figure 3-7). The specified porosity for the Magenta was 0.09, an estimate based on the measured porosity values of Culebra Dolomite (0.066 and 0.115, Lappin et al., 1989, Tables E-8 and E-9) at a location (H-10) with roughly comparable measured transmissivity ( $7.5 \times 10^{-8}$  m<sup>2</sup>/s, Lappin et al., 1989, Table 3-7). Storativity in the Magenta Dolomite was assumed to be comparable to that in the Culebra Dolomite.

The value of hydraulic conductivity in the Dewey Lake was assumed to be  $10^{-8}$  m/s, which is the same as the value used for Dewey Lake in the 1992 WIPP PA 3-D regional model and the same as the value used in the U.S. Geological Survey regional flow model (Davies, 1989). This value is typical for a fine-grained, silty sandstone. The value of freshwater head used for the Dewey Lake is 980 m. The value of porosity used for the Dewey Lake is 0.15, based on an analogue of the Wilcox sandstone, a silty/shaley sandstone (Davis and Dewiest, 1966, Table 10.1). The value of compressibility used for the Dewey Lake is  $10^{-10}$  Pa<sup>-1</sup>, which is the middle of the range for intact rock (Freeze and Cherry, 1979, Table 2.5).

Because other members of the Rustler Formation are relatively tight rock lithologies with low hydraulic conductivities, and very little transport of radionuclides is expected to occur within these units, they were assumed to have zero transmissivity. This assumption is "realistically conservative" because these units generally have very low transmissivities, and it partitions the flow that would have gone into these units into higher transmissivity units.

## **2.10.2 Culebra Flow and Physical Retardation**

In the Non-Salado baseline calculations, flow and transport within the Culebra was treated assuming 2-D, perfectly-confined, double-porosity conditions. Following the treatment in the 1992 WIPP PA calculations, advection of radionuclides was assumed to occur only in fractures, although radionuclides might diffuse into the matrix. In order to avoid overestimating the amount of diffusion in the baseline, model properties were assumed that limit the fracture surface area. This was implemented by assigning a value of 1 to the number of fractures present in the numerical transport model. Other transport parameters used in the baseline include fixed values of 0.001 for fracture porosity, and 0.08 for tortuosity. Longitudinal dispersion used a single value (100 m) equal to the median used in the 1992 WIPP PA calculations. The spatial distribution of transmissivity of the Culebra was explicitly implemented in the baseline model by sampling from the currently available transmissivity fields (LaVenue and RamaRao, 1992).

## **2.10.3 Chemical Retardation**

### **2.10.3.1 CONCEPTUAL MODEL FOR WATER-ROCK INTERACTION IN THE CULEBRA**

The Non-Salado baseline model assumed that advective transport occurs in the fractures with diffusion into the matrix. In terms of the accessibility of mineral assemblages for chemical interactions, it was assumed that no clay "linings" are present, and that minerals present in the bulk rock are available for chemical interactions.

### **2.10.3.2 DISTRIBUTION COEFFICIENTS FOR CHEMICAL RETARDATION OF ACTINIDES IN THE CULEBRA**

Distribution coefficients ( $K_d$ ) in the baseline model were assumed to be zero.

### **2.10.3.3 CHEMICAL RETARDATION OF ACTINIDES DUE TO MIXING OF DISPOSAL ROOM BRINES WITH CULEBRA BRINES**

In the SPM-2 baseline model, mixing effects were assumed to be negligible.

#### 2.10.3.4 COLLOID-FACILITATED RADIONUCLIDE TRANSPORT IN THE CULEBRA

For the Culebra, three subtypes of colloids were considered in the baseline model. “Soft-sphere” carrier colloids (chiefly humic materials) and actinide-intrinsic colloids are small enough to undergo matrix diffusion. Microbes (sterically stabilized carrier colloids) are too large to undergo matrix diffusion, and will be transported by fracture advection. Based on preliminary results of ongoing experimental activities, it is likely that actinide-intrinsic colloids will not be important in actinide transport, but they could not be eliminated from the baseline. Free water diffusion constants for the actinide intrinsic colloids and humic materials were estimated based on the sizes of those particles relative to the sizes of dissolved solutes. The largest colloidal particle that could undergo matrix diffusion was limited to about 0.5  $\mu\text{m}$ , which is the approximate mean size of pore throats in the Culebra (0.63  $\mu\text{m}$ ) (see Section 3.3.3 in *Systems Prioritization Method – Iteration 2 Baseline Position Paper: Non-Salado Flow and Transport*). Assuming that the sizes of dissolved species is on the order of 1  $\text{\AA}$ , the free water diffusion constants for macromolecular colloidal particles with mean diameters of about 0.5  $\mu\text{m}$  were estimated by reducing the free water diffusion constant of the dissolved species by a factor of 5,000 (i.e.,  $0.5 \times 10^{-6}$  meter  $\div 1 \times 10^{-10}$  meter). A macromolecular particle size of 0.5  $\mu\text{m}$  is large for a macromolecular colloidal particle, but not unusual for actinide intrinsic colloids (see Section 3.3.3 in *Systems Prioritization Method – Iteration 2 Baseline Position Paper: Non-Salado Flow and Transport*). Again, based on preliminary results of current experimental work, it was anticipated that the reduction factor value of 5,000 would be decreased substantially.

#### 2.10.4 Intrusion Holes and the Castile Brine Reservoir

The Non-Salado baseline model used a depleting reservoir model similar to that developed by Reeves et al. (1991). Each reservoir had a size and storativity representative of the reservoir hit by the WIPP-12 borehole. There were four reservoirs that conceptually covered an equal portion of the fraction of the repository footprint assumed to overlie brine reservoirs. This fraction, the “brine reservoir area fraction,” was as sampled in the 1992 WIPP PA. No credit was taken for reservoir depletion by boreholes that could theoretically hit reservoirs beyond the boundaries of the repository. The baseline model sampled on the positions of the intrusion holes, and release points in the Culebra were determined accordingly.

#### 2.10.5 Climate Change

For the Non-Salado baseline model, climate change was treated in a manner similar to that used in the 1992 WIPP PA (Swift, 1993; Swift et al., 1994). A simple conservative steady-state calculation was made with heads raised to the land surface along the northern boundary while the head remained fixed at its present steady-state value along the southern boundary.

## **2.10.6 Castile Brine Reservoirs**

For the baseline model, the properties of a Castile brine reservoir potentially present beneath the WIPP repository were assumed to be those of the WIPP-12 reservoir. For purposes of numerical modeling, reservoir properties were those in Table 2-5 (from Reeves et al., 1991, Table 2-1). The model implementation was somewhat different than that used in Reeves et al., however, in the interest of simplicity. First, a one-zone approach was used to assign transmissivities within the reservoir, rather than the two-zone (inner and outer) approach used by Reeves et al. Second, the reservoir was assumed to be completely isolated from the Castile. In the implementation of Reeves et al. (1991), undisturbed Castile anhydrites were assigned a small, but non-zero, permeability.

## **2.11 RH-TRU**

The SPM-2 baseline modeled the inventory, including RH-TRU, that is defined in the *Waste Isolation Pilot Plant Transuranic Waste Baseline Inventory Report* (U.S. DOE, 1995a).

## **2.12 EAs**

EAs were not modeled in the SPM-2 baseline.

Table 2-5. Modeling Parameters for a Hypothetical Brine Reservoir in the Castile Formation (Reeves et al., 1991, Table 2.1)

Parameter	Symbol	High End	Base Case	Low End	Range	Units
Initial pressure	$P_{bo}$	117.4	12.7	10.0*	7.0 - 17.4	MPa
Effective thickness	$\Delta z_b$	†	7.0	†	7.0 - 24.0	m
Transmissivity of inner ring	$T_{bi}$	$7 \times 10^{-2}$	$7 \times 10^{-4}$	$7 \times 10^{-6}$	$7 \times 10^{-6}$ to $7 \times 10^{-2}$	$m^2$
Distance to inner/outer zone contact	$r_{bi}$	900	300	100	100-900	m
Transmissivity of outer ring	$T_{bo}$	$7 \times 10^{-4}$	$7 \times 10^{-6}$	$7 \times 10^{-8}$	$7 \times 10^{-8}$ to $7 \times 10^{-4}$	$m^2/s$
Distance to outer ring/intact Castile contact	$r_{bo}$	8,600	2,000	100‡	30\8,600	m
Transmissivity of intact Castile	$T_c$	$1 \times 10^{-9}$	$1 \times 10^{-11}$	$1 \times 10^{-13}$	$7 \times 10^{-13}$ to $7 \times 10^{-9}$	$m^2/s$
<b>Porosity</b>						
Brine reservoir	$\phi_b$	0.01	0.005	0.001	0.001 - 0.01	
Intact Castile	$\phi_c$	NA	0.005	NA	constant	
<b>Bulk compressibility of medium</b>						
Brine reservoir	$C_{bR}$	$1 \times 10^{-8}$	$1 \times 10^{-9}$	$1 \times 10^{-10}$	$7 \times 10^{-10}$ to $7 \times 10^{-8}$	1/Pa
Intact Castile	$C_{bc}$	$4.8 \times 10^{-10}$	$4.8 \times 10^{-11}$	$4.8 \times 10^{-12}$	$7 \times 10^{-12}$ to $7 \times 10^{-10}$	1/Pa
Fluid density	$\rho$	NA	1,240	NA	constant	$kg/m^3$
Fluid viscosity	$\mu$	NA	$1.6 \times 10^{-3}$	NA	constant	Pa
Fluid compressibility	$c_w$	NA	$3 \times 10^{-10}$	NA	constant	1/Pa

\* A minimum pressure of 9.7 MPa is required to provide a driving force to cause flow from the brine reservoir depth to the Culebra.

† Sensitivity to effective thickness is included in the transmissivity of values.

‡ The minimum radial distance  $r_{bo}$ , the contact between the more permeable reservoir and the surrounding intact rock, cannot be less than  $r_{bi}$ .

### **3. ACTIVITIES, ACTIVITY OUTCOMES, OUTCOME PROBABILITIES, AND INPUT PARAMETERS FOR SPM-2 ANALYSIS**

#### **3.1 Introduction**

This section summarizes the SPM-2 activities, predictions of the potential outcomes of each activity (hereafter referred to as "potential outcomes"), probabilities of each outcome, and the parameter distributions<sup>2</sup> used to model each activity outcome. A complete list of the activities considered in the SPM-2 decision analysis appears in Table 3-1. Each activity was assigned an SPM-2 identifier.

The summary is organized by the following topics: Actinide Source Term, Gas Generation, Disposal Room, Seals and Rock Mechanics, Salado, Non-Salado, Engineered Alternatives (EAs), and Waste Acceptance Criteria (WAC). A short description of each activity is provided, followed by a discussion of the activity's potential outcomes and its outcome probabilities. The parameters to be used for SPM-2 calculations to determine the impact of the activity on the complementary cumulative distribution functions (CCDFs) and the RCRA concentrations are then summarized.

The elicitation process used to define these activities and their outcomes is described in Section 3.5 of Volume I of this report. Activities defined in the elicitation process were not actually evaluated in the SPM-2 analysis if:

- 1) the activity outcome would have a negligible effect on repository performance,
- 2) the activity was eliminated upon management review as a nonviable option, or
- 3) the activity could not be implemented in the codes at this time.

Some activities eliminated for reason (3) were dealt with in side investigations as described in Volume I, Section 3.4.2. The primary activity eliminated from SPM-2 consideration due to time constraints (i.e., (3) above) was the Gas Generation activity (GG I), which would have been represented as the RPM within BRAGFLO. The RPM was incorporated into BRAGFLO, but verification of its utility for SPM-2 calculations could not be completed, and it is being handled as a side investigation. Three other technical areas also had elicited activities that were not analyzed. These areas (with the number of elicited activities that were not analyzed) are: Disposal Room (2), Seals (4), and Non-Salado (5).

#### **3.2 Actinide Source Term**

The following two activities for the Actinide Source Term, AST 1.1 and AST 1.2, are mutually exclusive. That is, DOE/CAO can select one or the other, but not both.

---

<sup>2</sup> The elicited parameters distributions predicted for each outcome were in many cases defined by probability density functions (PDFs). In the cases where the results of outcomes are so defined, the probabilities contained within these PDFs are not to be confused with the probabilities given for the outcome that results in the PDF.

Table 3-1. SPM-2 Final Activity List

Activity	SPM-2 Indicator	Number of Outcomes	Probabilities of Outcomes	Parameters Influenced by Success or Failure of Outcomes		SPM-2 Modeling Codes
				Activity Constraints	Activity Constraints	
<b>Actinide Source Term</b>						
Dissolved Actinide Solubilities for Oxidation States +III - +VI	AST 1.1	2	0, 1	Solubility in (+III), (+IV), (+V), (+VI)	AST 1.1 and 1.2 are mutually exclusive	PANEL
Dissolved Actinide Solubilities for Oxidation States +III - +V	AST 1.2	2	0, 1	Solubility in (+III), (+IV), (+V)	AST 1.1 and 1.2 are mutually exclusive	PANEL
<b>Gas Generation<sup>a</sup></b>						
RPM and Supporting Data	GG 1	2	0.33, 0.67	Model and data	NA	BRAGFLO
<b>Disposal Room</b>						
Decomposed Waste Properties	DR 1	2	0, 1	Waste strength, k	None	CUTTINGS/ SPALLINGS
Blowout Releases	DR 2	10	See Table 3-4	Release reduction factor	None	CUTTINGS/ SPALLINGS
Non-Blowout Releases	DR 3	6	See Table 3-6	Release reduction factor	None	CUTTINGS/ SPALLINGS
<b>Seals and Rock Mechanics</b>						
Rock Mechanics	RM 1	2	0.05, 0.95	Model and Data	Must be done with SL 4	SANCHO
Studies of Short- and Long-Term Components	SL 4	2	0.05, 0.95	Seals Permeability	Must be done with RM 1	BRAGFLO

<sup>a</sup>This activity was elicited, but not modeled for the SPM-2 analysis.

Table 3-1. SPM-2 Final Activity List (Continued)

Activity	SPM-2 Indicator	Number of Outcomes	Parameters Influenced by Success or Failure of Outcomes			SPM-2 Modeling Codes
			Probabilities of Outcomes	Activity Constraints	Activity Constraints	
<b>Salado</b>						
Lab/Field Properties of Anhydrite	SAL 1	2	0.15, 0.85	None	$k, n, S_{ge}, S_{br}, P_{th}, C_{min}$	BRAGFLO
Halite Far-Field Pore Pressure	SAL 2	2	0.20, 0.80	None	Field Pore Pressure	BRAGFLO
Halite Lab/Field Properties	SAL 3	2	0.25, 0.75	None	$P_{th}, k, n, S_{b6}, S_{ge}$	BRAGFLO
Fingering/Channeling Studies - Existing Data	SAL 4.1	2	0.20, 0.80	None	$C_{min}$	Post-Processing
Fingering/Channeling Studies - New Data	SAL 4.2	2	0.05, 0.95	Requires SAL 1	$C_{min}$	Post-Processing
Anhydrite Fracture Studies	SAL 4.3	2	0.30, 0.70	Requires SAL 1	$C_{min}$	Post-Processing
<b>Non-Salado</b>						
Dewey Lake - Paper and Low-Effort Field Studies	NS 1	2	0, 1	None	Minimum $K_{ds}$	Scaled SECO-TP
Culebra Fracture/Matrix/Flow - Lab	NS 2	4	See Table 3-21	None	Diffusion surface area	Scaled SECO-TP
Culebra Fracture/Matrix/Flow - Field	NS 3	4	See Table 3-21	None	Diffusion surface area	Scaled SECO-TP
Multi-Well Tracer Test	NS 4	4	See Table 3-21	None	Diffusion surface area	Scaled SECO-TP
Sorbing Tracer Test	NS 5	2	0.05, 0.95	None	$K_{ds}$ in Culebra	Scaled SECO-TP

Table 3-1. SPM-2 Final Activity List (Continued)

Activity	SPM-2 Indicator	Number of Outcomes	Probabilities of Outcomes	Parameters Influenced by Success or Failure of Outcomes		Activity Constraints	SPM-2 Modeling Codes
<b>Non-Salado (Continued)</b>							
Chemical Retardation for Th, Np, Pu, U, and Am Concentrations and Transport of Colloid Carriers: HMWOC and Microbes	NS 7	2		K <sub>as</sub> in Culebra	Requires NS 6		Scaled SECO-TP
Enhanced Colloid Experimental Program	NS 8.1	2	0, 1	Concentrations and retardation mechanisms	None		Scaled SECO-TP
	NS 8.2	2	0, 1	Concentrations and retardation mechanisms	None		Scaled SECO-TP
<b>EAs</b>							
Passive Markers	EA 3	1	1	Drilling Rates	None		BRAGFLO and PANEL
Backfill with pH Buffer	EA 1	1	1	Room Porosity, Actinide Solubilities	None		BRAGFLO and PANEL
Backfill with pH Buffer and Waste Form Modification	EA 2	1	1	Room Porosity, Waste Strength, Solubilities	None		BRAGFLO and PANEL
<b>WAC</b>							
Non-Corroding Waste Containers	WAC 1	1	1	Reduce Gas Potential	None		BRAGFLO
Elimination of Humic-Containing Waste Drums (Not Funded)	WAC 2	1	1	No humic colloids	None		Scaled SECO-TP

### 3.2.1 AST 1.1 – Dissolved Actinide Solubilities for Oxidation States +III – +VI

#### 3.2.1.1 SHORT DESCRIPTION

Develop a model to determine the solubilities of oxidation states +III, +IV, +V, and +VI for the actinides Am, Np, Pu, Th, and U as a function of brine composition, pH, and other independent variables. This effort includes experiments, a literature search, data reduction, and translation of data into a form usable in future compliance assessment codes.

#### 3.2.1.2 OUTCOMES

Two potential outcomes were elicited for Activity AST 1.1: success and failure. The probability of success is 1; the probability of failure is 0. For the successful outcome, the parameters to be used to model the actinide source term for Activity AST 1.1 are those modifications to the SPM-2 baseline described below. For the outcome of failure, the parameters to be used are those in the unmodified SPM-2 baseline.

#### 3.2.1.3 PARAMETERS

For the successful outcome of Activity AST 1.1, the probability distributions for the concentrations of actinides with oxidation states +III, +IV, +V, and +VI for SPM-2 analysis are shown in Table 3-2. The mean is the actual log value that was used in the SPM-2 analysis based on a maximum concentration of 10 M/l. In fact, the maximum concentration used to calculate this mean should have been 1 M in all cases, shifting the mean down. Correcting this error, which was made during the preparation of the input would result in improved performance, but in the end has no impact on the Probability of Demonstrating Compliance (PDC) for this activity.

Table 3-2. Probability Distributions for Actinide Concentration for the oxidation states +III, +IV, +V, and +VI for SPM-2 Analysis for Activity AST 1.1

Oxidation State	$x_0$ (M/l)	$x_{25}$ (M/l)	$x_{75}$ (M/l)	$x_{95}$ (M/l)	Mean (log $(K_d)$ )
+III	$10^{-10}$	$10^{-8}$	$10^{-5}$	$10^{-2}$	-6.225
+IV	$10^{-10}$	$10^{-8}$	$10^{-6}$	$10^{-2}$	-6.575
+V	$10^{-10}$	$10^{-7}$	$10^{-3}$	$10^{-1}$	-5.025
+VI	$10^{-10}$	$10^{-7}$	$10^{-1}$	1	-4.2

Note:  $x_q$  satisfies  $P(X \leq x_q) = q$  where X is the actinide concentration.

For the successful outcome of AST 1.1, the oxidation states are to be partitioned as follows:

Am(+III) - 100%

Am(+V) - 0%

Np(+IV) and Np(+V) - Randomly partitioned between the two states using a uniform [0, 1] random variable

Np(+VI) - 0%

Th(+IV) - 100%

U(+VI) and Pu(+VI) - Uniformly distributed between 0 and 20%

Remaining U and Pu inventory - Randomly partitioned between the respective remaining oxidation states after sampling and removing U(+VI) and Pu(+VI)

### **3.2.2 AST 1.2 – Dissolved Actinide Solubilities for Oxidation States +III – +V**

Activity AST 1.2 is similar to AST 1.1 with a reduced scope. AST 1.2 differs from AST 1.1 in that it does not investigate solubilities for actinides in oxidation state +VI. Assumptions regarding oxidation state +VI for SPM-2 analysis for Activity AST 1.2 are to be based on information on partitioning U and Pu into oxidation state +VI obtained from the Los Alamos Source Term Test Program.

#### **3.2.2.1 SHORT DESCRIPTION**

Develop an expanded model for determining the solubilities of oxidation states +III, +IV, and +V for the actinides Am, Np, Pu, Th, and U as a function of brine composition, pH, and other independent variables. This effort includes experiments, a literature search, data reduction, and translation of data into a form usable in future compliance assessment codes.

#### **3.2.2.2 OUTCOMES**

Two potential outcomes were elicited for Activity AST 1.2: success and failure. The probability of success is 1; the probability of failure is 0. For the successful outcome, the parameters used to model the actinide source term for Activity AST 1.2 were those modifications to the SPM-2 baseline described below. For the outcome of failure, the parameters were those in the unmodified SPM-2 baseline.

#### **3.2.2.3 PARAMETERS**

For the successful outcome of Activity AST 1.2, the probability distribution for actinide concentrations for the oxidation states +III, +IV, and +V used in the SPM-2 analysis appear in Table 3-3.

Table 3-3. Probability Distribution for Actinide Concentrations for the Oxidation States +III, +IV, and +V for SPM-2 Analysis for Activity AST 1.1

Oxidation State	$x_0$ (M/l)	$x_{.25}$ (M/l)	$x_{.75}$ (M/l)	$x_{.95}$ (M/l)	Mean (log (concentration)) <sup>a</sup>
+III	$10^{-10}$	$10^{-8}$	$10^{-5}$	$10^{-2}$	-6.225
+IV	$10^{-10}$	$10^{-8}$	$10^{-6}$	$10^{-2}$	-6.575
+V	$10^{-10}$	$10^{-7}$	$10^{-3}$	$10^{-1}$	-5.025
+VI	1	1	1	1	0

<sup>a</sup> The mean is the actual log value used in the SPM-2 analysis based on a maximum concentration of 10 M/l.

Note:  $x_q$  satisfies  $P(X \leq x_q) = q$  where X is the actinide concentration.

For the successful outcome of AST 1.2, the oxidation states are to be partitioned as follows:

Am(+III) – 100%

Am(+V) – 0%

Np(+IV) and Np(+V) – Randomly partitioned between the two states using a uniform [0, 1] random variable

Np(+VI) – 0%

Th(+IV) – 100%

U(+VI) and Pu(+VI) – Uniformly distributed between 0 and 20%

Remaining U and Pu inventory – Randomly partitioned between the respective remaining oxidation states after sampling and removing U(+VI) and Pu(+VI)

### 3.3 Gas Generation

The following information describes the Gas Generation activity and the predicted potential outcomes. The time required for necessary code modifications and verification, however, prevented the inclusion of this activity in the SPM-2 analysis. Gas generation is being evaluated as a side investigation.

#### 3.3.1 GG 1 – RPM and Supporting Data

##### 3.3.1.1 SHORT DESCRIPTION

Replace the average-stoichiometric model with the RPM and conduct experiments to quantify parameters in the RPM. These parameters consist of rates of production for gas and water,

passivation amount, and rates for radiolysis. The RPM has been developed, but requires completion. The model has many parameters, some with values that cannot be supported by existing experimental or field data.

### 3.3.1.2 OUTCOMES

Two potential outcomes were elicited for Activity GG 1: success and failure. The probability of success is 67%; the probability of failure is 33%. For the successful outcome, the RPM will replace the average-stoichiometric model used in the baseline. For the outcome of failure, the average-stoichiometric model will not be replaced with the RPM, and the baseline will not be modified.

### 3.3.1.3 PARAMETERS

Unless explicitly changed in the elicitation record or by memorandum, the values for the parameters in the RPM are the same as those in the average-stoichiometric model. However, the RPM requires data for more parameters than the average-stoichiometric model. A portion of the complete set of required parameters appears in Brush et al., 1994, and P. Drez, "Waste Material Parameter and Radionuclide Inventories for SPM-2 Calculations Derived from Draft WTWBIR Rev. 1 and IDB Rev. 10 Databases," Drez Environmental Associates memorandum to File, January 3, 1995 (see Appendix).

Some input parameters are material inventory. These are provided in the *Waste Isolation Pilot Plant Transuranic Waste Baseline Inventory Report* (U.S. DOE, 1995a). There are a series of gas generation experiments underway, the results of which will impact specific parameter input for the RPM.

## 3.4 Disposal Room

Wicking, mobile brine saturation, and two-phase flow properties of the waste areas were discussed during the elicitation meetings as possible Disposal Room activities. All of these will be investigated in side investigations, and were not part of the SPM-2 baseline or activity sets.

### 3.4.1 DR 1 – Decomposed Waste Properties

The impact of this activity on brine inflow was not performed with the BRAGFLO code. Past PA calculations show little impact of these properties on Disposal Room modeling. However, the effect of increased waste strength was evaluated as part of the disturbed spillings releases in the context of an EA (see EA 2).

### 3.4.1.1 SHORT DESCRIPTION

Perform experiments to investigate the mechanical and physical properties of decomposed waste, and include the results in the Disposal Room model.

### 3.4.1.2 OUTCOMES

There were two potential outcomes elicited for Activity DR 1: success and failure. The probability of success is 1; the probability of failure is 0. This activity affects the porosity surface and, through the porosity surface, the permeability of the material in the waste room. For the successful outcome, the parameters to be used to model Activity DR 1 are those in the SPM-2 baseline, with the exception the porosity surface value, which is to be modified as described below. For the outcome of failure, the parameters to be used are those in the unmodified SPM-2 baseline.

### 3.4.1.3 PARAMETERS

For the successful outcome of Activity DR 1, the porosity surface in the baseline is to be modified as follows. To account for the effect of waste decomposition on disposal room porosity, the porosity surface value to be used is the baseline value reduced according to the following:

$$\phi' = \phi - 0.12 \left[ \frac{\phi_{\max} - \phi}{\phi_{\max} - \phi_{\min}} \right]$$

where  $\phi'$  is the porosity including waste decomposition effects,

$\phi$  is the baseline porosity from the porosity surface,

$\phi_{\max}$  is the maximum baseline porosity (porosity at emplacement), and

$\phi_{\min}$  is the minimum porosity associated with the baseline surface (fully consolidated value).

## 3.4.2 DR 2 – Blowout Releases

### 3.4.2.1 SHORT DESCRIPTION

This activity is a compilation of studies to calculate the effects of blowout releases resulting from human intrusion.

- Upgrade the modeling of flow in the compacted waste during a blowout from one-dimensional axisymmetric to 2-D axisymmetric to provide more accurate results and better predict the rate of gas flow.
- Improve the modeling of transport in the borehole by allowing for variation in the annular area between the borehole and the drill pipe (assume a two-stage annular area in the model).
- Introduce capability to model both isothermal and adiabatic gas flow during a blowout.
- Experimentally determine the effective surface area over which gas is assumed to flow from the waste into the borehole.

### 3.4.2.2 OUTCOMES

Twenty discrete outcomes for the release reduction factor were elicited for Activity DR 2, as shown in Figure 3-1.

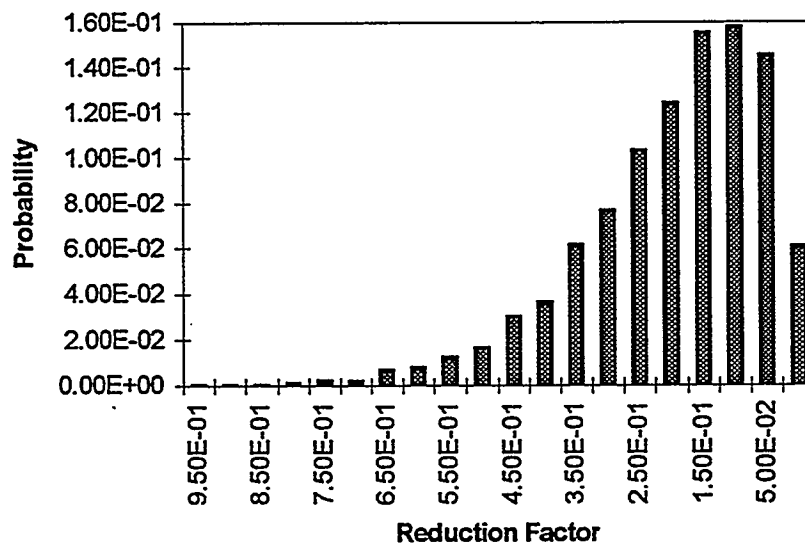


Figure 3-1. Probabilities for blowout releases for Activity DR 2.

The probabilities of the elicited outcomes (reduction factors) that correspond to Figure 3-1 are listed in Table 3-4. For the SPM-2 analysis, these 20 outcomes were grouped more coarsely into 10 outcomes, as shown in Table 3-5.

Table 3-4. DR 2 Elicited Outcomes and Their Probabilities

Reduction Factor	Probability
9.50E-01	4.69E-04
9.00E-01	2.67E-04
8.50E-01	4.61E-04
8.00E-01	8.67E-04
7.50E-01	2.43E-03
7.00E-01	1.94E-03
6.50E-01	6.60E-03
6.00E-01	7.85E-03
5.50E-01	1.25E-02
5.00E-01	1.64E-02
4.50E-01	3.02E-02
4.00E-01	3.65E-02
3.50E-01	6.15E-02
3.00E-01	7.66E-02
2.50E-01	1.03E-01
2.00E-01	1.24E-01
1.50E-01	1.55E-01
1.00E-01	1.58E-01
5.00E-02	1.45E-01
4.50E-03	6.04E-02

Table 3-5. Reduction Factors and Their Probabilities Used in the SPM-2 Analysis for the Successful Outcome of Activity DR 2

Reduction Factor	Probability
1	0
0.95	6.02e-4
0.85	1.03e-3
0.75	3.83e-3
0.65	1.15e-2
0.55	2.46e-2
0.45	5.66e-2
0.35	1.18e-1
0.25	2.03e-1
0.15	2.96e-1
0.05	2.84e-1

### 3.4.2.3 PARAMETERS

For each outcome of Activity DR 2, the blowout values to be used are those calculated from the SPM-2 baseline blowout model for releases multiplied by an associated reduction factor. The probability density function (PDF) for blowout releases and a list of the reduction factors appear in Figure 3-1.

### 3.4.3 DR 3 – Non-Blowout Releases

#### 3.4.3.1 SHORT DESCRIPTION

Activity DR 3 consists of a compilation of studies to calculate the effects of non-blowout releases resulting from a human intrusion.

- Estimate the volume of waste eroded into the mud as a percentage of the flow rate of the drilling fluid
- Incorporate the effect of waste strength into the model for waste entrainment in mud.

#### 3.4.3.2 OUTCOMES

A continuum of outcomes was elicited for Activity DR 3. Each outcome was associated with a release reduction factor for non-blowout releases. The PDF elicited for the release reduction factor is a loguniform distribution ranging from -2.3 to -0.3.

#### 3.4.3.3 PARAMETERS

For each outcome, the values for the non-blowout releases used in the analysis are those calculated from the SPM-2 baseline non-blowout model multiplied by an associated reduction factor. Six outcomes with the probabilities shown in Table 3-6 were used to approximate this continuum of outcomes.

## 3.5 Seals and Rock Mechanics

### 3.5.1 RM 1 – Rock Mechanics

Activity RM 1 must be performed in conjunction with Activity SL 4. RM 1 provides the basic Rock Mechanics models used by the Seals program in SL 4. By itself (apart from SL 4), RM 1 makes no contribution to the PDC for the WIPP disposal system.

**Table 3-6. Probability Distribution for the Reduction Release Factors for SPM-2 Analysis for Activity DR 3**

$R_f$	$P(x)$
1	0
0.32	0.20
0.13	0.20
0.05	0.20
0.02	0.20
0.008	0.20

### 3.5.1.1 SHORT DESCRIPTION

Replace MD model with the Multimechanism Deformation Coupled Fracture (MDCF) model and perform experiments to determine uncertainty distributions for input parameters to the MDCF model.

### 3.5.1.2 OUTCOMES

There were two potential outcomes elicited for Activity RM 1: success and failure. The probability of success is 0.95; the probability of failure is 0.05.

### 3.5.1.3 PARAMETERS

Activity RM 1 does not provide parameters for the SPM-2 models except to the extent that it provides the basis for models used in Activity SL 4.

## 3.5.2 SL 4 – Studies of Short and Long-Term Components

Activity SL 4 must be performed in conjunction with Activity RM 1.

### 3.5.2.1 SHORT DESCRIPTION

- Study short-term materials. Model short-term components. Design systems model. Perform intermediate tests. Perform field tests.
- Model long-term components. Design systems model. Perform intermediate tests. Perform compaction tests.

### 3.5.2.2 OUTCOMES

There were two potential outcomes elicited for Activity SL 4: success and failure. The probability of success is 0.9025; the probability of failure is 0.0975. For the successful outcome of the combined Activities RM 1 and SL 4, the parameters to be used for SPM-2 analysis are those discussed below.

### 3.5.2.3 PARAMETERS

Values of long-term component seal permeability to be used for Activities SL 4 + RM 1, short-term and long-term component studies, appear in Table 3-7.

Table 3-7. Short-Term and Long-Term Component Seal Permeability for Activities SL 4 + RM 1, Short-Term and Long-Term Component Studies

$X_{.00}$ (Minimum)	$X_{.01}$	$X_{.50}$	$X_{.99}$	$X_{1.00}$
$10^{-20}$	$10^{-19}$	$10^{-17}$	$10^{-16}$	$10^{-14}$

$$\text{Mean (log)} = -17.3$$

Note:  $x_q$  satisfies  $P(X \leq x_q) = q$  where  $X$  is the long-term seal permeability.

## 3.6 Salado

### 3.6.1 SAL 1 – Lab/Field Properties of Anhydrite

#### 3.6.1.1 SHORT DESCRIPTION

Activity SAL 1 is a combination of the following experimentation and modeling activities, aimed at obtaining better understanding of the properties of anhydrite:

- Lab testing on capillary and relative permeability of anhydrite as a function of saturation and hydrostatic stress.
- Pressure dependent permeability testing of anhydrite. Lab tests.
- Compilation of petrographic analyses for anhydrite.

- Analyze data from core-damage experiments of anhydrite.
- Lab tests on anhydrite porosity for stressed samples.
- Curve-fit modeling of two-phase flow in anhydrite.
- 2-D/3-D flow modeling for anhydrite.
- General fracture characterization studies for anhydrite.

### 3.6.1.2 OUTCOMES

There were two potential outcomes elicited for Activity SAL 1: success and failure. The probability of success is 85%; the probability of failure is 15%. For the successful outcome, the parameters to be used to model the anhydrite properties for Activity SAL 1 are those modifications to the SPM-2 baseline described below. For the outcome of failure, the parameters to be used are those in the unmodified SPM-2 baseline. Note: 2-D/3-D flow modeling for anhydrite was originally elicited as an activity. Subsequent management review identified this as a side investigation to be done to confirm the final SPM-2 baseline technical position, described in Section 2. The expected outcome for this activity, that is, the values for the lower limit of a brine mass storage parameter,  $C_{min}$ , are thus to be included in the successful outcome for SAL 1.

Success and failure were sampled once for all parameters. No attempt was made to otherwise induce correlations among the various parameter values.

### 3.6.1.3 PARAMETERS

For the successful outcome of Activity SAL 1, the values for the anhydrite properties to be used in the SPM-2 analysis are those below. The properties affected are anhydrite porosity, anhydrite permeability, critical gas saturation in anhydrite, critical brine saturation in anhydrite, the threshold pressure constant "M," and the brine mass storage parameter.

#### 3.6.1.3.1 Anhydrite Porosity

The PDF for the parameter distribution for anhydrite porosity for the successful outcome of Activity SAL 1 appears in Table 3-8.

Table 3-8. Parameter Distribution for Anhydrite Porosity for Activity SAL 1

Anhydrite Porosity Range (%)	Interval Probability
0.1 to 0.3	0.025
0.3 to 0.5	0.100
0.5 to 2.0	0.425
2.0 to 4.5	0.400
4.5 to 8.0	0.050
Mean = 0.0219	

### 3.6.1.3.2 Anhydrite Permeability

The parameter distribution for anhydrite permeability for the successful outcome of Activity SAL 1 appears in Table 3-9.

Table 3-9. Parameters for Anhydrite Permeability for Activity SAL 1

Anhydrite Laboratory Permeability Range Uniform Log (m <sup>2</sup> )	Interval Probability
10 <sup>-21</sup> to 10 <sup>-20</sup>	0.100
10 <sup>-20</sup> to 10 <sup>-19</sup>	0.320
10 <sup>-19</sup> to 10 <sup>-18</sup>	0.320
10 <sup>-18</sup> to 10 <sup>-17</sup>	0.170
10 <sup>-17</sup> to 10 <sup>-16</sup>	0.064
10 <sup>-16</sup> to 10 <sup>-15</sup>	0.026
Mean (log) = -18.6	

### 3.6.1.3.3 Critical Gas Saturation in Anhydrite

The parameter distribution for critical gas saturation in anhydrite for the successful outcome of Activity SAL 1 appears in Table 3-10.

Table 3-10. Parameter Distribution for Critical Gas Saturation in Anhydrite for Activity SAL 1

$S_{gc}(\%)$	Interval Probability
0.00 to 0.08	0.20
0.08 to 0.16	0.25
0.16 to 0.20	0.30
0.20 to 0.24	0.10
0.24 to 0.32	0.10
0.32 to 0.40	0.05

Mean = 0.16

3.6.1.3.4 Critical Brine Saturation in Anhydrite

The parameter distribution for critical brine saturation in anhydrite for the successful outcome of Activity SAL 1 appears in Table 3-11.

Table 3-11. Parameter Distribution for Critical Brine Saturation in Anhydrite for Activity SAL 1

$S_{br}(\%)$	Interval Probability
0.00 to 0.05	0.05
0.05 to 0.10	0.23
0.10 to 0.20	0.23
0.20 to 0.30	0.23
0.30 to 0.40	0.20
0.40 to 0.50	0.05
0.50 to 0.60	0.01

Mean = 0.209

### 3.6.1.3.5 Threshold pressure constant "M"

The parameter distribution for calculating threshold pressure (M) for the successful outcome of Activity SAL 1 appears in Table 3-12.

Table 3-12. Parameter M for Calculating Threshold Pressure for Activity SAL 1

Uniform Log (M)	Interval Probability
$5.6 \times 10^{-10}$ to $5.6 \times 10^{-9}$	0.4
$5.6 \times 10^{-9}$ to $5.6 \times 10^{-8}$	0.3
$5.6 \times 10^{-8}$ to $5.6 \times 10^{-7}$	0.2
$5.6 \times 10^{-7}$ to $5.6 \times 10^{-6}$	0.1

Mean (log) = -7.75

### 3.6.1.3.6 Brine Mass Storage Parameter

The brine mass storage parameter for the successful outcome of Activity SAL 1 to be used for SPM-2 analysis depends on the calculated results of BRAGFLO for repository pressure relative to lithostatic pressure. If the result of the BRAGFLO calculations for room pressure are below that required to initiate fracturing in the anhydrite interbed (i.e., the interbed remains unaltered), the brine mass storage parameter values for the successful outcome of Activity SAL 1 are those appearing in Table 3-13. If the result of the BRAGFLO is above that required to initiate fracturing in the anhydrite interbed (i.e., the interbed is altered), the brine mass storage parameter values for the successful outcome of Activity SAL 1 are those appearing in Table 3-14.

Table 3-13. Probability Distribution for  $C_{min}$  Values for Activity SAL 1, Without Alterations to the Interbed

$C_{min}$	Interval Probability
$1 \times 10^{-3}$ to $3 \times 10^{-3}$	0.38
$3 \times 10^{-3}$ to $1 \times 10^{-2}$	0.60
$1 \times 10^{-2}$ to $5 \times 10^{-2}$	0.02

Mean = 0.00526

Table 3-14. Probability Distribution for  $C_{min}$  Values for Activity SAL 1, With Alterations to the Interbed

$C_{min}$	Interval Probability
$1 \times 10^{-3}$ to $3 \times 10^{-3}$	0.83
$3 \times 10^{-3}$ to $1 \times 10^{-2}$	0.17

Mean = 0.00277

### 3.6.2 SAL 2 – Halite Far-Field Pore Pressure

#### 3.6.2.1 SHORT DESCRIPTION

Activity SAL 2 is a combination of the following experimental activities:

- Far-field halite testing.
- Lab tests on the intrinsic permeability of halite.

#### 3.6.2.2 OUTCOMES

Two potential outcomes were elicited for Activity SAL 2: success and failure. The probability of success is 0.80; the probability of failure is 0.20. For the successful outcome, the parameters to be used to model the halite far-field pore pressure for Activity SAL 2 are those modifications to the SPM-2 baseline described below. For the outcome of failure, the parameters to be used are those in the unmodified SPM-2 baseline.

#### 3.6.2.3 PARAMETERS

For the successful outcome of Activity SAL 2, the values for the anhydrite properties to be used for SPM-2 analysis are those below.

##### 3.6.2.3.1 Far-Field Pore Pressure in Halite

The distribution for far-field pore pressure values for modeling the successful outcome of Activity SAL 2 for SPM-2 analysis appears in Table 3-15.

Table 3-15. Distribution of Far-Field Pore Pressure Values for Activity SAL 2

$k_h$ (MPa)	Interval Probability
7 to 9	0.03
9 to 11	0.06
11 to 13	0.30
13 to 15	0.61
Mean = 13	

### 3.6.2.3.2 Far-Field Halite Permeability

The far-field halite permeability values for modeling the successful outcome of Activity SAL 2 for SPM-2 analysis appear in Table 3-16.

Table 3-16. Distribution of Far-Field Halite Permeability Values for Activity SAL 2

Uniform Log ( $m^2$ )	Probability
$10^{-21}$	0.5
$10^{-21}$ to $10^{-20}$	0.5
Mean (log) = -20.488	

## 3.6.3 SAL 3 – Halite Lab/Field Properties

### 3.6.3.1 SHORT DESCRIPTION

Activity SAL 3 is a combination of the following experimental and modeling activities:

- Lab tests on the intrinsic permeability of halite.
- Lab tests on halite porosity for stressed samples.
- Curve fit modeling of results from halite lab tests, gas and brine under different stresses, and two-phase flow.

### 3.6.3.2 OUTCOMES

Two potential outcomes were elicited for Activity SAL 3: success and failure. The probability of success is 0.75; the probability of failure is 0.25. For the successful outcome, the parameters to be used to model the halite properties for Activity SAL 3 are those modifications to the SPM-2 baseline described below. For the outcome of failure, the parameters to be used are those in the unmodified SPM-2 baseline.

### 3.6.3.3 PARAMETERS

For the successful outcome of Activity SAL 3, the probability distribution for far-field gas threshold pressure of halite to be used for SPM-2 analysis appears in Table 3-17.

Table 3-17. Values for Gas Threshold Pressure of Halite for Activity SAL 3

$P_{th}$ (MPa)	Interval Probability
0.1 to 0.3	0.05
0.3 to 1	0.10
1 to 3	0.15
3 to 10	0.25
10 to 30	0.30
30 to 100	0.15

Mean = 17.8

### 3.6.4 SAL 4 – Contaminated Brine Outflow

SAL 4 consists of three experimental and modeling activities that impact the baseline assumption for contaminated brine outflow. These experiments and analyses will investigate the amount of storage available to hold contaminated brine after it leaves the repository and before it reaches the accessible environment through the Salado anhydrites. All of these activities affect a single parameter used to check the amount of brine stored before release. This check is done strictly as a post-processing routine after all the major flow and transport modeling is completed.

### 3.6.4.1 SAL 4.1 – FINGERING/CHANNELING STUDIES – EXISTING DATA

#### 3.6.4.1.1 Short Description

Activity SAL 4.1 consists of a combination of the following experiments and modeling:

- Modeling preferential flow.
- 2-D/3-D flow modeling in the anhydrite. (Note: The expected potential outcomes of this activity modeling were included as part of the final SPM-2 baseline, and are to be confirmed in side investigations.)
- Analysis of existing data.

#### 3.6.4.1.2 Outcomes

Two potential outcomes were elicited for Activity SAL 4.1: success and failure. The probability of success is 0.80; the probability of failure is 0.20. For the successful outcome, the  $C_{min}$  parameter to be used to model the brine mass storage has the distribution described below. For the outcome of failure, the parameter distribution to be used is that in the unmodified SPM-2 baseline.

#### 3.6.4.1.3 Parameters

For the successful outcome of Activity SAL 4.1, if it is conducted without the other SAL activities, the probability distribution for the Salado brine mass storage parameter to be used for SPM-2 analysis is that shown in Table 3-18.

Table 3-18. Probability Intervals for the Brine Mass Storage Parameter for Activity SAL 4.1

$C_{min}$	Interval Probability
$1 \times 10^{-3}$ to $3.2 \times 10^{-3}$	0.10
$3.2 \times 10^{-3}$ to $4.2 \times 10^{-3}$	0.30
$4.2 \times 10^{-3}$ to $5.6 \times 10^{-3}$	0.50
$5.6 \times 10^{-3}$ to $1 \times 10^{-2}$	0.10

Mean = 0.0046

### 3.6.4.2 SAL 4.2 – FINGERING/CHANNELING STUDIES – NEW DATA

Activity SAL 4.2. is to be conducted only in conjunction with Activity SAL 1.

#### 3.6.4.2.1 Short Description

Activity SAL 4.2 is a combination of the following experimental and modeling activities:

- Modeling preferential flow.
- A new activity to collect spacially distributed geostatistical core samples.

#### 3.6.4.2.2 Outcomes

Two potential outcomes were elicited for Activity SAL 4.2: success and failure. The probability of success is 0.95; the probability of failure is 0.05. For the successful outcome, the  $C_{min}$  parameter to be used to model the brine mass storage has the distribution described below. For the outcome of failure, the parameter distribution to be used is that in the unmodified SPM-2 baseline.

#### 3.6.4.2.3 Parameters

For the successful outcome of Activity SAL 4.2, the probability distribution for the brine mass storage parameter to be used for SPM-2 analysis is that appearing in Table 3-19.

Table 3-19. Probability Intervals for the Brine Mass Storage Parameter for Activity SAL 4.2

$C_{min}$	Interval Probability
$1 \times 10^{-3}$ to $3.2 \times 10^{-3}$	0.05
$3.2 \times 10^{-3}$ to $4.2 \times 10^{-3}$	0.10
$4.2 \times 10^{-3}$ to $5.6 \times 10^{-3}$	0.45
$5.6 \times 10^{-3}$ to $1 \times 10^{-2}$	0.40

Mean = 0.0058

### 3.6.4.3 SAL 4.3 – ANHYDRITE FRACTURE STUDIES

#### 3.6.4.3.1 Short Description

Activity SAL 4.3 is a combination of the following experimental and modeling activities:

- Anhydrite fracture tests in field and laboratory.
- Fracture modeling for high pressure in anhydrite.

#### 3.6.4.3.2 Outcomes

Two potential outcomes were elicited for Activity SAL 4.3: success and failure. The probability of success is 0.70; the probability of failure is 0.30. For the successful outcome, the  $C_{\min}$  parameter to be used to model the brine mass storage parameter has the distribution described below. For the outcome of failure, the parameter distribution to be used is that in the unmodified SPM-2 baseline.

#### 3.6.4.3.3 Parameters

For the successful outcome of Activity SAL 4.3, the probability distribution for the brine mass storage parameter to be used for SPM-2 analysis is that appearing in Table 3-20.

Table 3-20. Probability Intervals for the Brine Mass Storage Parameter for Activity SAL 4.3

$C_{\min}$	Interval Probability
$1 \times 10^{-3}$ to $5.6 \times 10^{-3}$	0.05
$5.6 \times 10^{-3}$ to $7.4 \times 10^{-3}$	0.10
$7.4 \times 10^{-3}$ to $1 \times 10^{-2}$	0.85

Mean = 0.0082

## 3.7 Non-Salado

### 3.7.1 NS 1 – Dewey Lake - Paper and Low-Effort Field Studies

#### 3.7.1.1 SHORT DESCRIPTION

Determine a range of minimum acceptable sorption distribution coefficients ( $K_{ds}$ ) by incorporating density and porosity distributions determined from sample analysis, conservative estimates of the dispersivity coefficient and groundwater velocity, expected source term behavior, and the critical  $C/C_0$  value into a one-dimensional analytical solution of the advection-dispersion equation. Develop estimates of expected  $K_{ds}$  to compare with the range of minimum acceptable  $K_{ds}$ .

#### 3.7.1.2 OUTCOMES

Two potential outcomes were elicited for Activity NS 1: success and failure. The probability of success is 1; the probability of failure is 0. For the successful outcome, the parameters to be used to model the Dewey Lake are the modifications to the SPM-2 baseline described below.

#### 3.7.1.3 PARAMETERS

For the successful outcome of Activity NS 1, the Dewey Lake is to be modeled as follows:

Retardation in the Dewey Lakes effectively eliminates radionuclide releases from the Dewey Lakes to the accessible environment.

The following three Activities (NS 2, NS 3, and NS 4) may have correlated outcomes. They result in different possibilities assigned to the same range of outcomes. Each activity is described individually, but the outcomes for each and for allowable combinations are given in Table 3-21 and 3-22.

Table 3-21. Outcomes, Probabilities, and Parameter Values for Activities NS 2, NS 3, and NS 4

Outcome	Outcome Probabilities			Parameter Values	
	Activity NS 2	Activity NS 3	Activity NS 4	Specific Area for Matrix Diffusion	Fracture Spacing
1	0.1	0.05	0.02	0.52 - 1.04	3.0
2	0.25	0.15	0.08	1.04 - 2.08	1.5
3	0.45	0.50	0.45	2.08 - 4.16	0.75
4	0.2	0.30	0.45	4.16 - 20.78	0.30

Table 3-22. Parameter Determination for Activities NS 2, NS 3, and NS 4

Activity Outcome or Outcome Combination	Parameter Value
NS 2 <sub>i</sub>	P <sub>i</sub>
NS 2 <sub>i</sub> + NS 3 <sub>j</sub>	P <sub>j</sub>
NS 2 <sub>i</sub> + NS 4 <sub>k</sub>	MIN(P <sub>i</sub> , P <sub>k</sub> )
NS 2 <sub>i</sub> + NS 3 <sub>j</sub> + NS 4 <sub>k</sub>	MIN(P <sub>j</sub> , P <sub>k</sub> )
NS 4 <sub>k</sub>	P <sub>k</sub>

Note: NS 2<sub>i</sub> = Outcome i from Activity NS 2, where  
i = 1, 2, 3, or 4  
NS 3<sub>j</sub> = Outcome j from Activity NS 3, where  
j = 1, 2, 3, or 4  
NS 4<sub>k</sub> = Outcome k from Activity NS 4, where  
k = 1, 2, 3, or 4  
P<sub>i</sub> = Parameter value for outcome i  
P<sub>j</sub> = Parameter value for outcome j  
P<sub>k</sub> = Parameter value for outcome k

### 3.7.2 NS 2 – Culebra Fracture/Matrix/Flow - Lab

#### 3.7.2.1 SHORT DESCRIPTION

- Reexamine existing data (e.g., cores, core data, core permeability) to define a defensible value range for matrix and fracture properties and a spatial assignment of matrix permeability. Review the 1992 WIPP PA model to examine the extent of matrix participation arising from diffusion, coupled with examination of old results; perform scoping modeling. Perform 3-D simulation for future flow directions.
- Improve the understanding of the transmissivity field (T-field) over the repository from well H-19 pumping test, and review existing data. Conduct multiphase flow scoping calculations for increasing the effects of a given fracture.

#### 3.7.2.2 OUTCOMES

Four outcomes were elicited for Activity NS 2, defined by ranges in specific surface area for matrix diffusion in the Culebra. The probabilities for the four outcomes appear in column four of Table 3-21.

### **3.7.2.3 PARAMETERS**

For the successful outcome of Activity NS 2, the Culebra is to be modeled using the parameters in Table 3-21. The fracture spacing values in column three of Table 3-21 are to be used to model the Culebra for Activity NS 2. The fracture spacing is calculated from the midpoint of the range of the specific surface areas for matrix diffusion for each outcome, assuming an aquifer thickness of 7.7 m.

### **3.7.3 NS 3 – Culebra Fracture/Matrix/Flow - Field**

Activity NS 3 must be conducted in conjunction with NS 2, because it is an extension of NS 2.

#### **3.7.3.1 SHORT DESCRIPTION**

Drill additional wells over the repository to obtain information on the T-field. Implement a technically defensible model for compliance calculations (e.g., develop a new numerical model as needed for PA, including Quality Assurance (QA) and coding).

#### **3.7.3.2 OUTCOMES**

Four potential outcomes were elicited for Activity NS 2 combined with Activity NS 3, defined by ranges in specific surface for matrix diffusion in the Culebra. The probabilities for the four outcomes appear in column five of Table 3-21.

#### **3.7.3.3 PARAMETERS**

The values in column three of Table 3-21 are to be used to model the Culebra for Activity NS 3 in combination with NS 2. Activity NS 3 may also be conducted with Activity NS 4. If Activity NS 3 is conducted with Activity NS 4, the values to be used to model the Culebra are those discussed in Section 3.7.5.

### **3.7.4 NS 4 – Multi-Well Tracer Test**

#### **3.7.4.1 SHORT DESCRIPTION**

Perform multi-well tracer tests, the results of which are expected to permit the defense of more fractures in the model that would provide a greater surface area for matrix diffusion.

#### 3.7.4.2 OUTCOMES

Four potential outcomes were elicited for Activity NS 4, defined by ranges in specific surface for matrix diffusion in the Culebra. The probabilities for the four outcomes appear in column six of Table 3-21.

#### 3.7.4.3 PARAMETERS

Activity NS 4 may be conducted alone or with Activity NS 2 and/or Activity NS 3. The values in Table 3-20 are to be used to model the Culebra for Activity NS 4 if it is conducted without NS 2 or NS 3. They indicate the fracture spacing calculated from the midpoint of the range of the specific surface areas for matrix diffusion for each outcome of Activity NS 4, assuming an aquifer thickness of 7.7 m.

### 3.7.5 Parameters for the Combined Activities NS 2, NS 3, and NS 4

If Activity NS 4 is conducted with Activity NS 2 or NS 3, the value to be used to model the Culebra is the smaller of the fracture spacing values in Table 3-20, according to the algorithms shown in Table 3-21.

### 3.7.6 NS 5 – Sorbing Tracer Test

Activity NS 5 must be conducted in conjunction with Activity NS 6 or both Activity NS 6 and Activity NS 7.

#### 3.7.6.1 SHORT DESCRIPTION

Perform a field sorbing tracer test to confirm laboratory-derived  $K_{ds}$ .

#### 3.7.6.2 OUTCOMES

If Activity NS 5 is performed, data will be obtained that will contribute to the defensibility of laboratory-derived  $K_d$  values for use in WIPP PAs. The probability that this data will show that the laboratory-derived  $K_{ds}$  are defensible is 0.95. There is a 0.05 probability that the data resulting from this activity will show that laboratory-derived  $K_{ds}$  are not defensible. These probabilities are accounted for in the outcomes of NS 6 and NS 7.

### 3.7.6.3 PARAMETERS

There are no parameters directly associated with Activity NS 5. It must be performed with Activity NS 6 or both Activity NS 6 and Activity NS 7. Activity NS 5 influences the probability of obtaining defensible  $K_d$  values from Activities NS 6 and NS 7.

### 3.7.7 NS 6 – Chemical Retardation (U and Am)

Activity NS 6 was originally a single activity. However, it was combined with NS 7 for implementation in SPM-2.

#### 3.7.7.1 SHORT DESCRIPTION

Activity NS 6 has two components: the examination of the mechanisms of retardation, and the conceptual model to determine the partition coefficients ( $K_d$  values) for modeling.

- Perform experiments on mechanistic adsorption with U and neodymium (Nd) on Culebra substrates to provide the experimental basis for derivation of defensible  $K_d$  values for U and Am (Nd is an analog element for Am).
- Perform studies that will provide a conceptual model for the investigation of retardation in the fractured Culebra. Perform local petrography-geochemical evaluation of flow paths. Examine possible skin effects of the clay minerals at the fracture surface. Examine the clay mineral properties. Use subhorizontal fractures and matrix for potential solute with rock interactions. Use concentrations of clay minerals in the matrix adjacent to the fractures for the model.

#### 3.7.7.2 OUTCOMES

The first component of Activity NS 6 has two potential outcomes: success and failure. If NS 5 is not undertaken or if NS 5 fails, the probability of successful completion of the first component of Activity NS 6 is 0.8; and the probability of failure is 0.20. Conversely, if NS 5 succeeds, the probability of NS 6 being successful is 0.95, and the probability of failure is 0.05.

The second component of Activity NS 6 has two potential outcomes: successful demonstration of fracture advection with matrix diffusion and dual porosity, and inability to demonstrate fracture advection with matrix diffusion and dual porosity. The probability of the successful outcome of the second component is 0.75; the probability of the unsuccessful outcome is 0.25.

### 3.7.7.3 PARAMETERS

Matrix  $K_d$  values for use in modeling are determined by the outcome of the first and second components of Activity NS 6 and by the outcome of Activity NS 5.

For the outcome of success for component one and two of Activity NS 6, use the  $K_d$  values in Table 3-23 to model transport in the Culebra.

Table 3-23. Matrix  $K_d$  Values for Modeling Dissolved Actinide Transport in the Culebra for Activity NS 6

Actinide	$K_d$ Values	Mean (log ( $K_d$ ))	
		1992 WIPP PA	NS 6
Am	Those in the 1992 WIPP PA, multiplied by 0.10	-0.392	-1.392
Np	0	-1.55	0
Pu	0	-0.713	0
Th	0	-1.83	0
U	Those in the 1992 WIPP PA, multiplied by 0.10	-2.01	-3.01

For the outcome of conditional success of the first component of Activity NS 6 and the outcome of success for NS 5 and success of component two of NS 6, also use the  $K_d$  values in Table 3-23.

In all other cases, use the parameters in the unmodified SPM-2 baseline.

### 3.7.8 NS 7 – Chemical Retardation for Th, Np, Pu, U, and Am

Activity NS 7 is an experimental study that builds upon NS 6 and therefore, for SPM-2 analysis, was the only one of the two (NS 6, NS 7) analyzed.

#### 3.7.8.1 SHORT DESCRIPTION

Activity NS 7 has two components: the examination of the mechanisms of retardation, and the conceptual model to determine the partition coefficients ( $K_d$  values) for modeling.

- Perform experiments on mechanistic adsorption with U and neodymium (Nd) on Culebra substrates to provide the experimental basis for derivation of defensible  $K_d$  values for U and Am (Nd is an analog element for Am).
- Perform semi-empirical adsorption experiments to establish minimum  $K_d$  values for Th, Np, and Pu, and revise the  $K_d$  for U and Am.
- Perform studies that will provide a conceptual model for the investigation of retardation in the fractured Culebra. Perform local petrography-geochemical evaluation of flow paths. Examine possible skin effects of the clay minerals at the fracture surface. Examine the clay mineral properties. Use subhorizontal fractures and matrix for potential solute with rock interactions. Use concentrations of clay minerals in the matrix adjacent to the fractures for the model.

#### 3.7.8.2 OUTCOMES

The first component of Activity NS 7 has two potential outcomes: success and failure. If NS 5 is not successful or is not undertaken, the probability of successful completion of the first component of Activity NS 6 is 0.8; and the probability of failure is 0.2. If NS 5 is successful, the probability of success for the first component of NS 6 is 0.95; and the probability of failure is 0.05.

The second component of Activity NS 7 has two potential outcomes: successful demonstration of fracture advection with matrix diffusion and dual porosity, and inability to demonstrate fracture advection with matrix diffusion and dual porosity. The probability of the successful outcome of the second component is 0.75; the probability of the unsuccessful outcome is 0.25.

#### 3.7.8.3 PARAMETERS

$K_d$  values for use in SPM-2 modeling are determined by the outcomes of both the first and second components of Activity NS 7, and the outcome Activity NS 5.

For the outcome of success for the first and second components of Activity NS 7, the matrix  $K_{ds}$  to be used to model dissolved actinide transport in the Culebra in the model are those in Table 3-23. For a conditionally successful outcome of the first component and success of the second component, the values in Table 3-24 are to be used only if Activity NS 5 is successful.

For the outcome of failure of the first or second components for Activity NS 7, baseline  $K_{ds}$  are used.

Table 3-24.  $K_d$  Values for Modeling Dissolved Actinide Transport in the Culebra for Activity NS 7

Actinide	Elicited $K_d$ Distributions	Mean ( $\log(K_d)$ )	
		1992 WIPP PA	NS 7
Am	Same as 1992 WIPP PA	-0.392	-0.392
Np	25% probability value from 1992 WIPP PA as the distribution minimum	-1.55	-1.673
	75% probability value from 1992 WIPP PA as the distribution maximum		
	Same distribution shape as 1992 WIPP PA rescaled to fit above absolute values		
Pu	25% probability value from 1992 WIPP PA as the distribution minimum	-0.713	-0.74
	75% probability value from 1992 WIPP PA as the distribution maximum		
	Same distribution shape as 1992 WIPP PA rescaled to fit above absolute values		
Th	25% probability value from 1992 WIPP PA as the distribution minimum	-1.83	-1.85
	75% probability value from 1992 WIPP PA as the distribution maximum		
	Same distribution shape as 1992 WIPP PA rescaled to fit above absolute values		
U	Same as 1992 WIPP PA	-2.01	-2.01

### 3.7.9 NS 8.1 – Concentrations and Transport of Colloid Carriers: High-Molecular Weight Organic Compounds (HMWOCs) and Microbes

#### 3.7.9.1 SHORT DESCRIPTION

- Reduce the upper bound concentrations of mobile actinides that are present in the source term in the form of humic material and microbes.
- Quantify chemical and physical retardation of colloids in the Culebra through scoping studies and a literature search.

### 3.7.9.2 OUTCOMES

There were two potential outcomes elicited for each component of Activity NS 8.1: success and failure. The probability of success for the first component is 1. The probability of failure is 0. The probability of success for the second component is 1. The probability of failure is 0. For each component, if it succeeds, the baseline will be modified as described below. Component one succeeds if the model furnishes the required concentrations; component two succeeds if the data collected demonstrates retardation in the Culebra. For each component, if it fails, the baseline will not be modified.

### 3.7.9.3 PARAMETERS

For the successful outcome of Activity NS 8.1, the actinide concentrations to be used in SPM-2 analysis are those appearing in Table 3-25.

Table 3-25. Concentrations of Actinides for Activity NS 8.1

Form of Actinide	Concentration (M/l)
Carried by humic materials	$2 \times 10^{-6}$
Carried by microbes	$1 \times 10^{-7}$

Additional assumptions for the successful outcome of Activity NS 8.1 are as follows:

- Transport of microbes in the Culebra is by fracture advection.
- For humic materials, actinide transport in the Culebra is by fracture advection and matrix diffusion, and the free water diffusion constant is  $2 \times 10^{-8}$  cm<sup>2</sup>/sec.
- The release to the accessible environment is reduced by a factor of 10.
- For actinides transported in the Culebra by microbes, reduce the release to the accessible environment by a factor of 10.

### 3.7.10 NS 8.2 – Enhanced Colloid Experimental Program

Activity NS 8.2 will investigate concentration and transport properties of colloids. It combines the potential outcomes of the existing Actinide Source Term program that quantifies the mobile colloidal actinide concentrations in WIPP brine, and the Non-Salado Flow and Transport program that investigates colloid transport.

The goals for the Enhanced Colloid Experimental Program are to provide additional information that can be used to: 1) reduce the estimates of the upper bound concentrations of mobile colloidal actinides that are present in the source term in the forms of humic material and microbes; 2) demonstrate that actinide intrinsic and mineral fragments are not important constituents of the source term; 3) lower the estimate of the abundance of in situ natural organic matter in Culebra groundwaters; and 4) quantify and take credit for chemical and physical retardation of colloids in the Culebra.

#### 3.7.10.1 SHORT DESCRIPTION

- Develop a model for estimating the concentration of carrier colloids, HMWOCs, and microbial colloids in WIPP brine. The model will estimate concentrations of Am, Np, Pu, Th, and U in WIPP brine for each type of carrier colloid as a function of pH, Eh, and other variables.
- Evaluate transport of colloids with the core column flow apparatus and the sorption capacity of microbes with actinides Am, Np, Pu, and Th (not U).

#### 3.7.10.2 OUTCOMES

Two potential outcomes were elicited for each component of Activity NS 8.2: success and failure. The probability of success for the first component is 1; the probability of failure is 0. The probability of success for the second component is 1; the probability of failure is 0. For each component, if it succeeds, the baseline will be modified as described below. Component one succeeds if the model furnishes the required concentrations; component two succeeds if the data collected demonstrates retardation in the Culebra. For each component, if it fails, the baseline will not be modified. The probability of success for each component is 1. The probability of failure is 0.

#### 3.7.10.3 PARAMETERS

If the first component of Activity NS 8.2 succeeds, the parameters and distributions for the concentrations of actinide colloid carriers are those appearing in Table 3-26.

Table 3-26. Parameters and Distributions for Actinide Colloid Carriers – Mineral Fragments and Actinide Macromolecules for Activity NS 8.2

Colloidal Particle	Concentration (M/l)
Microbes	$1 \times 10^{-8}$
HMWOCs	$2 \times 10^{-8}$

If the second component of Activity NS 8.2 succeeds, the parameters and distributions for the concentrations of actinide colloid carriers are to be as follows:

- Microbes are transported by fracture advection; that is, they will not diffuse into the matrix.
- Humic materials are transported by fracture advection and matrix diffusion; the free water diffusion constant is  $1 \times 10^{-7}$  cm<sup>2</sup>/sec.
- A release factor of 100 is to be applied to actinides transported in the Culebra by microbes.
- A release factor of 100 is to be applied to actinides transported in the Culebra by humic materials.

### 3.8 EAs

The SPM-2 evaluation of EAs considered how implementing a given alternative (or combination of alternatives) effects WIPP performance in terms of the Compliance Indicator (CI), the order of magnitude cost, and the estimated implementation time. For example, if either the cost or schedule to implement a given alternative is too great, it was not considered a viable candidate for use at the WIPP site and was eliminated from further evaluation. For the purpose of SPM-2, three EAs were defined. These cases were chosen to evaluate performance improvements of the WIPP facility with respect to selected regulatory criteria, that is, backfill, backfill with waste form modification, and passive markers. A rigorous screening of EAs is not appropriate within the context of SPM-2.

The Engineered Alternatives Task Force (EATF) was established by the DOE in 1989 to evaluate the relative effectiveness and feasibility of implementing selected design enhancements (referred to as EAs) for WIPP. The primary goal of the EATF was to develop and evaluate EAs that could substantially enhance the containment performance of the WIPP repository. In addition

to EAs, WACs were formulated to evaluate potential improvements in WIPP performance resulting from selective emplacement of waste based on performance characteristics.

### 3.8.1 EA 1 – Backfill with pH Buffer

#### 3.8.1.1 SHORT DESCRIPTION

The first EA (EA 1) provides a backfill with an added pH buffer. This EA provides for improved repository performance by emplacing a backfill that will reduce brine inflow, and, subsequently, gas generation. The backfill will have a pH buffer additive to control pH to  $6.4 \pm 1.0$ , which will reduce actinide solubility. Overall actinide mobilization is reduced by both the reduction in brine inflow and reduced solubility due to pH control.

#### 3.8.1.2 OUTCOMES

There are two potential outcomes for the EA 1 activity: success and failure. If the activity succeeds, the baseline will be modified as described below. If the activity fails, the baseline will not be modified. If Activity EA 1 is undertaken, the probability of success is assumed to be 1 and the probability of failure is 0. Probabilities may differ as described below.

#### 3.8.1.3 PARAMETERS

For the successful outcome of EA 1, the parameters for SPM-2 analysis are as follows:

- Porosity Surface – 1992 WIPP PA porosity surface
- Gas Generation – Reduced due to less brine
- Actinide Solubility – As discussed below
- Spalling Release – No change

**Actinide Solubilities.** For the successful outcome of EA 1, there are two potential outcomes for actinide solubilities. Outcome 1 results in the solubilities in Table 3-27 with a 75% probability of success. There is a 25% probability of a second outcome, the results of which are the default solubilities without this EA, depending on which branch of the decision tree the calculation is on (i.e., baseline or some other branch or branches of the tree for activities). Neither estimated probabilities of success and failure were used in the SPM-2 analysis. Instead, the outcome of success alone was assumed. Decisions made on selecting EA 2 should look more carefully at the import of EA 2 where there is failure to reduce the actinide solubilities.

Table 3-27. Actinide Solubilities with EA 1 in Log (gram moles/liter)

Oxidation State	Minimum Log Molar Concentration	Maximum Log Molar Concentration
+III	-10	-5
+IV	-10	-8
+V	-10	-4
+VI	-10	-2

### 3.8.2 EA 2 – Backfill with pH Buffer and Waste Form Modification

#### 3.8.2.1 SHORT DESCRIPTION

EA 2 provides a backfill (such as clay) with a pH buffer and waste form modification (such as clay or grout injection into drums of waste). This EA provides an optimally effective barrier to brine inflow, thereby reducing the gas generation and actinide mobilization. The pH buffer additive controls pH to the range of  $6.4 \pm 1.0$  to reduce actinide solubility. The clay or grout injection into the waste drums will provide additional waste strength to reduce spillings releases.

#### 3.8.2.2 OUTCOMES

There are two potential outcomes for this activity: success and failure. If the activity succeeds, the baseline will be modified as described below. If the activity fails, the baseline will not be modified. If Activity EA 2 is undertaken, the probability of success is 1 and the probability of failure is 0. However, there are some concerns and uncertainties associated with this case in terms of potential competing effects. These are described in B. Butcher, R. Anderson, and B. Thompson, "SPM-2 EA Case 2," Sandia National Laboratories memorandum to N. Prindle, March 2, 1995 (see Appendix). These issues were addressed in the detailed design and performance testing of the selected materials for this EA. Therefore, there are no other changes in parameters other than those listed below.

#### 3.8.2.3 PARAMETERS

For the successful outcome of Activity EA 2, the parameters for SPM-2 analysis are as follows:

Porosity Surface – Range equals 0.1 to 0.4, expected value of 0.25, assume 100% saturation

Actinide Solubility – Same as for EA 1

Spalling Release – Linear from 0.001 to 0.1, expected value of 0.01 (comparable to grouted waste)

Puddle Factor – Use residual saturation wetting phase values from the baseline

### **3.8.3 EA 3 – Passive Markers**

#### **3.8.3.1 SHORT DESCRIPTION**

EA 3 takes credit for passive markers which reduce the probability of effective human intrusion drilling rates. The effective drilling rate is derived from considering historic drilling rates, projections of future drilling rates, and the probability of the effectiveness of passive markers.

#### **3.8.3.2 OUTCOMES**

There are two potential outcomes for this activity: success and failure. If the activity succeeds, the baseline will be modified as described below. If the activity fails, the baseline will not be modified. No Project consensus was reached on determining the probability of this outcome (L. R. Fitch, "Future Inadvertent Intrusion Rates," Westinghouse Electric Corporation letter to M. McFadden, March 21, 1995, in Appendix). Therefore, for the purposes of SPM-2, if Activity EA 3 is undertaken, the probability of success was assigned the value 1 and the probability of failure was assigned the value 0. This probability is a measure of the likelihood that the regulator will accept the derivation of the effective drilling rate.

#### **3.8.3.3 PARAMETERS**

For the successful outcome of EA 3, the parameters for SPM-2 analysis are as follows:

Porosity Surface – No change

Gas Generation – No change

Actinide Solubility – No change

Spalling Release – Reduced based on results of calculations

Effective Drilling Rate –  $0.2/\text{km}^2/10,000$  years

## **3.9 WAC**

WAC have been formulated to evaluate potential improvements in WIPP performance gained by selectively emplacing waste based on performance characteristics.

The SPM-2 evaluation of WAC alternatives considers how implementation of a given alternative (or combination of alternatives) effects WIPP performance in terms of the calculated CI, the order of magnitude cost, and the estimated implementation time. For example, if either the cost or schedule to implement a given alternative is too great, it is not a viable candidate for use at the WIPP site and it is eliminated from further evaluation. For the purpose of SPM-2, two alternative WACs were defined. A rigorous screening of WACs was not performed to select these alternatives. These cases were chosen to evaluate the improvements gained by elimination of soils and reduction of corroding metal inventory.

### **3.9.1 WAC 1 – Non-Corroding Waste Containers**

#### **3.9.1.1 SHORT DESCRIPTION**

WAC 1 uses noncorroding waste containers for all future wastes to reduce gas generation.

##### **3.9.1.1.1 Outcomes**

There are two potential outcomes for this activity: success and failure. If the activity succeeds, the baseline will be modified as described below. If the activity fails, the baseline will not be modified. If Activity WAC 1 is undertaken, the probability of success is 1 and the probability of failure is 0.

##### **3.9.1.1.2 Parameters**

For the successful outcome of Activity WAC 1, the baseline parameters are to be modified as follows:

- Porosity Surface – No change
- Gas Generation – 8.5% in gas generation reduction
- Actinide Solubility – No change
- Spalling Release – No change

## **3.9.2 WAC 2 – Elimination of Humic-Containing Waste Drums**

### **3.9.2.1 SHORT DESCRIPTION**

WAC 2 eliminates humic-containing waste drums to reduce colloids.

### **3.9.2.2 OUTCOMES**

There are two potential outcomes for this activity: success and failure. If the activity succeeds, the baseline will be modified as described below. If the activity fails, the baseline will not be modified. If Activity WAC 2 is undertaken, there is a probability of success is assumed, for SPM-2, to be 1 and the probability of failure is 0.

### **3.9.2.3 PARAMETERS**

Porosity Surface – No change  
Gas Generation – No change  
Actinide Solubility – No small colloids  
Spalling Release – No change

#### **4. COMPUTATIONAL IMPLEMENTATION OF THE SPM-2 CONCEPTUAL MODELS**

The SPM-2 conceptual models were identified through the SPM-2 position paper process, the SNL SPM-2 baseline process, the SPM-2 activity elicitation process, the DOE/CAO guidance for SPM-2, and the SNL management and DOE/CAO SPM steering team review processes. These conceptual models were put into the appropriate PA codes. It was discovered, however, after checking the operation of these models, that several were not behaving as expected. It was not known whether this was due to incorrect coding or whether the processes that were being demonstrated were not fully understood. SNL chose to eliminate these conceptual models from the analysis until a better understanding of the processes could be achieved or until any coding errors could be found and removed. Eliminating these models meant that these issues would be studied using side investigations.

The following models were eliminated from SPM-2. All other conceptual models defined for the SPM-2 technical baseline and activity sets were used in the analysis.

- 1) The altered anhydrite model was not applied to the DRZ and the TZ as requested. It was applied to the anhydrite material in the appropriate marker beds. These zones were assumed to have the porosity of the far-field halite and enhanced permeability, so that they would not choke any fluid flow.
- 2) The stratigraphic dip was not analyzed in the baseline. Instead, the repository was modeled as completely horizontal.
- 3) Gas generation by radiolysis was not analyzed. This means that there was no gas generation from the radiolysis mechanism. The other gas generation mechanisms were analyzed.
- 4) Multiple room closure porosity surfaces were not modeled. It was expected that the model analysis would have one porosity surface for the north end (empty, i.e., no waste and no backfill) and one porosity surface for the south end of the facility (waste and backfill as required). Instead, the south end was analyzed using the appropriate porosity surface, and the north end used fixed values for the closed state of an empty facility.
- 5) The disposal room waste region permeability was not analyzed as a dynamic function of porosity for fluid flowing in and through the room. Instead, it was modeled as having a fixed permeability. The dynamic permeability model was implemented for the purposes of human intrusion, i.e., cuttings, cavings, and spillings.
- 6) Brine wicking up through the waste was not analyzed. No wicking was assumed.

- 7) Gas dissolution in the brine was not analyzed. It was assumed that gas would not dissolve in the brine, and no gas was contained in the brine.
- 8) Multicomponent gas transport was not analyzed, i.e., multiple components in the gas phase, such as hydrogen, CO<sub>2</sub>, and/or VOCs, were not analyzed.
- 9) The reaction-path model (RPM) and the option of using the Ideal Gas Law were not analyzed for the SPM-2 activity sets. Instead, the SPM-2 baseline Gas Generation model was applied to all activity sets.

The baseline was modeled using a Latin Hypercube Sampling (LHS) size of 40. However, based on recommendations from the SNL WIPP PA Departments, in addition to the modeling changes listed above, the analysis of the CCDF was changed from a full Latin Hypercube analysis to a mean value approach. "We believe that the best course of meeting the 3/31/95 milestone and delivering the SPM product to DOE/CAO as a decision aid tool is to go forward with the mean value approach which is different from our traditional Latin Hypercube Sampling (LHS) approach" (H. Jow and D. Anderson, "PA Computational Approach to SPM2," Sandia National Laboratories memorandum to Les Shephard, March 1, 1995, in Appendix).

The mean value approach would give the zeroth order approximation of the mean of the CCDFs generated by using the LHS. This zeroth order approximation is believed to be a reasonable estimate of the mean of the CCDFs for decision analysis. The shortcoming of the mean value approach is not an inability to include the evaluation of the uncertainty distributions of parameter values. That is, if an activity causes the mean to shift, as most SPM-2 activities do, the SPM-2 analysis will capture and show this effect. However, if an activity does not move the mean of the distribution, but only narrows the range of the distribution, the SPM-2 analysis will not capture the effect. In exchange for this limitation, the SPM-2 analysis was able to look at a much richer and broader suite of activities than would have been possible using LHS methods.

The CCDF for total release was derived from the two component releases. The same random drilling histories were used to construct each CCDF. The total release corresponding to the first simulated history is the sum of the direct release for the first simulated history, and the groundwater release for the first simulated history. The component releases for all other simulated histories can be similarly added to produce a distribution of total release. This distribution is then compared against the long-term containment requirements of 40 CFR 191.13(a). This comparison, in conjunction with comparison values calculated for the hazardous constituent concentrations, produces the SPM-2 CI.

## 5. REFERENCES

- Beauheim, R. L., R. M. Roberts, T. F. Dale, M. D. Fort, and W. A. Stensrud. 1993. *Hydraulic Testing of Salado Formation Evaporites at the Waste Isolation Pilot Plant Site: Second Interpretive Report*. SAND92-0533. Albuquerque, NM: Sandia National Laboratories.
- Beauheim, R. L., S. M. Howarth, P. Vaughn, S. W. Webb, and K. W. Larson. 1994. "Integrated Modeling and Experimental Programs to Predict Brine and Gas Flow at the Waste Isolation Pilot Plant," *Geoval 94, Paris, France, October 11-14, 1994*. SAND94-0599C. Albuquerque, NM: Sandia National Laboratories.
- Brush, L. H., J. W. Garner, and L. J. Storz. 1994. "Development of a Gas-Generation Model for the Waste Isolation Pilot Plant," *Scientific Basis for Nuclear Waste Management XVII, Materials Research Society Symposium Proceedings, Boston, MA, November 29-December 3, 1993*. Eds. A. Barkatt and R. A. Van Konynenburg. Pittsburgh, PA: Materials Research Society. Vol. 333, 241-246.
- Cygan, R. T. 1991. *The Solubility of Gases in NaCl Brine and a Critical Evaluation of Available Data*. SAND90-2848. Albuquerque, NM: Sandia National Laboratories.
- Davies, P. B. 1989. *Variable-Density Ground-Water Flow and Paleohydrology in the Waste Isolation Pilot Plant (WIPP) Region, Southeastern New Mexico*. Open-File Report 88-490. Albuquerque, NM: U.S. Geological Survey.
- Davies, P. B. 1991. *Evaluation of the Role of Threshold Pressure in Controlling Flow of Waste-Generated Gas into Bedded Salt at the Waste Isolation Pilot Plant*. SAND90-3246. Albuquerque, NM: Sandia National Laboratories.
- Davis, S. N., and R. J. M. Dewiest. 1966. *Hydrogeology*. New York, NY: John Wiley and Sons.
- Freeze, R. A., and J. A. Cherry. 1979. *Groundwater*. Englewood Cliffs, NJ: Prentice-Hall.
- Lappin, A. R., R. L. Hunter, D. P. Garber, P. B. Davies, R. L. Beauheim, D. J. Borns, L. H. Brush, B. M. Butcher, T. Cauffman, M. S. Y. Chu, L. S. Gomez, R. V. Guzowski, H. J. Iuzzolino, V. Kelley, S. J. Lambert, M. G. Marietta, J. W. Mercer, E. J. Nowak, J. Pickens, R. P. Rechar, M. Reeves, K. L. Robinson, and M. D. Siegel, eds. 1989. *Systems Analysis, Long-Term Radionuclide Transport, and Dose Assessments, Waste Isolation Pilot Plant (WIPP), Southeastern New Mexico; March 1989*. SAND89-0462. Albuquerque, NM: Sandia National Laboratories.

- LaVenue, A. M., and B. S. RamaRao. 1992. *A Modeling Approach to Address Spatial Variability within the Culebra Dolomite Transmissivity Field*. SAND92-7306. Albuquerque, NM: Sandia National Laboratories.
- Luker, R. S., T. W. Thompson, and B. M. Butcher. 1991. "Compaction and Permeability of Simulated Waste," *Rock Mechanics as a Multidisciplinary Science: Proceedings of the 32nd U.S. Symposium, The University of Oklahoma, Norman, OK, July 10-12, 1991*. Ed. J-C. Roegiers. SAND90-2368C. Brookfield, VT: A. A. Balkema. 693-702.
- Mercer, J. W. 1983. *Geohydrology of the Proposed Waste Isolation Pilot Plant Site, Los Medanos Area, Southeastern New Mexico*. Water-Resources Investigations Report 83-4016. Albuquerque, NM: U.S. Geological Survey.
- Mualem, Y. 1976. "A New Model for Predicting the Hydraulic Conductivity of Unsaturated Porous Media," *Water Resources Research*. Vol. 12, no. 3, 513-522.
- Munson, D. E., A. F. Fossum, and P. E. Senseny. 1989. *Advances in Resolution of Discrepancies Between Predicted and Measured In Situ WIPP Room Closures*. SAND88-2948. Albuquerque, NM: Sandia National Laboratories.
- Nowak, E. J., D. F. McTigue, and R. Beraun. 1988. *Brine Inflow to WIPP Disposal Rooms: Data, Modeling, and Assessment*. SAND88-0112. Albuquerque, NM: Sandia National Laboratories.
- Reeves, M., G. A. Freeze, V. A. Kelley, J. F. Pickens, D. T. Upton, and P. B. Davies. 1991. *Regional Double-Porosity Solute Transport in the Culebra Dolomite Under Brine-Reservoir-Breach Release Conditions: An Analysis of Parameter Sensitivity and Importance*. SAND89-7069. Albuquerque, NM: Sandia National Laboratories.
- Sandia WIPP Project. 1992. *Preliminary Performance Assessment for the Waste Isolation Pilot Plant, December 1992. Volume 3: Model Parameters*. SAND92-0700/3. Albuquerque, NM: Sandia National Laboratories.
- Swift, P. N. 1993. "Long-Term Climate Variability at the Waste Isolation Pilot Plant, Southeastern New Mexico, USA," *Environmental Management*. SAND91-7055J. Vol. 17, no. 1, 83-97.
- Swift, P. N., B. L. Baker, K. Economy, J. W. Garner, J. C. Helton, and D. K. Rudeen. 1994. *Incorporating Long-Term Climate Change in Performance Assessment for the Waste Isolation Pilot Plant*. SAND93-2266. Albuquerque, NM: Sandia National Laboratories.

- U.S. DOE. 1990. "Appendix B: Waste Analysis Plan," *Waste Isolation Pilot Plant No-Migration Variance Petition*. DOE/WIPP 89-003, Revision 1. Carlsbad, NM: Westinghouse Electric Corporation, Waste Isolation Division. Appendices A and B, Vol. II.
- U.S. DOE. 1993. "Chapter C: Waste Analysis Plan," *Resource Conservation and Recovery Act Part B Permit Application*. DOE/WIPP 91-005, Revision 3. Carlsbad, NM: Waste Isolation Pilot Plant. Vol. I, c-i – c-64.
- U.S. DOE. 1995a. *Waste Isolation Pilot Plant Transuranic Waste Baseline Inventory Report*. CAO-94-1005, Revision 1. [Carlsbad, NM]: WIPP Technical Assistance Contractor for U.S. Department of Energy. Vols. 1-2.
- U.S. DOE. 1995b. *Waste Isolation Pilot Plant No-Migration Variance Petition*. DOE/CAO-95-2043. Carlsbad, NM: United States Department of Energy, Waste Isolation Pilot Plant, Carlsbad Area Office.
- van Genuchten, M. Th. 1980. "A Closed-Form Equation for Predicting the Hydraulic Conductivity of Unsaturated Soils," *Soil Science Society of America Journal*. Vol. 44, no. 5, 892-898. (Copy on file in the Nuclear Waste Management Library, Sandia National Laboratories, Albuquerque, NM.)
- Van Genuchten, R. 1978. *Calculating the Unsaturated Hydraulic Conductivity with a New Closed-Form Analytical Model*. Research Report 78-WR-08. Princeton, NJ: Princeton University, Department of Civil Engineering.
- Wawersik, W. R., and C. M. Stone. 1989. *Application of Hydraulic Fracturing to Determine Virgin In Situ Stress State Around Waste Isolation Pilot Plant - In Situ Measurements*. SAND85-1776. Albuquerque, NM: Sandia National Laboratories.
- Webb, S. W. 1992. *Brine Inflow Sensitivity Study for Waste Isolation Pilot Plant Boreholes: Results of One-Dimensional Simulations*. SAND91-2296. Albuquerque, NM: Sandia National Laboratories.
- Webb, S. W., and K. W. Larson. 1996. *The Effect of Stratigraphic Dip on Brine Inflow and Gas Migration at the Waste Isolation Pilot Plant*. SAND94-0932. Albuquerque, NM: Sandia National Laboratories.
- WIPP PA (Performance Assessment) Division. 1991. *Preliminary Comparison with 40 CFR 191, Subpart B for the Waste Isolation Pilot Plant, December 1991. Volume 3: Reference Data*. Eds. R. P. Rechard, A. C. Peterson, J. D. Schreiber, H. J. Iuzzolino,

M. S. Tierney, and J. S. Sandha. SAND91-0893/3. Albuquerque, NM: Sandia National Laboratories.

WIPP PA (Performance Assessment) Department. 1992a. *Preliminary Performance Assessment for the Waste Isolation Pilot Plant, December 1992. Volume 1: Third Comparison with 40 CFR 191, Subpart B.* SAND92-0700/1. Albuquerque, NM: Sandia National Laboratories.

WIPP PA (Performance Assessment) Department. 1992b. *Preliminary Performance Assessment for the Waste Isolation Pilot Plant, December 1992. Volume 2: Technical Basis.* SAND92-0700/2. Albuquerque, NM: Sandia National Laboratories.

WIPP PA (Performance Assessment) Department. 1993a. *Preliminary Performance Assessment for the Waste Isolation Pilot Plant, December 1992. Volume 4: Uncertainty and Sensitivity Analyses for 40 CFR 191, Subpart B.* SAND92-0700/4. Albuquerque, NM: Sandia National Laboratories.

WIPP PA (Performance Assessment) Department. 1993b. *Preliminary Performance Assessment for the Waste Isolation Pilot Plant, December 1992. Volume 5: Uncertainty and Sensitivity Analyses of Gas and Brine Migration for Undisturbed Performance.* SAND92-0700/5. Albuquerque, NM: Sandia National Laboratories.

**APPENDIX:  
MEMORANDA AND LETTERS REGARDING REFERENCE DATA**

Brush, June 18, 1993 .....	A-5
Butcher, Anderson, and Thompson, March 2, 1995.....	A-49
Drez, January 3, 1995 .....	A-55
Fewell and Sanchez, December 12, 1995.....	A-63
Fitch, March 21, 1995.....	A-77
Jow and Anderson, March 1, 1995.....	A-83
McFadden, December 19, 1994.....	A-87

Intentionally Left Blank

**APPENDIX A:  
MEMORANDA AND LETTERS REGARDING REFERENCE DATA**

**Brush, June 18, 1993**

Date: 6/18/93  
To: M.S. Tierney  
From: L.H. Brush  
Subject: Likely Gas-Generation Reactions and Current Estimates of Gas-Generation Rates for the Long-Term WIPP Performance Assessment

**Butcher, March 2, 1995**

Date: 3/2/95  
To: N. Prindle  
From: B.M. Butcher, R. Anderson, B. Thompson  
Subject: SPM-2 EA Case 2

**Drez, January 3, 1995**

Date: 1/3/95  
To: File  
From: P. Drez  
Subject: Waste Material Parameter and Radionuclide Inventories for SPM-2 Calculations Derived from Draft WTWBIR Rev. 1 and IDB Rev. 10 Databases.

**Fewell and Sanchez, March 29, 1995**

Date: 3/29/95  
To: F. Mendenhall and N. Prindle  
From: M. Fewell and P. Sanchez  
Subject: Soil-Based VOC and Semi-VOC Concentration in the Gas Phase for SPM-2

**Fitch, March 21, 1995**

Date: 3/21/95  
To: M. McFadden  
From: Fitch  
Subject: Future Inadvertent Intrusion Rates

**Jow and Anderson, March 1, 1995**

Date: 3/1/95  
To: L. Shepard  
From: H. Jow and D. Anderson  
Subject: PA Computational Approach to SPM2

**McFadden, December 19, 1994**

Date: 12/19/94  
To: R. Lincoln  
From: M. McFadden  
Subject: Systems Prioritization Method Information Needs and Product Requirements.

**Brush, June 18, 1993**

Date: 6/18/93  
To: M.S. Tierney  
From: L.H. Brush  
Subject: Likely Gas-Generation Reactions and Current Estimates of Gas-Generation Rates for the Long-Term WIPP Performance Assessment

Intentionally Left Blank

date: June 18, 1993

to: M. S. Tierney, 6342

from: L. H. Brush, 6348

subject: Likely Gas-Generation Reactions and Current Estimates of Gas-Generation Rates for the Long-Term WIPP Performance Assessment

### INTRODUCTION

This memorandum identifies likely gas-generation reactions (Table 1), provides current estimates of humid and inundated gas-generation rates (Tables 2 and 3), and calculates the gas-generation potential for radiolysis of H<sub>2</sub>O in brine by <sup>239</sup>Pu for the 1993 long-term WIPP performance-assessment (PA) calculations. A. R. Lappin, 6305, has provided estimates of gas-generation potentials for other processes.

I understand that because of severe time constraints and the higher priorities assigned to other changes in the models to be used for the 1993 PA calculations, you will not have time to incorporate the current version of the gas-generation model J. W. Garner and I provided to P. Vaughn in February 1993. Therefore, I understand you will use the same gas-generation model used in the 1991 and 1992 calculations. This approach consists of listing likely gas-generation reactions, calculating the average stoichiometric gas-production ratio of these reactions, estimating average gas-production rates, and allowing gas production to proceed until the total quantity of gas expected (the gas-generation potential) is attained for a given set of assumptions. I refer to this model as the "average-stoichiometry model." The assumptions include (but are not necessarily limited to): (1) the inventory of reactants (steels and other Fe-base alloys, Al and Al-base alloys, and, perhaps, other metals; cellulose, plastics, and rubbers); (2) the extent to which these materials are convertible to gas (this is especially important in the case of plastics and rubbers); (3) whether sufficient H<sub>2</sub>O will be available (this is especially significant in the case of reactions that occur only in the presence of brine, such as anoxic corrosion of steels). Of course, assumptions such as these are also necessary for the gas-generation model Garner and I are developing.

Given the severe time constraints and the higher priorities assigned to other improvements in the PA models, I concur with your

decision to retain the average-stoichiometry model used in the 1991 and 1992 PA calculations. However, I recommend using additional gas-generation reactions, if possible, and current estimates of gas-generation rates. I describe these reactions and rates below. Of course, I realize that there may not be time to make any changes in the average-stoichiometry model at this point.

Garner and I will continue to develop a thermodynamic and kinetic reaction-path gas-generation model. The current version of this model includes the following processes: (1) corrosion of steels and other Fe-base materials by  $O_2$ ,  $H_2O$ ,  $H_2S$  and  $CO_2$ ; (2) passivation of steels by  $CO_2$ ; (3) depassivation of steels by destabilization of  $FeCO_3$ ; (4) microbial degradation of cellulose with  $O_2$ ,  $NO_3^-$ ,  $Fe(III)$  hydroxide, or  $SO_4^{2-}$  as the electron acceptor; (5) consumption of  $CO_2$  by  $Ca(OH)_2$  (in cementitious materials) and  $CaO$  (a potential backfill additive). The main differences between the reaction-path model and the average-stoichiometry model used in the 1991 and 1992 PA calculations are that: (1) the reaction-path model includes more gas-producing reactions than the average-stoichiometry model; (2) the reaction-path model includes gas-consuming reactions; (3) the reaction-path model includes interactions among gas-producing and gas-consuming processes, such as passivation of steels by microbially-produced  $CO_2$  and depassivation of steels due to consumption of  $CO_2$  by  $Ca(OH)_2$  and  $CaO$ . We will provide you with the latest version of this model as soon as you are ready to incorporate it in the PA models.

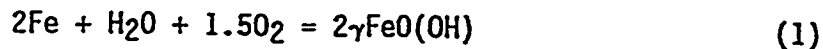
## CORROSION

Oxic corrosion of steel waste containers (drums and boxes), Fe-base alloys in the waste, and, perhaps, other metals would consume  $O_2$  in mine air trapped in WIPP disposal rooms at the time of filling and sealing. Oxic corrosion would also consume  $O_2$  produced by radiolysis of  $H_2O$  in brine. After depletion of the  $O_2$  initially present, anoxic corrosion of Fe-base and other metals could produce significant quantities of  $H_2$ , at least in microenvironments without radiolytically produced  $O_2$ . Other metals that could consume  $O_2$  and produce  $H_2$  include (but are not necessarily limited to) Al, Al-base alloys, Pb, and Pu. Oxic and anoxic corrosion could also consume significant quantities of brine and  $H_2O$  vapor.

### Oxic Corrosion

Brush (1990) concluded that oxic corrosion of steels, other Fe-base alloys, and, perhaps, other metals would not have a significant, direct effect on the gas and  $H_2O$  budget of WIPP disposal rooms. However, this process could be important from the standpoint of the  $O_2$  budget of the repository. The  $O_2$  budget will in turn affect how soon the repository becomes anoxic after filling and sealing, the extent to which microenvironments dominated by brine radiolysis remain oxic, whether gas is consumed or produced, and which gases are consumed and

produced. The O<sub>2</sub> budget will also affect the oxidation state of radionuclides and hence their chemical behavior. Therefore, Garner and I have added the following reaction to the reaction-path gas-generation model to simulate oxid corrosion:



We are using this reaction because N. R. Sorensen, 1832, observed that  $\gamma\text{FeO(OH)}$  (lepidocrocite) was the most abundant corrosion product in oxic, inundated experiments carried out for the Strategic Petroleum Reserve Project. Sorensen also observed  $\text{Fe}_3\text{O}_4$  as a major corrosion product and  $\beta\text{FeO(OH)}$  as a minor corrosion product. Therefore, Garner and I may also add an equation simulating the formation of  $\text{Fe}_3\text{O}_4$ . (Addition of an equation for  $\beta\text{FeO(OH)}$  would not change the stoichiometry of Reaction 1).

For my best estimate of the O<sub>2</sub>-consumption rate for oxid corrosion, I recommend 5 moles per m<sup>2</sup> of steel per year, the value (rounded off to one significant figure) reported by Molecke (1979). Lappin et al. (1989) estimated that there are 6 m<sup>2</sup> of steels and other Fe-base alloys per drum of CH TRU waste, 4 m<sup>2</sup> for CH TRU waste containers and an estimated 2 m<sup>2</sup> for the Fe-base alloys in CH TRU waste. (These values do not include steel or other Fe-base alloys in canisters or plugs to be used for RH TRU waste, any steels or other Fe-base alloys contained in RH TRU waste, or steels or other Fe-base alloys used for ground support in the WIPP underground workings.) Therefore, this rate is equivalent to 30 moles of O<sub>2</sub> per drum of CH TRU waste per year. I computed the oxid-corrosion rate as follows.

The rate at which Fe is consumed by Reaction 1 is:

$$\begin{aligned} & ((2 \text{ moles Fe}) / (1.5 \text{ moles O}_2)) \cdot 5 \text{ moles O}_2 / (\text{m}^2 \cdot \text{yr}) \\ & = 6.67 \text{ moles Fe} / (\text{m}^2 \cdot \text{yr}). \end{aligned} \quad (2)$$

(Only one of the figures in this and the following equations are significant, but I did not round off until the end of these calculations.) This rate is equivalent to:

$$\begin{aligned} & 6.67 \text{ moles} / (\text{m}^2 \cdot \text{yr}) \cdot 5.5847 \cdot 10^{-2} \text{ kg/mole} \\ & = 3.7231 \cdot 10^{-1} \text{ kg} / (\text{m}^2 \cdot \text{yr}). \end{aligned} \quad (3)$$

In Equation 2, "5.5847 · 10<sup>-2</sup> kg" is the mass of a mole of metallic Fe. The thickness of the layer of Fe removed from the surface per year is:

$$3.7231 \cdot 10^{-1} \text{ kg}/(\text{m}^2 \cdot \text{yr}) / 7.86 \cdot 10^3 \text{ kg}/\text{m}^3$$

$$= 5 \cdot 10^{-5} \text{ m}/\text{yr}.$$

(4) →

In Equation 4, " $7.86 \cdot 10^3 \text{ kg}/\text{m}^3$ " is the density of metallic Fe. This rate is equivalent to about  $50 \text{ } \mu\text{m}$  of steel per year (Table 2). I cannot compare these estimates of  $\text{O}_2$ -consumption or corrosion rates with previous estimates because I did not estimate these rates for oxidic corrosion of steels for the 1991 and 1992 PA calculations (see Brush, 1991).

My minimum estimates of  $\text{O}_2$ -consumption and corrosion rates for oxidic corrosion of steels and other Fe-base alloys under inundated conditions, 0 moles per  $\text{m}^2$  of steel per year or 0 moles of  $\text{O}_2$  per drum of CH TRU waste per year and  $0 \text{ } \mu\text{m}$  of steel per year (Table 2), are based on the possibility of passivation by formation of an adherent corrosion product (see Anoxic Corrosion below), or by precipitation of salts on the surfaces of corroding metals due to the consumption of  $\text{H}_2\text{O}$  during oxidic corrosion of steels, other Fe-base alloys, and, perhaps, other metals. Although laboratory studies have not demonstrated these mechanisms yet, they are possible, especially (in the case of the latter mechanism) if microbial degradation of cellulose and brine radiolysis also consume significant quantities of  $\text{H}_2\text{O}$ .

My maximum estimates of  $\text{O}_2$ -consumption and corrosion rates for oxidic corrosion of steels and other Fe-base alloys under inundated conditions (Table 2) are based on estimates of the effects of pH on these rates. I have not yet considered the effects of total pressure, the partial pressures of gases expected in WIPP disposal rooms, or temperature on oxidic corrosion. However, I have considered the effects of these factors on anoxic corrosion (see below); the analysis for anoxic corrosion suggests that pH is the most important of these factors. In the case of oxidic corrosion,  $\text{O}_2$ -consumption and corrosion rates are inversely proportional to pH. I used the inverse relationship between pH and oxidic-corrosion rates observed experimentally for applications other than the WIPP Project and estimates of the range of pH expected in WIPP disposal rooms after filling and sealing to estimate the maximum values of these rates.

I assume that the  $\text{O}_2$ -consumption rate of 5 moles per  $\text{m}^2$  of steel per year (Molecke, 1979), which I used for my best estimate of this and other rates under inundated conditions (Table 2), pertains to Reaction 1 at a neutral or nearly neutral pH. Furthermore, I expect that the pH in WIPP disposal rooms will vary between about 3 and 12. Although obtained with deionized  $\text{H}_2\text{O}$ , the results of Uhlig and Revie (1963) suggest that the  $\text{O}_2$ -consumption and corrosion rates for oxidic corrosion of steels are constant or essentially constant between a pH of about 4 and 10, that these rates are higher by about a factor of 1.5 at a pH of 3, and that they are lower by a factor of 0.6 at a pH of 11 and by a factor of 0.4 at a pH of 12. Therefore, the possibility of pH values as low as 3 in WIPP disposal rooms necessitates multiplying my

best estimates in Table 2 by a factor of 1.5:

$$1.5 \cdot 5 \text{ moles/m}^2 = 8 \text{ moles}/(\text{m}^2 \cdot \text{yr}); \quad (5a)$$

$$1.5 \cdot 30 \text{ moles}/(\text{drum} \cdot \text{yr}) = 50 \text{ moles}/(\text{drum} \cdot \text{yr}); \quad (5b)$$

$$1.5 \cdot 50 \text{ } \mu\text{m}/\text{yr} = 80 \text{ } \mu\text{m}/\text{yr}. \quad (5c)$$

These are my maximum estimates, rounded to one significant figure, of these rates under inundated conditions (Table 2). Because they are maximum estimates, I have rounded them up in all three cases. The effects of basic conditions on oxidic corrosion need not be considered at this point because, although they decrease these rates, my minimum estimates are already 0 moles of O<sub>2</sub> per m<sup>2</sup> of steel per year, 0 moles of O<sub>2</sub> per drum of CH TRU waste per year, and 0 μm of steel per year because of possible passivation (see above).

My best estimates of O<sub>2</sub>-consumption and corrosion rates for oxidic corrosion of steels and other Fe-base alloys under humid conditions are 0.5 moles of O<sub>2</sub> per m<sup>2</sup> of steel per year, 3 moles of O<sub>2</sub> per drum of CH TRU waste per year, and 5 μm of steel per year (Table 3). I arbitrarily assume that these rates are one tenth of my current best estimates for oxidic corrosion under inundated conditions (Table 2). I did not estimate these rates for oxidic corrosion of steels for the 1991 and 1992 PA calculations (Brush, 1991).

My arbitrary minimum estimates of O<sub>2</sub>-consumption and corrosion rates for oxidic corrosion of steels and other Fe-base alloys under humid conditions are also 0 moles of O<sub>2</sub> per m<sup>2</sup> of steel per year, 0 moles of O<sub>2</sub> per drum of CH TRU waste per year, and 0 μm of steel per year (Table 3).

My maximum estimates of O<sub>2</sub>-consumption and corrosion rates for oxidic corrosion of steel and other Fe-base alloys under humid conditions are 5 moles of O<sub>2</sub> per m<sup>2</sup> of steel per year, 30 moles of O<sub>2</sub> per drum of CH TRU waste per year, and 50 μm of steel per year (Table 2). I arbitrarily assume that these rates are identical to my current best estimates for oxidic corrosion under inundated conditions (Table 2).

If oxidic-corrosion rates under humid conditions affect the overall performance of the repository significantly, laboratory studies will be necessary to replace these arbitrary estimates with experimentally-based results.

#### Anoxic Corrosion

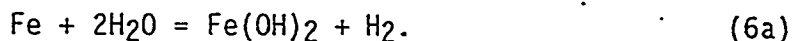
Anoxic corrosion of steels, other Fe-base alloys, and, perhaps, other metals may, if brine is present, produce significant quantities

of H<sub>2</sub> and consume significant quantities of H<sub>2</sub>O (Lappin et al., 1989; Brush, 1990).

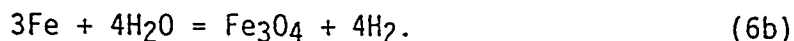
I used thermodynamic calculations and laboratory studies carried out for applications other than the WIPP Project to predict the behavior of steels and other Fe-base alloys under expected WIPP conditions (see Brush, 1990). I am extending these thermodynamic calculations to support of the development of the reaction-path gas-generation model (see INTRODUCTION above).

R. E. Westerman and M. R. Telander of Pacific Northwest Laboratory (PNL) are carrying out laboratory studies of anoxic corrosion for the WIPP Project. So far, they have studied two heats each of the low-C steels ASTM A 366 and ASTM A 570 under inundated conditions (specimens immersed in Brine A) and humid conditions (specimens suspended above Brine A) with initially pure atmospheres of N<sub>2</sub>, CO<sub>2</sub>, and H<sub>2</sub>S at low pressures (about 1 to 15 atm) at 30 ± 5°C. ASTM A 366 simulates the waste drums to be emplaced in the repository; ASTM A 570 simulates the boxes. Brine A is a synthetic brine that, although developed to simulate fluids equilibrated with K<sup>+</sup>- and Mg<sup>2+</sup>-bearing minerals in overlying potash-rich zones prior to entering the repository (Molecke, 1983), is coincidentally similar in composition to intergranular brines from the Salado Fm. at or near the stratigraphic horizon of the WIPP underground workings. Westerman and Telander have also conducted experiments with these steels under inundated conditions with initially pure N<sub>2</sub>, CO<sub>2</sub>, and H<sub>2</sub> at high pressures (about 35 or 70 atm). Finally, they have performed preliminary experiments with these steels in simulated backfill materials (crushed salt and a mixture of 70 wt % crushed salt and 30 wt % bentonite) at low pressures. Westerman and Telander also plan to study anoxic corrosion of Al and Al-base materials.

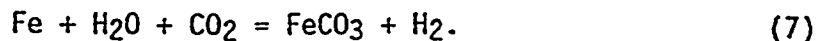
Telander and Westerman (in prep.) have identified three likely anoxic-corrosion reactions. At low fugacities (similar to partial pressures) of CO<sub>2</sub> and H<sub>2</sub>S, the reaction observed in 3-, 6-, 12-, and 24-month experiments appears to be:



However, Brush (1990) calculated that Fe(OH)<sub>2</sub> is unstable with respect to Fe<sub>3</sub>O<sub>4</sub>. Therefore, significant quantities of steels and other Fe-base alloys could eventually corrode via the reaction:



At relatively high CO<sub>2</sub> fugacities, the experimentally observed reaction is:



Formation of the adherent corrosion product  $\text{FeCO}_3$  (siderite) by this reaction will passivate steels and, presumably, other Fe-base alloys after the consumption of various quantities of  $\text{CO}_2$ . Currently, laboratory studies at PNL suggest a range of 0.33 to 2.2 moles of  $\text{CO}_2$  per  $\text{m}^2$  of steel for the amount of  $\text{CO}_2$  required for passivation, depending on the  $\text{CO}_2$  partial pressure and the pH of the brine. However, I do not recommend revision of the average-stoichiometry gas-generation model to include passivation. To avoid potential criticism, inclusion of this process would also necessitate the inclusion of depassivation, the simulation of which would require a reaction-path model such as the one Garner and I are developing.

Finally, at relatively high  $\text{H}_2\text{S}$  fugacities, the experimentally observed reaction appears to be:



Laboratory studies at PNL suggest that this reaction also passivates steels and other Fe-base alloys. However, I do not recommend revision of the average-stoichiometry model to include passivation by this reaction for the reasons given in connection with Equation 3 (above).

A literature review by Telander and Westerman (in prep.) and thermodynamic calculations for the reaction-path model have identified another possible reaction involving  $\text{H}_2\text{S}$ :



The literature reviewed by Telander and Westerman (in prep.) suggests that this reaction does not passivate steels and other Fe-base alloys. Table 1 summarizes these anoxic-corrosion reactions.

In addition to these corrosion reactions, there exist numerous likely reactions among Fe-bearing corrosion products such as  $\text{Fe}(\text{OH})_2$ ,  $\text{Fe}_3\text{O}_4$ ,  $\text{FeCO}_3$ ,  $\text{FeS}$ , and  $\text{FeS}_2$ . Garner and I are incorporating these reactions in the reaction-path model to predict, among other things, if and when depassivation of steels will occur. I do not recommend revising the average-stoichiometry model to include reactions among corrosion products.

My best estimates of  $\text{H}_2$ -production and corrosion rates for anoxic corrosion of steels and other Fe-base alloys under inundated conditions are based on data reported by Telander and Westerman (in prep.) They obtained average  $\text{H}_2$ -production rates of 0.19, 0.21, 0.16, and 0.10 moles per  $\text{m}^2$  of steel per year in experiments carried out under

inundated conditions with initially pure N<sub>2</sub> at low pressures (about 10 to 15 atm) for 3, 6, 12, and 24 months, respectively. Because there are 6 m<sup>2</sup> of steels and other Fe-base alloys per drum of CH TRU waste (Lappin et al., 1989), these rates are equivalent to 1.14, 1.26, 0.96, and 0.60 moles of H<sub>2</sub> per drum of CH TRU waste per year. The average corrosion rates in the 3-, 6-, 12-, and 24-month runs were 1.97, 1.72, 1.23, and 0.99 μm of steel per year. For my best estimates, I prefer values of 0.1 moles of H<sub>2</sub> per m<sup>2</sup> of steel per year or 0.6 moles of H<sub>2</sub> per drum of CH TRU waste per year and 1 μm of steel per year (see Table 2). These rates, from the 24-month experiments at PNL, are less by as much as about a factor of two than the rates observed in the 3-, 6-, and 12-month runs. Therefore, my best estimates are now half or about half those provided for the 1991 and 1992 PA calculations (Brush, 1991), 0.2 moles of H<sub>2</sub> per m<sup>2</sup> of steel per year, 1 mole of H<sub>2</sub> per drum of CH TRU waste per year, and 2 μm of steel per year, for which I used the 6-month results.

Strictly speaking, my best estimates of H<sub>2</sub>-production and corrosion rates for anoxic corrosion of steels and other Fe-base alloys under inundated conditions (Table 2) pertain only to Reaction 6a, the reaction which apparently occurs with initially pure N<sub>2</sub> at low and high pressures. However, I arbitrarily assume that, at any given pH, Reactions 6b, 7, 8a, and 8b occur at the same rate as Reaction 6a. Therefore, my best estimates also apply to these reactions. Clearly, Reaction 7 proceeded much faster than Reaction 6a in low-pressure, inundated experiments at PNL, at least prior to passivation (below). However, this was probably because the pH of Brine A was much lower in runs with initially pure CO<sub>2</sub> at low pressures than in runs with initially pure N<sub>2</sub> at low pressures. I describe the effects of pH in the discussion of my maximum estimates for anoxic corrosion under inundated conditions (below):

My minimum estimates of H<sub>2</sub>-production and corrosion rates for anoxic corrosion of steels and other Fe-base alloys under inundated conditions (Table 2) are based on passivation observed by Telander and Westerman (in prep.) in 6-, 12-, and 24-month, low-pressure (about 12 to 15 atm) experiments with initially pure CO<sub>2</sub>. In these runs, the H<sub>2</sub>-production and corrosion rates were high initially but decreased to 0 moles of H<sub>2</sub> per m<sup>2</sup> of steel per year or, 0 moles of H<sub>2</sub> per drum of CH TRU waste per year and 0 μm of steel per year after about 3 or 4 months due to passivation by Reaction 7 (above). Passivation at these pressures apparently required 0.33 moles of CO<sub>2</sub> per m<sup>2</sup> of steel, a very small quantity relative to the total microbial CO<sub>2</sub> production potential. My minimum estimates of these rates are identical to those provided for the 1991 and 1992 PA calculations (Brush, 1991). However, Telander and Westerman (in prep.) have now completed 12- and 24-month experiments, which confirm the results of the 6-month runs. Furthermore, since preparing their report, Westerman and Telander have also observed passivation in 6- and 12-month, high-pressure (about 36 to 40 atm) runs. These high-pressure tests partially address the concerns of those who claimed that high CO<sub>2</sub> partial pressures and concomitant acidification of brine would destabilize the passivating

film of  $\text{FeCO}_3$  and restart anoxic corrosion and  $\text{H}_2$  production. Experiments carried out to date suggest that these high  $\text{CO}_2$  partial pressures increase the quantity of  $\text{CO}_2$  required to passivate steels somewhat, from 0.33 to 2.2 moles per  $\text{m}^2$  of steel. However, this requirement is still very small relative to the total microbial  $\text{CO}_2$  production potential. On the other hand, these high  $\text{CO}_2$  partial pressures apparently decrease the time required for passivation somewhat, from about 3 or 4 months to 2 months.

At least two other passivation mechanisms are possible. First, after a few days of  $\text{H}_2$  production, Telander and Westerman (in prep.) have observed passivation of steels under inundated conditions with initially pure  $\text{H}_2\text{S}$  at low pressures (about 5 to 6 atm) for up to about 200 days. This is probably due to formation of the adherent corrosion product  $\text{FeS}_2$  (pyrite) by Reaction 8a (above). Based on preliminary results obtained with the reaction-path model, Garner and I think that  $\text{FeS}_2$  formation may be unlikely in WIPP disposal rooms. This is because  $\text{H}_2\text{S}$  fugacities high enough and  $\text{CO}_2$  and  $\text{H}_2$  fugacities low enough to stabilize  $\text{FeS}_2$  may be unlikely, given expected stoichiometries for microbial gas-production reactions. Therefore, passivation by  $\text{FeCO}_3$  appears more likely than passivation by  $\text{FeS}_2$ . However, the latter is still possible.

A second passivation mechanism is precipitation of salts on the surfaces of corroding metals due to the consumption of  $\text{H}_2\text{O}$  during anoxic corrosion (see Oxidic Corrosion above).

The results of laboratory studies of anoxic corrosion at PNL demonstrate that passivation of steels, at least by  $\text{FeCO}_3$ , is a real phenomenon under at least some combinations of conditions expected in WIPP disposal rooms. However, based on preliminary results of modeling studies, Garner and I believe that depassivation of steels is also possible, especially if consumption of  $\text{CO}_2$  by  $\text{Ca}(\text{OH})_2$  (in hydrated cementitious materials) and  $\text{CaO}$  (a potential backfill additive) decrease the fugacity of  $\text{CO}_2$  below values required to stabilize  $\text{FeCO}_3$ . Nevertheless, minimum estimates of 0 moles of  $\text{H}_2$  per  $\text{m}^2$  of steel per year or 0 moles of  $\text{H}_2$  per drum of CH TRU waste per year and 0  $\mu\text{m}$  of steel per year seem justified at this time.

For my maximum estimates of  $\text{H}_2$ -production and corrosion rates for anoxic corrosion of steels and other Fe-base alloys under inundated conditions (Table 2), I estimated the effects of pH, pressure, and temperature on these rates. These  $\text{H}_2$ -production and corrosion rates are: (1) inversely proportional to pH; (2) proportional to the partial pressures of  $\text{CO}_2$  and, probably,  $\text{H}_2\text{S}$  (both of these gases decrease the pH of any brine they are in contact with as their partial pressures increase); (3) proportional to the partial pressure of  $\text{N}_2$  and hence the total pressure; (4) inversely proportional to the partial pressure of  $\text{H}_2$ ; (5) probably proportional to temperature. I used estimated or experimentally measured relationships between these parameters and the  $\text{H}_2$ -production and corrosion rates, and estimates of the extreme values of these parameters in the repository after filling and sealing to

estimate the maximum values of these rates.

Telander and Westerman (in prep.) reported that the pH of Brine A, initially 6.7, increased to values of 8.3, 8.3, and 8.4 after the 6-, 12-, and 24-month, low-pressure experiments with initially pure N<sub>2</sub>. (They did not report the pH of Brine A after the 3-month runs.) Therefore, the best estimates of these rates (Table 2) pertain to Reaction 6a at a neutral or nearly neutral pH. I expect that the pH in WIPP disposal rooms will vary between about 3 and 12. Although obtained for applications other than the WIPP Project, the results of Uhlig and Revie (1963) and Grauer et al. (1991) suggest that the H<sub>2</sub>-production and corrosion rates for anoxic corrosion of steels are constant or essentially constant between a pH of about 4 and 10, that these rates are higher by about a factor of 50 at a pH of 3, and that they are lower by a factor of 0.05 at a pH of 11 and by a factor of 0.005 at a pH of 12. Therefore, the possibility of pH values as low as 3 in WIPP disposal rooms necessitates multiplying my best estimates in Table 2 by a factor of 50:

$$50 \cdot 0.10 \text{ moles/m}^2 = 5 \text{ moles}/(\text{m}^2 \cdot \text{yr}); \quad (9a)$$

$$50 \cdot 0.60 \text{ moles}/(\text{drum} \cdot \text{yr}) = 30 \text{ moles}/(\text{drum} \cdot \text{yr}); \quad (9b)$$

$$50 \cdot 1 \text{ } \mu\text{m}/\text{yr} = 50 \text{ } \mu\text{m}/\text{yr}. \quad (9c)$$

If acidification is caused by CO<sub>2</sub> or, perhaps, H<sub>2</sub>S (see below), the increase in rates described above may only be temporary due to passivation of steels by FeCO<sub>3</sub> or, perhaps, FeS<sub>2</sub>. However, organic acids produced by microbial degradation of cellulose in the waste (below) could also acidify the brines in WIPP disposal rooms. These acids may not result in passivation of steels. The effects of basic conditions on anoxic corrosion need not be considered here because, although they decrease these rates, my minimum estimates are already 0 moles of H<sub>2</sub> per m<sup>2</sup> of steel per year or 0 moles of H<sub>2</sub> per drum of CH TRU waste per year and 0 μm of steel per year because of passivation (see above).

Based on the results of 6-month experiments, Telander and Westerman (in prep.) reported that an N<sub>2</sub> partial pressure of 73 atm increased the average corrosion rate of steels by about a factor of two from that observed at an N<sub>2</sub> partial pressure of 10 atm. Because 73 atm is about half of lithostatic pressure at the depth of the WIPP underground workings, I assume that total pressure (the effects of which should be equivalent to those of high N<sub>2</sub> partial pressure) could increase the H<sub>2</sub>-production and corrosion rates for steels and other Fe-base alloys by as much as a factor of four. Therefore, the effect of lithostatic pressure on the rates estimated for the lowest pH expected in the repository necessitates multiplying the rates obtained from Equations

9a, 9b, and 9c by a factor of four:

$$4 \cdot 5 \text{ moles/m}^2 = 20 \text{ moles}/(\text{m}^2 \cdot \text{yr}); \quad (10a)$$

$$4 \cdot 30 \text{ moles}/(\text{drum} \cdot \text{yr}) = 120 \text{ moles}/(\text{drum} \cdot \text{yr}); \quad (10b)$$

$$4 \cdot 50 \text{ } \mu\text{m}/\text{yr} = 200 \text{ } \mu\text{m}/\text{yr}. \quad (10c)$$

High  $\text{CO}_2$  and  $\text{H}_2\text{S}$  partial pressures should increase the  $\text{H}_2$ -production and corrosion rates for anoxic corrosion of steels and other Fe-base alloys under inundated conditions, at least prior to passivation, because the solubilities of these gases in aqueous solutions are proportional to their partial pressures and they form the weak, diprotic acids  $\text{H}_2\text{CO}_3$  and  $\text{H}_2\text{S}$  after dissolution. Although weak, these acids do deprotonate to some extent, thus acidifying solutions in contact with these gases. However, I have already included the effects acidification on anoxic corrosion (see above).

The results of 6- and 12-month experiments carried out by Telander and Westerman (in prep.) suggest that  $\text{H}_2$  partial pressures of 35, 69, and 70 atm decreased the average corrosion rate of steels by about a factor of five from that observed at the  $\text{H}_2$  partial pressures in the low-pressure runs. High  $\text{H}_2$  partial pressures have the opposite effect of high  $\text{N}_2$  partial pressures (or total pressure) because  $\text{H}_2$  is a product of Reactions 6a, 6b, 7, 8a, and 8b. The effects of high  $\text{H}_2$  partial pressures on anoxic corrosion need not be addressed further because, although they decrease these rates, my minimum estimates are already 0 moles of  $\text{H}_2$  per  $\text{m}^2$  of steel per year or 0 moles of  $\text{H}_2$  per drum of CH TRU waste per year and 0  $\mu\text{m}$  of steel per year because of passivation.

Telander and Westerman (in prep.) have carried out all of their laboratory studies of anoxic corrosion at  $30 \pm 5^\circ\text{C}$ . I assume that the temperature during their experiments was normally distributed about a value of  $30^\circ\text{C}$ . Therefore, their average rates pertain to this temperature. I also assume a temperature of  $30 \pm 3^\circ\text{C}$  in WIPP disposal rooms after filling and sealing. This is slightly above the in situ temperature of  $27^\circ\text{C}$  at a subsurface depth of 2,150 feet because of the small amount of heat produced by RH TRU waste and, to a much lesser extent, by CH TRU waste. Finally, I assume that a  $10^\circ\text{C}$  increase in temperature would increase the rates of Reactions 6a, 6b, 7, 8a, and 8b by a factor of two. Therefore, the effect of a temperature of  $33^\circ\text{C}$  on the rates estimated for the lowest pH and highest total pressure expected in the repository, based on experiments carried out at  $30 \pm 5^\circ\text{C}$ , requires multiplying the rates obtained from Equations 10a, 10b, and 10c by a factor of 1.23 (obtained from  $2^{((33 - 30)/10)}$ ):

$$1.23 \cdot 20 \text{ moles}/(\text{m}^2 \cdot \text{yr}) = 20 \text{ moles}/(\text{m}^2 \cdot \text{yr}); \quad (11a)$$

$$1.23 \cdot 120 \text{ moles}/(\text{drum} \cdot \text{yr}) = 100 \text{ moles}/(\text{drum} \cdot \text{yr}); \quad (11b)$$

$$1.23 \cdot 200 \text{ } \mu\text{m}/\text{yr} = 200 \text{ } \mu\text{m}/\text{yr}. \quad (11c)$$

These are my maximum estimates, rounded to one significant figure, of these rates under inundated conditions (Table 2). They are significantly higher than those provided for the 1991 and 1992 PA calculations (Brush, 1991), 0.4 moles of H<sub>2</sub> per m<sup>2</sup> of steel per year or 2 moles of H<sub>2</sub> per drum of CH TRU waste per year and 3 μm of steel per year, because the combined effects of pH, high N<sub>2</sub> partial pressure or total pressure, and temperature have a much greater effect on these rates than high N<sub>2</sub> partial pressure, the only factor I included in my previous estimates of the maximum rates under inundated conditions.

My best estimates of H<sub>2</sub>-production and corrosion rates for anoxic corrosion of steels and other Fe-base alloys under humid conditions are 0 moles of H<sub>2</sub> per m<sup>2</sup> of steel per year or 0 moles of H<sub>2</sub> per drum of CH TRU waste per year and 0 μm of steel per year (Table 3). These rates are less than those provided for the 1991 and 1992 PA calculations (Brush, 1991), 0.02 moles of H<sub>2</sub> per m<sup>2</sup> of steel per year or 0.1 moles of H<sub>2</sub> per drum of CH TRU waste per year and 0.2 μm of steel per year, which I arbitrarily assumed were one tenth of the best estimates provided at that time for inundated conditions. As of 1991, no H<sub>2</sub> production or corrosion had occurred in 3- and 6-month humid, low-pressure experiments with initially pure N<sub>2</sub> or CO<sub>2</sub>, except for very limited H<sub>2</sub> production due to corrosion of some of the bottom 10% of the specimens splashed with brine during pretest preparation procedures. Since then, Telander and Westerman (in prep.) have obtained identical results from 6- and 12-month runs. These results confirm and extend the results of the 3- and 6-month runs. Therefore, I have reduced my best estimates as described above.

My minimum estimates of H<sub>2</sub>-production and corrosion rates for anoxic corrosion of steels and other Fe-base alloys under humid conditions are also 0 moles of H<sub>2</sub> per m<sup>2</sup> of steel per year or 0 moles of H<sub>2</sub> per drum of CH TRU waste per year and 0 μm of steel per year (Table 3). These minimum estimates are identical to those provided for the 1991 and 1992 PA calculations (Brush, 1991).

My arbitrary maximum estimates of H<sub>2</sub>-production and corrosion rates for anoxic corrosion of steels and other Fe-base alloys under humid conditions are 0.01 moles of H<sub>2</sub> per m<sup>2</sup> of steel per year or 0.06 moles of H<sub>2</sub> per drum of CH TRU waste per year and 0.1 μm of steel per year (Table 3). I arbitrarily assume that these rates are one tenth of my current best estimates for anoxic corrosion under inundated conditions. My maximum estimates for humid conditions are less than those provided for the 1991 and 1992 PA calculations (Brush, 1991), 0.2 moles of H<sub>2</sub>

per m<sup>2</sup> of steel per year, 1 mole of H<sub>2</sub> per drum of CH TRU waste per year, and 2 μm of steel per year, which I arbitrarily assumed were identical to the best estimates provided at that time for inundated conditions.

If anoxic-corrosion rates under humid conditions significantly affect the behavior of the repository, additional laboratory studies will be necessary to replace these arbitrary estimates with actual experimental results.

## MICROBIAL ACTIVITY

Microbial degradation of cellulose and, perhaps, plastics and rubbers in the waste to be emplaced in WIPP disposal rooms may, if sufficient brine or H<sub>2</sub>O vapor, nutrients, and viable microorganisms are present, produce or consume significant quantities of various gases and produce or consume significant quantities of H<sub>2</sub>O (Lappin et al., 1989; Brush, 1990). The gases produced could include CO<sub>2</sub>, CH<sub>4</sub>, H<sub>2</sub>S, N<sub>2</sub>, and NH<sub>3</sub>; the gases consumed could include CO<sub>2</sub>, H<sub>2</sub> and O<sub>2</sub>.

Brush (1990) applied the conceptual model of sequential usage of electron acceptors by microorganisms in natural environments (see, for example, Froelich et al., 1979; Berner, 1980) to WIPP disposal rooms. In natural environments, the observed sequence is aerobic respiration, NO<sub>3</sub><sup>-</sup> reduction, reduction of Mn(IV) oxides and hydroxides, reduction of Fe(III) oxides and hydroxides, SO<sub>4</sub><sup>2-</sup> reduction, and methanogenesis. Alternatively, reduction of Mn(IV) oxides and hydroxides may precede NO<sub>3</sub><sup>-</sup> reduction. Based on which potential electron acceptors will be present in significant quantities in the repository after filling and sealing, I concluded that denitrification, SO<sub>4</sub><sup>2-</sup> reduction, fermentation, and methanogenesis are potentially significant microbial processes (see Brush, 1990).

A. J. Francis and J. B. Gillow of Brookhaven National Laboratory (BNL) are carrying out laboratory studies of microbial gas production for the WIPP Project. Currently, they are conducting short- and long-term (up to 24-month) studies of microbial degradation of papers under inundated conditions with and without addition of electron acceptors and bentonite, amendment with nutrients, and inoculation with halophilic microorganisms from the WIPP Site and vicinity. They are also planning similar experiments under humid conditions and experiments with other potential substrates such as irradiated and unirradiated plastics and rubbers.

### Aerobic Microbial Activity

I concluded that aerobic microbial activity will not affect the gas and H<sub>2</sub>O budgets of WIPP disposal rooms directly (see Brush, 1990). However, this process could affect the O<sub>2</sub> budget of the repository significantly. The O<sub>2</sub> budget will in turn affect the chemical behavior

of the repository (see Oxidic Corrosion above). Furthermore, Francis and Gillow (in prep.) have observed significant aerobic microbial activity. Therefore, Garner and I have added it to the reaction-path gas-generation model.

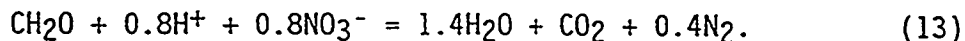
During aerobic microbial activity (or any other microbial process) the degradation of organic matter is complex and involves several intermediate steps usually mediated by different microorganisms. Geochemists have described microbial processes by writing simplified overall equations. Berner (1980) used the following equation to represent aerobic microbial activity:



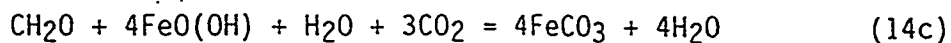
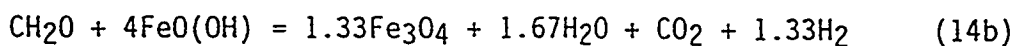
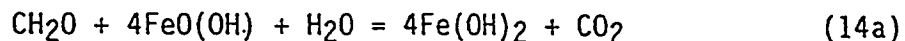
This equation uses the formula  $\text{CH}_2\text{O}$  (a simplified formula for glucose) to represent the substrate (mainly papers and other cellulose in the case of the WIPP) and does not include the synthesis of cellular material (biomass) by microorganisms. These approximations are certainly adequate for the average-stoichiometry gas-generation model, but may not be for the reaction-path model.

#### Anaerobic Microbial Activity

I also concluded that microbial denitrification could significantly affect the gas and  $\text{H}_2\text{O}$  budgets of WIPP disposal rooms (see Brush, 1990). Furthermore, Francis and Gillow (in prep.) have observed production of significant quantities of  $\text{N}_2\text{O}$ , a precursor of  $\text{N}_2$  and an indicator of denitrification. According to Berner (1980), the overall equation for denitrification is:

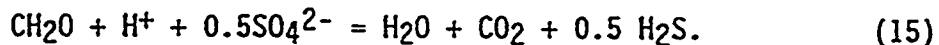


Microbial reduction of Fe(III) oxides and hydroxides will not affect on the gas and  $\text{H}_2\text{O}$  budgets of WIPP disposal rooms significantly (Brush, 1990). However, Fe(III) reduction could affect the  $\text{O}_2$  budget, which will in turn affect the chemical behavior of the repository (see Oxidic Corrosion). Therefore, Garner and I added five possible Fe(III)-reduction reactions to the reaction-path model:





Finally, microbial  $\text{SO}_4^{2-}$  reduction could affect the repository gas and  $\text{H}_2\text{O}$  budgets significantly (Brush, 1990). Francis and Gillow (in prep.) have not analyzed for  $\text{H}_2\text{S}$ , a product of  $\text{SO}_4^{2-}$  reduction. However, they have observed blackening, an indicator of  $\text{SO}_4^{2-}$  reduction, in some of their experiments. Berner (1980) gave the following overall equation for  $\text{SO}_4^{2-}$  reduction:



Finally, Brush (1990) concluded that microbial fermentation and methanogenesis could significantly affect the gas and  $\text{H}_2\text{O}$  budgets of WIPP disposal rooms. Francis and Gillow (in prep.) have not analyzed for  $\text{CH}_4$ , a product of methanogenesis. However, it would be almost impossible to rule out methanogenesis in the repository if other microbial processes are expected. Berner's (1980) overall equation for methanogenesis is:



However, the simultaneous presence of  $\text{CO}_2$  and  $\text{H}_2$  in the repository could facilitate the following reaction proposed by Francis and Gillow (in prep.):



Garner and I will include both of these equations in the reaction-path model and will probably use Equation 16b whenever both  $\text{CO}_2$  and  $\text{H}_2$  are present.

Francis and Gillow (in prep.) observed aerobic respiration, denitrification, and  $\text{SO}_4^{2-}$  reduction in their long-term study of microbial degradation of papers under inundated conditions. So far, the gas-production rates observed in these experiments have all been within the range estimated by Brush (1991) for the 1991 and 1992 PA calculations. There is probably no justification, at least on the basis of the results obtained by Francis and Gillow to date, for reducing the previously-estimated range. On the other hand, there is certainly no justification for extending it. Therefore, I recommend using the previously-provided rates again. My best estimate of the total microbial gas production rates from all of the processes

described in Reactions 12 through 16a (above) under inundated conditions is 0.1 moles of gas ( $\text{CO}_2$ ,  $\text{CH}_4$ ,  $\text{H}_2\text{S}$  and  $\text{N}_2$ ) per kg of cellulose per year. There are 10 kg of cellulose per drum of CH TRU waste (Brush, 1990). (These values do not include any cellulose in RH TRU waste.) Therefore, this rate is equivalent to 1 mole of gas per drum of CH TRU waste per year. My minimum estimate for inundated conditions is 0 moles of gas per kg of cellulose per year or 0 moles of gas per drum of CH TRU waste per year. My maximum estimate is 0.5 moles of gas per kg of cellulose per year or 5 moles of gas per drum of CH TRU waste per year.

Methanogenesis by Reaction 16b could consume significant quantities of  $\text{CO}_2$  and especially  $\text{H}_2$ . Francis and Gillow (in prep.) have not observed this reaction yet. However, if it occurs under expected WIPP conditions, this reaction could consume a significant fraction of the  $\text{CO}_2$  produced by microbial activity, the  $\text{H}_2$  produced by anoxic corrosion, or even both, depending on the ratio of  $\text{CO}_2$  to  $\text{H}_2\text{O}$  in the repository and the extent to which it proceeds. I have not estimated rates for this reaction yet. Predictions of the effects of this methanogenic reaction on the gas and  $\text{H}_2\text{O}$  budgets of the repository will require measurements of its rates of gas consumption under expected WIPP conditions and its incorporation in the reaction-path model Garner and I are developing. However, it may be possible to estimate the rate of Reaction 16b from studies carried out for application other than the WIPP Project.

Because Francis and Gillow (in prep.) have not reported any results for humid conditions yet, I recommend using the same microbial gas-production rates provided for the 1991 and 1992 PA calculations (Brush, 1991). My arbitrary best estimate of the total microbial gas production rates from all of the processes described in Reactions 12 through 16a (above) under humid conditions is 0.01 moles of gas per kg of cellulose per year or 0.1 moles of gas per drum of CH TRU waste per year. My arbitrary minimum estimate for humid conditions is 0 moles of gas per kg of cellulose per year or 0 moles of gas per drum of CH TRU waste per year. My arbitrary maximum estimate is 0.1 mole of gas per kg of cellulose per year or 1 mole of gas per drum of CH TRU waste per year. I have not estimated any rates for methanogenesis by Reaction 16b yet.

Francis and Gillow are now carrying out laboratory studies of microbial gas production under conditions at BNL. Results from these studies will eventually replace these arbitrary estimates.

## RADIOLYSIS

The rates of gas production from radiolysis of  $\text{H}_2\text{O}$  in brine and sludges in WIPP disposal rooms and radiolysis of cellulose, plastics and rubbers in the waste will probably be significantly less than those expected from anoxic corrosion or microbial activity (Molecke, 1979;

Brush, 1990). However, even if these radiolytic gas-production rates are low, Garner and I will include radiolysis in the reaction-path gas-generation model we are developing to: (1) determine if, in the event that the rates and quantities of gas produced by anoxic corrosion and microbial activity turn out to be smaller than expected, radiolysis is still a minor gas-production mechanism; (2) predict the O<sub>2</sub> budget of the repository (see Oxidative Corrosion above).

D. T. Reed and S. Okajima of Argonne National Laboratory (ANL) have quantified gas production from  $\alpha$  radiolysis of WIPP brines as a function of dissolved <sup>239</sup>Pu concentration and brine composition. It is possible to use their results to calculate gas-production rates for other Pu isotopes, particulate Pu in contact with brine (colloids suspended in brine, undissolved particles in the waste, and precipitated particles), and other actinide elements dissolved, suspended, or otherwise in contact with brine. However, I did not have time to do so prior to submission of these estimates to PA. Instead, I considered only dissolved <sup>239</sup>Pu. I am currently gathering the information required to extend these calculations to include other Pu isotopes, particulate Pu, and important isotopes of other actinide elements. Eventually, Garner and I may include some or all of these other factors in the reaction-path model.

Reed and Okajima (in prep.) have observed H<sub>2</sub> production, but not O<sub>2</sub> production, from brine radiolysis in experiments carried out with <sup>239</sup>Pu. Recently, they have observed production of both H<sub>2</sub> and O<sub>2</sub> in runs conducted with <sup>238</sup>Pu. These studies and previous laboratory studies reviewed by Reed and Okajima (in prep.) suggest that, given sufficiently high absorbed doses, the O<sub>2</sub> production rate eventually approaches 50% that of H<sub>2</sub> in both pure H<sub>2</sub>O and brines. Strictly speaking, O<sub>2</sub> is not a direct product of the radiolytic decomposition of H<sub>2</sub>O. Instead, O<sub>2</sub> forms by the breakdown of O-containing intermediate species, such as H<sub>2</sub>O<sub>2</sub> in pure H<sub>2</sub>O and, possibly, ClO<sub>3</sub><sup>-</sup> (chlorate) or ClO<sub>4</sub><sup>-</sup> (perchlorate) in brines. On the other hand, it is possible that these intermediate species will react with electron donors (reductants), such as steels, other Fe-base alloys, other metals, or organic matter, before they produce significant O<sub>2</sub>. However, to simplify brine radiolysis for the reaction-path model, Garner and I are using the equation:



Initially, we will assume that this process produces O<sub>2</sub> immediately. We may include a realistic induction period to account for the necessary build-up of O-containing intermediate species once the laboratory studies under way at ANL quantify the absorbed dose required to initiate O<sub>2</sub> production. We will then be able to calculate the time required to attain this dose as a function of the dissolved and suspended concentrations of radionuclides in WIPP brines. Until these results become available, the reaction-path model may overestimate the

time required for the repository to become anoxic and overestimate the proportion of the waste that remains oxidic in microenvironments in which brine radiolysis is the predominant redox-determining process.

Reed and Okajima (in prep.) reported  $G(H_2)$  values of 1.1 to 1.4 molecules per 100 eV for Brine A and ERDA-6, two synthetic WIPP brines, and DH-36 and G-Seep, two brines collected from the WIPP underground workings. The observed  $G(H_2)$  values are independent of the dissolved  $^{239}\text{Pu}$  concentration in these experiments. Garner and I plan to use units of moles of  $H_2$ ,  $O_2$ , or  $H_2$  plus  $O_2$  per  $m^3$  of brine per year in the reaction-path model. Therefore, I converted the results of Reed and Okajima (in prep.) from units of molecules per 100 eV to units of moles per  $m^3$  of brine as follows.

For a dissolved  $^{239}\text{Pu}$  concentration of 1 M, there are  $2.39 \cdot 10^2$  g of  $^{239}\text{Pu}$  per L of brine. The current estimate of the quantity of Pu to be emplaced in WIPP disposal rooms and the quantities of brine expected in the repository imply that there will not be enough Pu present to support an average Pu concentration of 1 M (see below). However, a local Pu concentration of 1 M may be possible in microenvironments in which Pu is highly soluble. Because there are  $1 \cdot 10^3$  L of brine per  $m^3$  of brine, the mass of  $^{239}\text{Pu}$  per  $m^3$  of brine is:

$$2.39 \cdot 10^2 \text{ g/L} \cdot 1 \cdot 10^3 \text{ L/m}^3 = 2.39 \cdot 10^5 \text{ g/m}^3. \quad (18)$$

(Only two of the figures in this and the following equations are significant, but I did not round off until the end of these calculations.) The activity of  $^{239}\text{Pu}$  per  $m^3$  of brine is:

$$2.39 \cdot 10^5 \text{ g/m}^3 \cdot 0.0613 \text{ Ci/g} = 1.46507 \cdot 10^4 \text{ Ci/m}^3. \quad (19)$$

In Equation 19, "0.0613 Ci/g" is the specific activity of  $^{239}\text{Pu}$ . The disintegration rate of  $^{239}\text{Pu}$  per  $m^3$  of brine is:

$$\begin{aligned} & 1.46507 \cdot 10^4 \text{ Ci/m}^3 \cdot 3.7 \cdot 10^{10} \text{ (d/s)/Ci} \\ & = 5.42076 \cdot 10^{14} \text{ d/(m}^3 \cdot \text{s)}. \end{aligned} \quad (20)$$

In Equation 20, "d" is the abbreviation for "disintegrations," not "days!" The energy-deposition rate per  $m^3$  of brine is:

$$\begin{aligned} & 5.42076 \cdot 10^{14} \text{ d/(m}^3 \cdot \text{s)} \cdot 5.15 \text{ MeV/d} \\ & = 2.79169 \cdot 10^{15} \text{ MeV/(m}^3 \cdot \text{s)}. \end{aligned} \quad (21)$$

In Equation 21, "5.15 MeV/d" is the average energy of an  $\alpha$  particle emitted during the disintegration of  $^{239}\text{Pu}$ . Changing units gives:

$$2.79169 \cdot 10^{15} \text{ MeV}/(\text{m}^3 \cdot \text{s}) \cdot 1 \cdot 10^6 \text{ eV/MeV} \cdot 3.15576 \cdot 10^7 \text{ s/yr} \\ = 8.80991 \cdot 10^{28} \text{ eV}/(\text{m}^3 \cdot \text{yr}). \quad (22)$$

I used a value of 1.25 molecules per 100 eV for  $G(\text{H}_2)$  (the midpoint of the range of 1.1 to 1.4 molecules per 100 eV reported by Reed and Okajima (in prep.) for Brine A, ERDA-6, DH-36, and G-Seep) to calculate the number of molecules of  $\text{H}_2$  produced per  $\text{m}^3$  of brine per year:

$$8.80991 \cdot 10^{28} \text{ eV}/(\text{m}^3 \cdot \text{yr}) \cdot 1.25 \cdot 10^{-2} \text{ molecules/eV} \\ = 1.10124 \cdot 10^{27} \text{ molecules}/(\text{m}^3 \cdot \text{yr}). \quad (23)$$

The number of moles of  $\text{H}_2$  produced per  $\text{m}^3$  of brine per year is:

$$1.10124 \cdot 10^{27} \text{ molecules}/(\text{m}^3 \cdot \text{yr}) / 6.0225 \cdot 10^{23} \text{ molecules/mole} \\ = 1.8 \cdot 10^3 \text{ moles}/(\text{m}^3 \cdot \text{yr}). \quad (24)$$

In Equation 24, " $6.0225 \cdot 10^{23}$  molecules/mole" is Avogadro's number. Of course, " $1.8 \cdot 10^3$  moles/ $(\text{m}^3 \cdot \text{yr})$ " is actually the midpoint of a range of 1.6 to  $2.0 \cdot 10^3$  moles/ $(\text{m}^3 \cdot \text{yr})$ .

I repeated these calculations for dissolved  $^{239}\text{Pu}$  concentrations of  $1 \cdot 10^{-1}$ ,  $1 \cdot 10^{-2}$ ,  $1 \cdot 10^{-3}$ ,  $1 \cdot 10^{-4}$ ,  $1 \cdot 10^{-5}$ ,  $1 \cdot 10^{-6}$ ,  $1 \cdot 10^{-7}$ ,  $1 \cdot 10^{-8}$ , and  $1 \cdot 10^{-9}$  M (see Table 4). Again, the quantity of Pu to be emplaced in WIPP disposal rooms and the quantities of brine expected in the repository imply that there will not be enough Pu present to support some of these average Pu concentrations (see below). I calculated  $\text{O}_2$ -production rates for the same dissolved  $^{239}\text{Pu}$  concentrations in these brines by assuming a value of 0.625 molecules per 100 eV for  $G(\text{O}_2)$  (half the midpoint of the observed range for  $G(\text{H}_2)$ ) and neglecting the induction period for  $\text{O}_2$  production from the breakdown of O-containing intermediate species (Table 4). (Bear in mind that O-containing intermediate species may react with electron donors in WIPP disposal rooms before they produce significant  $\text{O}_2$ .) Finally, I calculated total radiolytic gas-production rates by adding the  $\text{H}_2$ - and  $\text{O}_2$ -production rates (Table 4).

I converted these rates from units of moles of  $\text{H}_2$ ,  $\text{O}_2$ , and  $\text{H}_2$  plus  $\text{O}_2$  per  $\text{m}^3$  of brine per year to units of  $\text{H}_2$ ,  $\text{O}_2$ , and  $\text{H}_2$  plus  $\text{O}_2$  per equivalent drum of CH TRU waste per year to compare them with the rates of gas production from anoxic corrosion and microbial activity. I

multiplied each of the rates in Table 4 by 135, 305, 525, or 815 m<sup>3</sup> of brine per WIPP disposal room to convert them to units of moles of H<sub>2</sub>, O<sub>2</sub>, and H<sub>2</sub> plus O<sub>2</sub> per room per year. B. M. Butcher used these estimates of the residual gas-accessible void volume in a WIPP disposal room and immediate vicinity for his recent calculations of gas-storage capacities. I then assumed that these volumes could become inundated. Of course, brine volumes less than 135 m<sup>3</sup> are entirely possible. Next, I divided Butcher's volumes by 6,800 drums of CH TRU waste per room to obtain units of moles of H<sub>2</sub>, O<sub>2</sub>, and H<sub>2</sub> plus O<sub>2</sub> per drum per year. Tables 5, 6, and 7 give these rates for H<sub>2</sub>, O<sub>2</sub>, and H<sub>2</sub> plus O<sub>2</sub>, respectively.

To calculate the maximum average Pu concentrations as a function of brine volume and time (Table 8), I used the quantities of brine required to saturate the residual gas-accessible void volume in a WIPP disposal room (see above) and referred to the PA code DECAF to obtain the initial Pu inventory and decay predictions used for the most recent PA calculations (WIPP Performance Assessment Department, 1992). (PA personnel will also use this inventory for the round of calculations to be presented to the EPA in February 1994.) At each time (0, 100, 200, 500, 1,000, 2,000, 5,000, and 10,000 years), I added the quantities of <sup>238</sup>Pu, <sup>239</sup>Pu, <sup>240</sup>Pu, <sup>241</sup>Pu, <sup>242</sup>Pu, and <sup>244</sup>Pu present in both CH and RH TRU waste in the column labeled "Scaled Inventory" in the output files from the PA code DECAF. "Scaled inventory" refers to the quantity of Pu (or other) isotopes present in one WIPP disposal panel. I then divided these sums by 12.65, the number of equivalent WIPP disposal rooms in one panel. Next, I calculated the percentage of each isotope of Pu present at each time and calculated the average molecular weight of Pu at that time. I assumed that the molecular weight of each isotope has an integral value equal to its mass number. I then divided the total mass of Pu by 135,000, 305,000, 525,000, or 815,000 L, the quantities of brine present in 135, 305, 525, or 815 m<sup>3</sup> of brine, respectively. Finally, I divided the results by the average molecular weight of Pu at that time to obtain the concentrations shown in Table 8.

Clearly, both the dissolved <sup>239</sup>Pu and the volume of brine to which this concentration pertain will strongly affect the H<sub>2</sub>-, O<sub>2</sub>-, and H<sub>2</sub>-plus O<sub>2</sub>-production rates from brine radiolysis. If the dissolved <sup>239</sup>Pu concentration is low enough, these gas-production rates are obviously insignificant (see Tables 5, 6, and 7). On the other hand, if the dissolved <sup>239</sup>Pu concentration and the <sup>239</sup>Pu inventory are high enough, these gas-production rates can equal or even exceed those of anoxic corrosion and microbial activity, at least locally. Given a range of 135 to 815 m<sup>3</sup> of brine per room, the range of Pu solubilities and the Pu inventory assumed for WIPP disposal rooms will determine the range of radiolytic gas-production rates.

For my best estimates of the rates of gas production from brine radiolysis, I chose 6.0 · 10<sup>-10</sup> M, the midpoint of the range of Pu(V) solubilities estimated by the Radionuclide-Source-Term Expert Panel (Trauth et al., 1992). (The Expert Panel also estimated the same

midpoint for the range of Pu(IV) solubilities.) For  $^{239}\text{Pu}$ , this dissolved concentration yields rates of  $1.1 \cdot 10^{-6}$  moles of  $\text{H}_2$  per  $\text{m}^3$  per year,  $5.4 \cdot 10^{-7}$  moles of  $\text{O}_2$  per  $\text{m}^3$  per year, and  $1.6 \cdot 10^{-6}$  moles of  $\text{H}_2$  plus  $\text{O}_2$  per  $\text{m}^3$  per year, equivalent to rates of  $6.6 \cdot 10^{-8}$  moles of  $\text{H}_2$  per drum per year,  $3.3 \cdot 10^{-8}$  moles of  $\text{O}_2$  per drum per year, and  $9.9 \cdot 10^{-8}$  moles of  $\text{H}_2$  plus  $\text{O}_2$  per drum per year (Table 2). To convert from units of moles per  $\text{m}^3$  per year to moles per drum per year, I used the average of the rates for 305 and 525  $\text{m}^3$  of brine per room in Tables 5, 6, and 7.

For my minimum estimates of the rates of gas production from brine radiolysis, I used the lower limit of the range of Pu solubilities estimated by the Expert Panel and 135  $\text{m}^3$ , the lower limit of the range of residual gas-accessible void volume expected in a WIPP disposal room. (Of course, there could be less than 135  $\text{m}^3$  of brine in a room.) The Expert Panel estimated that, for expected repository conditions, the lower limit of the range of Pu solubilities is  $2.5 \cdot 10^{-17}$  M, the value estimated for Pu(V). For  $^{239}\text{Pu}$ , this dissolved concentration yields rates of  $4.5 \cdot 10^{-14}$  moles of  $\text{H}_2$  per  $\text{m}^3$  per year,  $2.2 \cdot 10^{-14}$  moles of  $\text{O}_2$  per  $\text{m}^3$  per year, and  $6.7 \cdot 10^{-14}$  moles of  $\text{H}_2$  plus  $\text{O}_2$  per  $\text{m}^3$  per year, equivalent to rates of  $8.9 \cdot 10^{-16}$  moles of  $\text{H}_2$  per drum per year,  $4.5 \cdot 10^{-16}$  moles of  $\text{O}_2$  per drum per year, and  $1.3 \cdot 10^{-15}$  moles of  $\text{H}_2$  plus  $\text{O}_2$  per drum per year (Table 2).

It may be more difficult to defend estimates of the maximum rates of gas production from brine radiolysis. The Expert Panel estimated that the upper limit of the range of Pu solubilities is  $5.5 \cdot 10^{-4}$  M, the value estimated for Pu(V). Assuming that all of the Pu present is  $^{239}\text{Pu(V)}$ , this estimate and 815  $\text{m}^3$  of brine per room (the upper limit of the range of residual gas-accessible void volume) yield upper limits of  $9.9 \cdot 10^{-1}$  moles of  $\text{H}_2$  per  $\text{m}^3$  of brine per year,  $5.0 \cdot 10^{-1}$  moles of  $\text{O}_2$  per  $\text{m}^3$  per year, and  $1.5 \cdot 10^0$  moles of  $\text{H}_2$  plus  $\text{O}_2$  per  $\text{m}^3$  per year (Table 2). Again, the current estimate of the quantity of Pu to be emplaced in the repository and 815  $\text{m}^3$  of brine per WIPP disposal room imply that there will not be enough Pu present to support an average Pu concentration of  $5.5 \cdot 10^{-4}$  M (see above). These rates are equivalent to  $1.2 \cdot 10^{-1}$  moles of  $\text{H}_2$  per drum of CH TRU waste per year,  $6.0 \cdot 10^{-2}$  moles of  $\text{O}_2$  per drum per year, and  $1.8 \cdot 10^{-1}$  moles of  $\text{H}_2$  plus  $\text{O}_2$  per drum per year (Table 2). These are my favorite estimates of the maximum gas-production rates from brine radiolysis. I like them because the Expert Panel is responsible for defending  $5.5 \cdot 10^{-4}$  M as the upper limit of the range of Pu solubilities. A reasonable way to estimate the probability distribution for values within the range of gas-production rates from brine radiolysis is to assume the same probability distribution estimated by the Expert Panel for Pu(V) solubilities.

However, I believe that  $5.5 \cdot 10^{-4}$  M may not be a defensible upper limit of the range of Pu solubilities. Pu(III) is probably more soluble than Pu(IV) and Pu(V), the only oxidation states for which the Expert Panel estimated solubilities. Furthermore, Pu(VI) could well turn out to be more soluble than Pu(III)! Presumably, the Expert Panel

did not estimate solubilities of Pu(III) and Pu(VI) because it accepted the hypothesis that Pu(III) and Pu(VI) will be unstable with respect to Pu(IV) and Pu(V) in WIPP disposal rooms and that Pu(IV) and Pu(V) will thus control the solubility of Pu. This hypothesis may be impossible to defend given the results of laboratory studies by Reed and Okajima (in prep.) in which Pu(VI) remained stable in WIPP brines for lengthy periods. They observed that Pu(VI) is the predominant form of Pu in Brine A and G Seep during stability experiments carried out for periods of over 300 and 400 days. (Stability runs are necessary to demonstrate that Pu remains in solution during an experiment to quantify gas production by brine radiolysis.) Reed and Okajima (in prep.) observed dissolved Pu(VI) concentrations on the order of  $10^{-3}$  and  $10^{-4}$  M in Brine A and G Seep during 300- and 400-day stability runs. Furthermore, they observed a Pu(VI) concentration of  $2 \cdot 10^{-2}$  M in G Seep during an 80- or 90-day stability run. Because these experiments did not contain high concentrations of the inorganic ligand  $\text{CO}_3^{2-}$ , which could significantly increase both the stability and the solubility of Pu(VI), or any organic ligands, which could also increase the stability and solubility of Pu(VI), the results are clearly not worst-case. Nevertheless,  $^{239}\text{Pu}$  concentrations on the order of  $10^{-2}$  M would, if the inventory of  $^{239}\text{Pu}$  were high enough, imply upper limits of the ranges of gas-production rates from brine radiolysis on the order of  $10^1$  moles of  $\text{H}_2$ ,  $\text{O}_2$ , and  $\text{H}_2$  plus  $\text{O}_2$  per  $\text{m}^3$  of brine per year (see Table 4) or  $10^0$  moles of  $\text{H}_2$ ,  $\text{O}_2$ , and  $\text{H}_2$  plus  $\text{O}_2$  per drum of CH TRU waste per year (Tables 5, 6, and 7). These rates are similar to those expected from anoxic corrosion and microbial activity under inundated conditions.

If a significant fraction of Pu in WIPP disposal rooms is actually present as Pu(VI), its chemical behavior would probably be similar to that of its oxidation-state analog U(VI). G. R. Choppin observed dissolved U(VI) concentrations of about  $1 \cdot 10^{-4}$  M in approximately 600-day dissolution experiments in Brine A at a pH of about 8 and  $2 \cdot 10^{-3}$  M in 250-day precipitation runs under the same conditions at Florida State University. (Dissolution and precipitation experiments, also referred to as undersaturation and supersaturation runs, bracket the solubility by approaching equilibrium from opposite directions.) These results are similar to those of the ANL stability runs. Even worse, the Expert Panel's estimate of  $1.0 \cdot 10^0$  M for the upper limit of the range of the solubility of U(VI) could apply to Pu(VI) as well. This would, if the inventory of  $^{239}\text{Pu}$  were high enough, imply upper limits of the ranges of gas-production rates from brine radiolysis on the order of  $10^3$  moles of  $\text{H}_2$ ,  $\text{O}_2$ , and  $\text{H}_2$  plus  $\text{O}_2$  per  $\text{m}^3$  of brine per year (Table 4) or  $10^2$  moles of  $\text{H}_2$ ,  $\text{O}_2$ , and  $\text{H}_2$  plus  $\text{O}_2$  per drum of CH TRU waste per year (Tables 5, 6, and 7). These rates are much higher than those expected from anoxic corrosion and microbial activity under inundated conditions.

Similarly, if a significant fraction of Pu is present as Pu(III), the Expert Panel's estimate of  $1.4 \cdot 10^0$  M for the upper limit of the range of the solubilities of Am(III) and Cm(III) could apply to Pu(III). This would also imply very high upper limits of the ranges of

gas-production rates from brine radiolysis.

It is important to point out that such high solubilities may not persist indefinitely. For example, H. Nitsche of Lawrence Berkeley Laboratory observed dissolved Pu concentrations between about  $1 \cdot 10^{-4}$  and  $1 \cdot 10^{-3}$  M for over 1 year in a precipitation experiment started with initially pure Pu(VI) in Brine A at a pH of about 7. However, after about 400 days, the concentration of Pu dropped to between  $1 \cdot 10^{-7}$  and  $1 \cdot 10^{-6}$  M. This suggests that Pu(VI) may be unstable with respect to other, less soluble oxidation states and that, given enough time, the solubility of Pu will decrease to the ranges estimated by the Expert Panel for Pu(IV) and Pu(V). Therefore, it would probably be difficult at this time to defend upper limits of the ranges of gas-production rates from brine radiolysis based on a dissolved Pu(VI) concentration of  $2 \cdot 10^{-2}$  M observed by Reed and Okajima (in prep.) during an 80- or 90-day stability experiment. It might even be difficult to defend upper limits based on Pu(VI) concentrations on the order of  $10^{-4}$  or  $10^{-3}$  M in several-hundred-day solubility or stability runs. These are the maximum average Pu concentrations that can be supported by the current inventory (see Table 8). Furthermore, even if Pu is highly soluble under some combinations of conditions in WIPP disposal rooms, brine radiolysis would, like anoxic corrosion, probably be self-limiting. This is because neither anoxic corrosion nor brine radiolysis seems to occur under humid conditions. Therefore, small quantities of brine in the repository may produce H<sub>2</sub> (in the case of anoxic corrosion) or H<sub>2</sub> and O<sub>2</sub> (in the case of brine radiolysis), increase the pressure, prevent additional brine inflow or even cause brine outflow, and thus prevent or greatly reduce additional gas production, at least by these mechanisms. However, I still feel that it may be difficult to rule out the possibility of very high (relative to anoxic corrosion and microbial activity) upper limits of the ranges of gas-production rates from brine radiolysis, at least in some microenvironments with high Pu solubilities. Furthermore, if the average Pu solubility turns out to be high, increasing the quantity of Pu to be emplaced in WIPP disposal rooms could significantly affect the gas budget of the repository, and perhaps its performance.

I calculated the gas-production potential for radiolysis of H<sub>2</sub>O in brine by <sup>239</sup>Pu as follows. According to the initial Pu inventory and decay predictions used for the most recent PA calculations (WIPP Performance Assessment Department, 1992), there will be 568,600 g of <sup>239</sup>Pu in CH TRU waste and 14,280 g of <sup>239</sup>Pu in RH TRU waste per WIPP disposal panel at the time of emplacement. After 10,000 years, there will be 426,300 g of <sup>239</sup>Pu in CH TRU waste and 10,710 g of <sup>239</sup>Pu in RH TRU waste per panel. The mass of <sup>239</sup>Pu in one panel that will decay during the 10,000-year period of performance of the repository is:

$$(568,600 \text{ g} + 14,280 \text{ g}) - (426,300 \text{ g} + 10,710 \text{ g}) = 145,870 \text{ g}. \quad (25)$$

(I do not know how many of the figures in this and the following

equations are significant, but I suspect not more than one!) The mass of  $^{239}\text{Pu}$  in an equivalent drum of CH TRU waste that will decay in 10,000 years is:

$$145,870 \text{ g/panel} / 86,000 \text{ drums/panel} = 1.69616 \text{ g/drum.} \quad (26)$$

I have included the  $^{239}\text{Pu}$  in RH TRU waste in an "equivalent drum of CH TRU waste" for the sake of completeness, but this only increases the mass of  $^{239}\text{Pu}$  per drum by about 2.5%! The number of  $^{239}\text{Pu}$  disintegrations per drum in 10,000 years will be:

$$\begin{aligned} 1.69616 \text{ g/drum} / 239 \text{ g/mole} \cdot 6.0225 \cdot 10^{23} \text{ d/mole} \\ = 4.27411 \cdot 10^{21} \text{ d.} \end{aligned} \quad (27)$$

Assuming that all of the Pu in a drum dissolves in brine at the time of emplacement and remains dissolved throughout the 10,000-year period of performance of the repository is the worst-case assumption from the standpoint of radiolytic gas production. This assumption results in initial dissolved total Pu concentrations of  $1.60 \cdot 10^{-3}$ ,  $7.09 \cdot 10^{-4}$ ,  $4.12 \cdot 10^{-4}$ , or  $2.65 \cdot 10^{-4}$ , depending on the volume of brine per WIPP disposal room (see Table 8). Half of these values are higher than  $5.5 \cdot 10^{-4}$  M, the upper limit of the range of Pu solubilities estimated by the Expert Panel. However, the laboratory studies of radionuclide chemistry described above have yielded dissolved Pu(VI) concentrations higher than  $1.60 \cdot 10^{-3}$  M, at least so far. The total quantity of energy deposited in brine by decay of  $^{239}\text{Pu}$  in 10,000 years is:

$$4.27411 \cdot 10^{21} \text{ d} \cdot 5.15 \text{ MeV/d} = 2.20117 \cdot 10^{28} \text{ eV.} \quad (28)$$

The number of moles of  $\text{H}_2$  formed is:

$$\begin{aligned} 2.20117 \cdot 10^{28} \text{ eV} \cdot 1.25 \text{ molecules/100 eV} / \\ 6.0225 \cdot 10^{23} \text{ molecules/mole} = 4.57 \cdot 10^2 \text{ moles/drum.} \end{aligned} \quad (29)$$

In Equation 29, "1.25 molecules per 100 eV" is the midpoint of the range of  $G(\text{H}_2)$  (1.1 to 1.4 molecules per 100 eV) reported by Reed and Okajima (in prep.) for three WIPP brines (see above) and " $6.0225 \cdot 10^{23}$  molecules/mole is Avogadro's number. Therefore, " $4.57 \cdot 10^2$  moles/drum" is actually the midpoint of a range of 4.02 to  $5.12 \cdot 10^2$  moles per drum.

In addition to about 500 moles of H<sub>2</sub> per drum, the O<sub>2</sub>-production potential for brine radiolysis by <sup>239</sup>Pu could be as high as about 250 moles per drum, depending on the induction period for O<sub>2</sub> production from the breakdown of O-containing intermediate species (above). However, Garner and I believe that oxidic corrosion and aerobic microbial activity (above) will rapidly consume any O<sub>2</sub> produced by brine radiolysis. Therefore, we omit O<sub>2</sub> from the discussion that follows.

Although these results includes decay of <sup>239</sup>Pu but none of the other radionuclides in TRU waste, they are of the same order of magnitude as the H<sub>2</sub>-production potential of 900 moles per drum from anoxic corrosion of steel CH TRU waste containers (drums and boxes) and steels and other Fe-base alloys in CH TRU waste (Brush, 1990). They are also similar to my calculated gas-production potential of 600 moles per drum from microbial degradation 100% of the cellulose and 50% of the rubbers in CH TRU waste.

However, values of 500 moles of H<sub>2</sub> per drum and 750 moles of H<sub>2</sub> plus O<sub>2</sub> per drum for the gas-production potential from brine radiolysis by <sup>239</sup>Pu are probably far larger than what will actually be produced in WIPP disposal rooms. The assumption that all of the energy from decay of <sup>239</sup>Pu will be deposited in brine is probably far too pessimistic. It is much more likely that a significant fraction of this decay energy will be deposited in undissolved, particulate, Pu-bearing solids or other solids with which Pu is associated (cellulose such as paper towels, articles of clothing, rubber gloves, other solids in sludges, etc.)

Preliminary results obtained after adding brine radiolysis to the PA code PANEL also suggest that actual radiolytic gas production will be much smaller than the gas-production potentials calculated above. (The addition of brine radiolysis to PANEL is the first step in the addition of brine radiolysis to the reaction-path gas-generation model.) PANEL calculates the quantities of radionuclides dissolved in brine in WIPP disposal rooms as a function of time. Currently, it uses either an internal analytical model or the two-phase flow code BRAGFLO to predict the quantity of Salado- or Castile-Fm. brine present as a function of time. It then uses Latin hypercube sampling of solubilities estimated by the Expert Panel to predict the solubilities of Pu and other important actinide elements, and uses the initial inventory and decay rates of individual isotopes of these elements to calculate the relative abundance of each dissolved radionuclide as a function of time. Garner added the equations used to calculate the gas-production potential from decay of <sup>239</sup>Pu (above) to PANEL and extended them to include other important  $\alpha$ -emitting radionuclides in the WIPP inventory. For his preliminary calculations, Garner used predictions of brine inflow and outflow from BRAGFLO runs made for the last round of PA calculations (WIPP Performance Assessment Department, 1992), which included the average-stoichiometry gas-generation model. The brine volume in a panel varied with time in each vector (simulation). However, the gas-generation rates from anoxic corrosion and microbial activity and the dissolved concentration of each

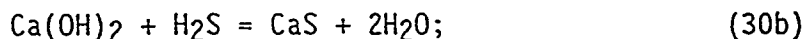
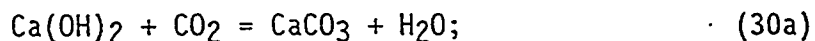
radioactive element did not vary within a given vector, unless brine was completely consumed or the quantity of a radioactive element in the inventory limited its concentration to a value less than the sampled solubility.

The largest quantity of H<sub>2</sub> produced by brine radiolysis during the 10,000-year period of performance of the repository was 90 moles per drum, a value significantly smaller than the 500-mole-per-drum H<sub>2</sub>-production potential from decay of <sup>239</sup>Pu calculated above. In this vector, the <sup>241</sup>Am was the largest contributor to radiolytic H<sub>2</sub> production. Furthermore, 50% of the 70 vectors produced less than 2 moles of H<sub>2</sub> per drum, a value less than 0.5% of the H<sub>2</sub>-production potential.

Clearly, the difference between the H<sub>2</sub>-production potential and the values calculated using PANEL suggest that gas production in WIPP disposal rooms may actually be far less than the gas-production potentials. The main reasons for this appear to be: (1) calculations of gas-production potentials often include worst-case assumptions; (2) these calculations also neglect interactions between or among processes; these interactions may significantly decrease the amount of gas produced.

#### CONSUMPTION OF GASES

The compounds Ca(OH)<sub>2</sub> (in hydrated cementitious materials and CaO (a potential backfill additive) could consume significant quantities of CO<sub>2</sub> and H<sub>2</sub>S by the reactions:



In bench-scale laboratory experiments, Ca(OH)<sub>2</sub>, dissolved in WIPP brines, reacts very rapidly with gaseous CO<sub>2</sub>. Dissolved, hydrated CaO, solid Ca(OH)<sub>2</sub> and solid CaO would probably also react very rapidly with gaseous CO<sub>2</sub>. However, the effects of transport phenomena must be incorporated in predictions of the rates of CO<sub>2</sub> and, perhaps, H<sub>2</sub>S uptake by these compounds in WIPP disposal rooms. Furthermore, estimates of the quantities of hydrated cementitious materials and the concentrations of Ca(OH)<sub>2</sub> in these materials are necessary for room-

scale predictions. Therefore, I have not estimated rates for these reactions yet.

#### REFERENCES

- Berner, R. A. (1980). *Early Diagenesis: A Theoretical Approach*. Princeton University Press, Princeton, NJ.
- Brush, L. H. (1990). *Test Plan for Laboratory and Modeling Studies of Repository and Radionuclide Chemistry for the Waste Isolation Pilot Plant*, SAND90-0266, Sandia National Laboratories, Albuquerque, NM.
- Brush, L. H. (1991). *Current Estimates of Gas Production Rates, Gas Production Potentials, and Expected Chemical Conditions Relevant to Radionuclide Chemistry for the Long-Term WIPP Performance Assessment*. In WIPP Performance Assessment Division, *Preliminary Comparison with 40 CFR Part 191, Subpart B for the Waste Isolation Pilot Plant*, December 1991, SAND91-0893/3, Sandia National Laboratories, Albuquerque, NM, pp. A-27 to A-36.
- Brush, L. H., M. A. Molecke, R. E. Westerman, A. J. Francis, J. B. Gillow, R. H. Vreeland, and D. T. Reed (1992). *Laboratory Studies of Gas Generation for the Waste Isolation Pilot Plant*. Presented at the Materials Research Society's Symposium on the Scientific Basis for Nuclear Waste Management, Boston, Ma., November 30 to December 4, 1992.
- Francis, A. J., and J. B. Gillow. *Effects of Microbial Processes on Gas Generation under Expected WIPP Conditions: Annual Report through 1992*. SAND93-7036, Sandia National Laboratories, Albuquerque, NM, in prep.
- Froelich, P. N., G. P. Klinkhammer, M. L. Bender, N. A. Luedtke, G. R. Heath, D. Cullen, P. Dauphin, D. Hammond, B. Hartman, and V. Maynard (1979). *Early Oxidation of Organic Matter in Pelagic Sediments of the Eastern Equatorial Atlantic: Suboxic Diagenesis*, *Geochimica et Cosmochimica Acta*, Vol. 43, pp. 1075-1090.
- Grauer, R., B. Knecht, P. Kreis, and J. P. Simpson (1991). *Hydrogen Evolution from Corrosion of Iron and Steel in Intermediate Level Waste Repositories*. In T. A. Abrajano, Jr., and L. H. Johnson, Eds., *Scientific Basis for Nuclear Waste Management XIV, Symposium held November 26-29, 1990, Boston, Massachusetts, U.S.A., Materials Research Society Symposia Proceedings, Vol. 44*, Materials Research Society, Pittsburgh, PA, pp. 295-302.
- Lappin, A. R., R. L. Hunter, D. P. Garber, and P. B. Davies, Eds. (1989). *Systems Analysis, Long-Term Radionuclide Transport, and Dose Assessments, Waste Isolation Pilot Plant (WIPP), Southeastern New Mexico; March, 1989*. SAND89-0462, Sandia National Laboratories, Albuquerque, NM.

- Molecke, M. A. (1979). Gas Generation from Transuranic Waste Degradation: Data Summary and Interpretation. SAND79-1245, Sandia National Laboratories, Albuquerque, NM.
- Molecke, M. A. (1983). A Comparison of Brines Relevant to Nuclear Waste Experimentation. SAND83-0516, Sandia National Laboratories, Albuquerque, NM.
- Reed, D. T., and S. Okajima. Radiation Effects Studies in Support of the Waste Isolation Pilot Plant: Progress Report for Fiscal Year 1992. SAND??-????, Sandia National Laboratories, Albuquerque, NM, in prep..
- Telander, M. R., and R. E. Westerman. Hydrogen Generation by Metal Corrosion in Simulated WIPP Environments: Progress Report for Period November 1989 - December 1992. SAND92-7347, Sandia National Laboratories, Albuquerque, NM, in prep.
- Trauth, K. M., S. C. Hora, R. P. Rechar, and D. R. Anderson (1992). The Use of Expert Judgement to Quantify Uncertainty in Solubility and Sorption Parameters for Waste Isolation Plant Performance Assessment, SAND92-0479, Sandia National Laboratories, Albuquerque, NM.
- Uhlig, H. H., and R. W. Revie (1963). Corrosion and Corrosion Control: An Introduction to Corrosion Science and Engineering. John Wiley and Sons, New York, NY.
- WIPP Performance Assessment Department (1992). Preliminary Performance Assessment for the Waste Isolation Pilot Plant, December 1992. Volume 4: Uncertainty and Sensitivity Analysis for 40 CFR 191, Subpart B. SAND92-0700/4, Sandia National Laboratories, Albuquerque, NM..

TABLE 1. GAS-GENERATION REACTIONS

Reaction	Abbreviation
Oxic corrosion of steels and other Fe-base materials:	
1. $2\text{Fe} + \text{H}_2\text{O} + 1.5\text{O}_2 = 2\gamma\text{FeO}(\text{OH})$	Fe to $\gamma\text{FeO}(\text{OH})^1$
Anoxic corrosion of steels and other Fe-base materials:	
6a. $\text{Fe} + 2\text{H}_2\text{O} = \text{Fe}(\text{OH})_2 + \text{H}_2$	Fe to $\text{Fe}(\text{OH})_2^2$
6b. $3\text{Fe} + 4\text{H}_2\text{O} = \text{Fe}_3\text{O}_4 + 4\text{H}_2$	Fe to $\text{Fe}_3\text{O}_4^2$
7. $\text{Fe} + \text{H}_2\text{O} + \text{CO}_2 = \text{FeCO}_3 + \text{H}_2$	Fe to $\text{FeCO}_3^2$
8a. $\text{Fe} + 2\text{H}_2\text{S} = \text{FeS}_2 + 2\text{H}_2$	Fe to $\text{FeS}_2^2$
8b. $\text{Fe} + \text{H}_2\text{S} = \text{FeS} + \text{H}_2$	Fe to $\text{FeS}^2$
Microbial degradation of cellulose and, perhaps, plastics and rubbers:	
12. $\text{CH}_2\text{O} + \text{O}_2 = \text{H}_2\text{O} + \text{CO}_2$	Aerobic respiration <sup>1</sup>
13. $\text{CH}_2\text{O} + 0.8\text{H}^+ + 0.8\text{NO}_3^-$ $= 1.4\text{H}_2\text{O} + \text{CO}_2 + 0.4\text{N}_2$	Denitrification <sup>2</sup>

TABLE 1. GAS-GENERATION REACTIONS (cont.)

Reaction	Abbreviation
Microbial degradation of cellulose and, perhaps, plastics and rubbers (cont.):	
14a. $\text{CH}_2\text{O} + 4\text{FeO}(\text{OH}) + \text{H}_2\text{O}$ $= 4\text{Fe}(\text{OH})_2 + \text{CO}_2$	Fe(III) reduction <sup>1</sup>
14b. $\text{CH}_2\text{O} + 4\text{FeO}(\text{OH})$ $= 1.33\text{Fe}_3\text{O}_4 + 1.67\text{H}_2\text{O} + \text{CO}_2 + 1.33\text{H}_2$	Fe(III) reduction <sup>1</sup>
14c. $\text{CH}_2\text{O} + 4\text{FeO}(\text{OH}) + \text{H}_2\text{O} + 3\text{CO}_2$ $= 4\text{FeCO}_3 + 4\text{H}_2\text{O}$	Fe(III) reduction <sup>1</sup>
14d. $\text{CH}_2\text{O} + 4\text{FeO}(\text{OH}) + 4\text{H}_2\text{S}$ $= 4\text{FeS} + 7\text{H}_2\text{O} + \text{CO}_2$	Fe(III) reduction <sup>1</sup>
14e. $\text{CH}_2\text{O} + 4\text{FeO}(\text{OH}) + 8\text{H}_2\text{S}$ $= 4\text{FeS}_2 + 7\text{H}_2\text{O} + \text{CO}_2 + 4\text{H}_2$	Fe(III) reduction <sup>1</sup>
15. $\text{CH}_2\text{O} + \text{H}^+ + 0.5\text{SO}_4^{2-}$ $= \text{H}_2\text{O} + \text{CO}_2 + 0.5 \text{H}_2\text{S}$	$\text{SO}_4^{2-}$ reduction <sup>2</sup>
16a. $2\text{CH}_2\text{O} = \text{CH}_4 + \text{CO}_2$	Methanogenesis <sup>2</sup>
16b. $\text{CO}_2 + 4\text{H}_2 = \text{CH}_4 + 2\text{H}_2\text{O}$	Methanogenesis <sup>2</sup>

TABLE 1. GAS-GENERATION REACTIONS (cont.)

Reaction	Abbreviation
Radiolysis:	
17. $H_2O = H_2 + 0.5O_2$	Radiolysis of brine <sup>1</sup>
Consumption of gases by cementitious materials and backfill additives:	
25a. $Ca(OH)_2 + CO_2 = CaCO_3 + H_2O$	$Ca(OH)_2$ to $CaCO_3$ <sup>2</sup>
25b. $Ca(OH)_2 + H_2S = CaS + 2H_2O$	$Ca(OH)_2$ to $CaS$
26a. $CaO + CO_2 = CaCO_3$	$CaO$ to $CaCO_3$ <sup>2</sup>
26b. $CaO + H_2S = CaS + H_2O$	$CaO$ to $CaS$ <sup>2</sup>

1. Probably will not have a significant, direct effect on the gas and H<sub>2</sub>O budget of WIPP disposal rooms, but could be important from the standpoint of the O<sub>2</sub> budget of the repository (see text).
2. Could have a significant, direct effect on the gas and H<sub>2</sub>O budget of the repository (see text).

TABLE 2. INUNDATED GAS-PRODUCTION RATES

Process	Gas-Production Rate		
	Minimum	Best	Maximum
<b>Oxic corrosion of steels and other Fe-base materials:</b>			
moles O <sub>2</sub> /(m <sup>2</sup> steel · yr)	0	- 5	- 8
moles O <sub>2</sub> /(drum · yr)	0 <sup>1</sup>	- 30 <sup>1</sup>	- 50 <sup>1</sup>
μm steel/yr	0	50	80
<b>Anoxic corrosion of steels and other Fe-base materials:</b>			
moles H <sub>2</sub> /(m <sup>2</sup> steel · yr)	0	0.1	20
moles H <sub>2</sub> /(drum · yr)	0 <sup>1</sup>	0.6 <sup>1</sup>	100 <sup>1</sup>
μm steel/yr	0	1	200
<b>Microbial degradation of cellulose (Reactions 12 through 16b):</b>			
moles gas/(kg cellulose · yr)	0 <sup>2</sup>	0.1 <sup>2</sup>	0.5 <sup>2</sup>
moles gas/(drum · yr)	0 <sup>1, 2</sup>	1 <sup>1, 2</sup>	5 <sup>1, 2</sup>
<b>Microbial degradation of cellulose (Reaction 16b):</b>			
moles gas/(kg cellulose · yr)	Not est. <sup>3</sup>	Not est. <sup>3</sup>	Not est. <sup>3</sup>
moles gas/(drum · yr)	Not est. <sup>3</sup>	Not est. <sup>3</sup>	Not est. <sup>3</sup>

TABLE 2. INUNDATED GAS-PRODUCTION RATES (cont.)

Reaction	Gas-Production Rate <sup>1</sup>		
	Minimum	Best	Maximum
Radiolysis of brine:			
moles H <sub>2</sub> /(m <sup>3</sup> · yr)	4.5 · 10 <sup>-14</sup>	1.1 · 10 <sup>-6</sup>	9.9 · 10 <sup>-1</sup>
moles H <sub>2</sub> /(drum · yr)	8.9 · 10 <sup>-16</sup>	6.6 · 10 <sup>-8</sup>	1.2 · 10 <sup>-1</sup>
moles O <sub>2</sub> /(m <sup>3</sup> · yr)	2.2 · 10 <sup>-14</sup>	5.4 · 10 <sup>-7</sup>	5.0 · 10 <sup>-1</sup>
moles O <sub>2</sub> /(drum · yr)	4.5 · 10 <sup>-16</sup>	3.3 · 10 <sup>-8</sup>	6.0 · 10 <sup>-2</sup>
moles (H <sub>2</sub> + O <sub>2</sub> )/(m <sup>3</sup> · yr)	6.7 · 10 <sup>-14</sup>	1.6 · 10 <sup>-6</sup>	1.5 · 10 <sup>0</sup>
moles (H <sub>2</sub> + O <sub>2</sub> )/(drum · yr)	1.3 · 10 <sup>-15</sup>	9.9 · 10 <sup>-8</sup>	1.8 · 10 <sup>-1</sup>
Consumption of CO <sub>2</sub> by cementitious materials and backfill additives:			
moles gas/(drum · yr)	Not est. <sup>4</sup>	Not est. <sup>4</sup>	Not est. <sup>4</sup>

1. Estimates do not include steels or other Fe-base alloys associated with RH TRU waste or steels or other Fe-base alloys used for ground support.
2. Gases produced by Reactions 12 through 16a could include CO<sub>2</sub>, CH<sub>4</sub>, H<sub>2</sub>S, N<sub>2</sub>, and NH<sub>3</sub> (see text).
3. Not estimated yet, but gases consumed by Reaction 16b could include significant quantities of CO<sub>2</sub> and especially H<sub>2</sub> (see text).
4. Not estimated yet, but gases consumed by Ca(OH)<sub>2</sub> and CaO in cementitious materials and backfill additives could include significant quantities of CO<sub>2</sub> and, perhaps, H<sub>2</sub>S (see text).

TABLE 3. HUMID GAS-PRODUCTION RATES

Process	Gas-Production Rate		
	Minimum	Best	Maximum
<b>Oxic corrosion of steels and other Fe-base materials:</b>			
moles O <sub>2</sub> /(m <sup>2</sup> steel · yr)	0	- 0.5	- 5
moles O <sub>2</sub> /(drum · yr)	0 <sup>1</sup>	- 3 <sup>1</sup>	- 30 <sup>1</sup>
μm steel/yr	0	5	50
<b>Anoxic corrosion of steels and other Fe-base materials:</b>			
moles H <sub>2</sub> /(m <sup>2</sup> steel · yr)	0	0	0.01
moles H <sub>2</sub> /(drum · yr)	0 <sup>1</sup>	0 <sup>1</sup>	0.06 <sup>1</sup>
μm steel/yr	0	0	0.1
<b>Microbial degradation of cellulose (Reactions 12 through 16b):</b>			
moles gas/(kg cellulose · yr)	0 <sup>2</sup>	0.01 <sup>2</sup>	0.1 <sup>2</sup>
moles gas/(drum · yr)	0 <sup>1, 2</sup>	0.1 <sup>1, 2</sup>	1 <sup>1, 2</sup>
<b>Microbial degradation of cellulose (Reaction 16b):</b>			
moles gas/(kg cellulose · yr)	Not set. <sup>3</sup>	Not est. <sup>3</sup>	Not est. <sup>3</sup>
moles gas/(drum · yr)	Not est. <sup>3</sup>	Not est. <sup>3</sup>	Not est. <sup>3</sup>

TABLE 3. HUMID GAS-PRODUCTION RATES (cont.)

Process	Gas-Production Rate		
	Minimum	Best	Maximum
<b>Radiolysis of brine:</b>			
moles H <sub>2</sub> /(m <sup>3</sup> · yr)	0	0	0
moles H <sub>2</sub> /(drum · yr)	0	0	0
moles O <sub>2</sub> /(m <sup>3</sup> · yr)	0	0	0
moles O <sub>2</sub> /(drum · yr)	0	0	0
moles (H <sub>2</sub> + O <sub>2</sub> )/(m <sup>3</sup> · yr)	0	0	0
moles (H <sub>2</sub> + O <sub>2</sub> )/(drum · yr)	0	0	0
<b>Consumption of gases by cementitious materials and backfill additives:</b>			
moles gas/(drum · yr)	Not est. <sup>4</sup>	Not est. <sup>4</sup>	Not est. <sup>4</sup>

1. Estimates do not include steels or other Fe-base alloys associated with RH TRU waste or steels or other Fe-base alloys used for ground support.
2. Gases produced by Reactions 12 through 16a could include CO<sub>2</sub>, CH<sub>4</sub>, H<sub>2</sub>S, N<sub>2</sub>, and NH<sub>3</sub> (see text).
3. Not estimated yet, but gases consumed by Reaction 16b could include significant quantities of CO<sub>2</sub> and especially H<sub>2</sub> (see text).
4. Not estimated yet, but gases consumed by Ca(OH)<sub>2</sub> and CaO in cementitious materials and backfill additives could include significant quantities of CO<sub>2</sub> and, perhaps, H<sub>2</sub>S (see text).

TABLE 4. RADIOLYTIC GAS-PRODUCTION RATES (mol/m<sup>3</sup> of brine·yr)<sup>1, 2</sup>

Dissolved <sup>239</sup> Pu Conc. (M)	Gas-Production Rate		
	H <sub>2</sub>	O <sub>2</sub>	H <sub>2</sub> + O <sub>2</sub>
1 · 10 <sup>0</sup>	1.8 · 10 <sup>3</sup>	0.9 · 10 <sup>3</sup>	2.7 · 10 <sup>3</sup>
1 · 10 <sup>-1</sup>	1.8 · 10 <sup>2</sup>	0.9 · 10 <sup>2</sup>	2.7 · 10 <sup>2</sup>
1 · 10 <sup>-2</sup>	1.8 · 10 <sup>1</sup>	0.9 · 10 <sup>1</sup>	2.7 · 10 <sup>1</sup>
1 · 10 <sup>-3</sup>	1.8 · 10 <sup>0</sup>	0.9 · 10 <sup>0</sup>	2.7 · 10 <sup>0</sup>
1 · 10 <sup>-4</sup>	1.8 · 10 <sup>-1</sup>	0.9 · 10 <sup>-1</sup>	2.7 · 10 <sup>-1</sup>
1 · 10 <sup>-5</sup>	1.8 · 10 <sup>-2</sup>	0.9 · 10 <sup>-2</sup>	2.7 · 10 <sup>-2</sup>
1 · 10 <sup>-6</sup>	1.8 · 10 <sup>-3</sup>	0.9 · 10 <sup>-3</sup>	2.7 · 10 <sup>-3</sup>
1 · 10 <sup>-7</sup>	1.8 · 10 <sup>-4</sup>	0.9 · 10 <sup>-4</sup>	2.7 · 10 <sup>-4</sup>
1 · 10 <sup>-8</sup>	1.8 · 10 <sup>-5</sup>	0.9 · 10 <sup>-5</sup>	2.7 · 10 <sup>-5</sup>
1 · 10 <sup>-9</sup>	1.8 · 10 <sup>-6</sup>	0.9 · 10 <sup>-6</sup>	2.7 · 10 <sup>-6</sup>

1. Rates in moles per m<sup>3</sup> of brine per year calculated from experimentally measured values of G(H<sub>2</sub>) (see text).
2. Values in bold type may exceed the maximum average Pu concentration or average gas-production rate depending on the quantity of brine present and time (see text).

TABLE 5. RADIOLYTIC H<sub>2</sub>-PRODUCTION RATES (mol/drum-yr)<sup>1, 2</sup>

Dissolved <sup>239</sup> Pu Conc. (M)	Brine Volume (m <sup>3</sup> /room)			
	135	305	525	815
1 · 10 <sup>0</sup>	3.6 · 10 <sup>1</sup>	8.1 · 10 <sup>1</sup>	1.4 · 10 <sup>2</sup>	2.2 · 10 <sup>2</sup>
1 · 10 <sup>-1</sup>	3.6 · 10 <sup>0</sup>	8.1 · 10 <sup>0</sup>	1.4 · 10 <sup>1</sup>	2.2 · 10 <sup>1</sup>
1 · 10 <sup>-2</sup>	3.6 · 10 <sup>-1</sup>	8.1 · 10 <sup>-1</sup>	1.4 · 10 <sup>0</sup>	2.2 · 10 <sup>0</sup>
1 · 10 <sup>-3</sup>	3.6 · 10 <sup>-2</sup>	8.1 · 10 <sup>-2</sup>	1.4 · 10 <sup>-1</sup>	2.2 · 10 <sup>-1</sup>
1 · 10 <sup>-4</sup>	3.6 · 10 <sup>-3</sup>	8.1 · 10 <sup>1-3</sup>	1.4 · 10 <sup>-2</sup>	2.2 · 10 <sup>-2</sup>
1 · 10 <sup>-5</sup>	3.6 · 10 <sup>-4</sup>	8.1 · 10 <sup>-4</sup>	1.4 · 10 <sup>-3</sup>	2.2 · 10 <sup>-3</sup>
1 · 10 <sup>-6</sup>	3.6 · 10 <sup>-5</sup>	8.1 · 10 <sup>-5</sup>	1.4 · 10 <sup>-4</sup>	2.2 · 10 <sup>-4</sup>
1 · 10 <sup>-7</sup>	3.6 · 10 <sup>-6</sup>	8.1 · 10 <sup>-6</sup>	1.4 · 10 <sup>-5</sup>	2.2 · 10 <sup>-5</sup>
1 · 10 <sup>-8</sup>	3.6 · 10 <sup>-7</sup>	8.1 · 10 <sup>-7</sup>	1.4 · 10 <sup>-6</sup>	2.2 · 10 <sup>-6</sup>
1 · 10 <sup>-9</sup>	3.6 · 10 <sup>-8</sup>	8.1 · 10 <sup>-8</sup>	1.4 · 10 <sup>-7</sup>	2.2 · 10 <sup>-7</sup>

1. Rates in moles per drum per year calculated from values in moles per m<sup>3</sup> of brine per year (see text).
2. Values in bold type may exceed the maximum average H<sub>2</sub>-production rate depending on the quantity of brine present and time (see text).

TABLE 6. RADIOLYTIC O<sub>2</sub>-PRODUCTION RATES (mol/drum·yr)<sup>1, 2</sup>

Dissolved <sup>239</sup> Pu Conc. (M)	Brine Volume (m <sup>3</sup> /room)			
	135	305	525	815
1 · 10 <sup>0</sup>	1.8 · 10 <sup>1</sup>	4.0 · 10 <sup>1</sup>	6.9 · 10 <sup>1</sup>	1.1 · 10 <sup>2</sup>
1 · 10 <sup>-1</sup>	1.8 · 10 <sup>0</sup>	4.0 · 10 <sup>0</sup>	6.9 · 10 <sup>0</sup>	1.1 · 10 <sup>1</sup>
1 · 10 <sup>-2</sup>	1.8 · 10 <sup>-1</sup>	4.0 · 10 <sup>-1</sup>	6.9 · 10 <sup>-1</sup>	1.1 · 10 <sup>0</sup>
1 · 10 <sup>-3</sup>	1.8 · 10 <sup>-2</sup>	4.0 · 10 <sup>-2</sup>	6.9 · 10 <sup>-2</sup>	1.1 · 10 <sup>-1</sup>
1 · 10 <sup>-4</sup>	1.8 · 10 <sup>-3</sup>	4.0 · 10 <sup>-3</sup>	6.9 · 10 <sup>-3</sup>	1.1 · 10 <sup>-2</sup>
1 · 10 <sup>-5</sup>	1.8 · 10 <sup>-4</sup>	4.0 · 10 <sup>-4</sup>	6.9 · 10 <sup>-4</sup>	1.1 · 10 <sup>-3</sup>
1 · 10 <sup>-6</sup>	1.8 · 10 <sup>-5</sup>	4.0 · 10 <sup>-5</sup>	6.9 · 10 <sup>-5</sup>	1.1 · 10 <sup>-4</sup>
1 · 10 <sup>-7</sup>	1.8 · 10 <sup>-6</sup>	4.0 · 10 <sup>-6</sup>	6.9 · 10 <sup>-6</sup>	1.1 · 10 <sup>-5</sup>
1 · 10 <sup>-8</sup>	1.8 · 10 <sup>-7</sup>	4.0 · 10 <sup>-7</sup>	6.9 · 10 <sup>-7</sup>	1.1 · 10 <sup>-6</sup>
1 · 10 <sup>-9</sup>	1.8 · 10 <sup>-8</sup>	4.0 · 10 <sup>-8</sup>	6.9 · 10 <sup>-8</sup>	1.1 · 10 <sup>-7</sup>

1. Rates in moles per drum per year calculated from experimentally measured values of G(H<sub>2</sub>) (see text).
2. Values in bold type may exceed the maximum average O<sub>2</sub>-production rate depending on the quantity of brine present and time (see text).

TABLE 7. RADIOLYTIC GAS- (H<sub>2</sub> + O<sub>2</sub>)-PRODUCTION RATES (mol/drum-yr)<sup>1, 2</sup>

Dissolved <sup>239</sup> Pu Conc. (M)	Brine Volume (m <sup>3</sup> /room)			
	135	305	525	815
1 · 10 <sup>0</sup>	5.4 · 10 <sup>1</sup>	1.2 · 10 <sup>2</sup>	2.1 · 10 <sup>2</sup>	3.2 · 10 <sup>2</sup>
1 · 10 <sup>-1</sup>	5.4 · 10 <sup>0</sup>	1.2 · 10 <sup>1</sup>	2.1 · 10 <sup>1</sup>	3.2 · 10 <sup>1</sup>
1 · 10 <sup>-2</sup>	5.4 · 10 <sup>-1</sup>	1.2 · 10 <sup>0</sup>	2.1 · 10 <sup>0</sup>	3.2 · 10 <sup>0</sup>
1 · 10 <sup>-3</sup>	5.4 · 10 <sup>-2</sup>	1.2 · 10 <sup>-1</sup>	2.1 · 10 <sup>-1</sup>	3.2 · 10 <sup>-1</sup>
1 · 10 <sup>-4</sup>	5.4 · 10 <sup>-3</sup>	1.2 · 10 <sup>-2</sup>	2.1 · 10 <sup>-2</sup>	3.2 · 10 <sup>-2</sup>
1 · 10 <sup>-5</sup>	5.4 · 10 <sup>-4</sup>	1.2 · 10 <sup>-3</sup>	2.1 · 10 <sup>-3</sup>	3.2 · 10 <sup>-3</sup>
1 · 10 <sup>-6</sup>	5.4 · 10 <sup>-5</sup>	1.2 · 10 <sup>-4</sup>	2.1 · 10 <sup>-4</sup>	3.2 · 10 <sup>-4</sup>
1 · 10 <sup>-7</sup>	5.4 · 10 <sup>-6</sup>	1.2 · 10 <sup>-5</sup>	2.1 · 10 <sup>-5</sup>	3.2 · 10 <sup>-5</sup>
1 · 10 <sup>-8</sup>	5.4 · 10 <sup>-7</sup>	1.2 · 10 <sup>-6</sup>	2.1 · 10 <sup>-6</sup>	3.2 · 10 <sup>-6</sup>
1 · 10 <sup>-9</sup>	5.4 · 10 <sup>-8</sup>	1.2 · 10 <sup>-7</sup>	2.1 · 10 <sup>-7</sup>	3.2 · 10 <sup>-7</sup>

1. Rates in moles per drum per year calculated from experimentally measured values of G(H<sub>2</sub>) (see text).
2. Values in bold type may exceed the maximum average gas-production rate depending on the quantity of brine present and time (see text).

TABLE 8. MAXIMUM AVERAGE Pu CONCENTRATIONS IN BRINES IN WIPP DISPOSAL ROOMS (M)<sup>1</sup>

Time (yr)	Brine Volume (m <sup>3</sup> /room)			
	135	305	525	815
0	1.60 · 10 <sup>-3</sup>	7.09 · 10 <sup>-4</sup>	4.12 · 10 <sup>-4</sup>	2.65 · 10 <sup>-4</sup>
100	1.56 · 10 <sup>-3</sup>	6.91 · 10 <sup>-4</sup>	4.02 · 10 <sup>-4</sup>	2.59 · 10 <sup>-4</sup>
200	1.54 · 10 <sup>-3</sup>	6.84 · 10 <sup>-4</sup>	3.97 · 10 <sup>-4</sup>	2.56 · 10 <sup>-4</sup>
500	1.52 · 10 <sup>-3</sup>	6.73 · 10 <sup>-4</sup>	3.91 · 10 <sup>-4</sup>	2.52 · 10 <sup>-4</sup>
1,000	1.49 · 10 <sup>-3</sup>	6.61 · 10 <sup>-4</sup>	3.84 · 10 <sup>-4</sup>	2.47 · 10 <sup>-4</sup>
2,000	1.44 · 10 <sup>-3</sup>	6.39 · 10 <sup>-4</sup>	3.71 · 10 <sup>-4</sup>	2.39 · 10 <sup>-4</sup>
5,000	1.31 · 10 <sup>-3</sup>	5.78 · 10 <sup>-4</sup>	3.36 · 10 <sup>-4</sup>	2.16 · 10 <sup>-4</sup>
10,000	1.11 · 10 <sup>-3</sup>	4.92 · 10 <sup>-4</sup>	2.86 · 10 <sup>-4</sup>	1.84 · 10 <sup>-4</sup>

1. Calculations include all isotopes of Pu expected in the repository, not just <sup>239</sup>Pu (see text).

Distribution:

J. N. Butler, Harvard University  
A. J. Francis, Brookhaven National Laboratory  
J. B. Gillow, Brookhaven National Laboratory  
D. T. Reed, Argonne National Laboratory  
R. H. Vreeland, West Chester University  
R. E. Westerman, Pacific Northwest Laboratory  
6115 P. B. Davies  
6119 F. Gelbard, Acting  
6121 J. R. Tillerson  
6303 W. D. Weart  
6305 S. A. Goldstein  
6305 A. R. Lappin  
6306 A. L. Stevens  
6342 D. R. Anderson  
6342 Staff  
6343 V. Harper-Slaboszewicz  
6345 R. C. Lincoln  
6345 Staff  
6347 D. R. Schafer  
6347 Staff  
6348 J. T. Holmes  
6348 Staff  
6352 SWCF (6): RC (WBS 1.1.1.1.3), RC/AC (WBS 1.1.1.1.3), RC/MA  
(WBS 1.1.1.1.3), RC/R (WBS 1.1.1.1.3), RC/BA (WBS 1.1.1.1.3),  
RC/GGM (WBS 1.1.1.2.5)

Intentionally Left Blank

**Butcher, March 2, 1995**

Date: 3/2/95  
To: N. Prindle  
From: B.M. Butcher, R. Anderson, B. Thompson  
Subject: SPM-2 EA Case 2

**Intentionally Left Blank**

# Sandia National Laboratories

Albuquerque, New Mexico 87185-1341

date: March 2, 1995

to: Nancy Prindle, 6705, MS 1335

*B. M. Butcher for*

from: Barry Butcher, 6378, MS 1341, Rip Anderson, 6749, Bill Thompson, WTAC

subject: SPM-2 EA Case 2

Case 2 of the proposed SPM-2 Engineering alternatives is described as "backfill (clay-like) and waste modification (clay injected into the drums to eliminate void volume and surround the waste) with pH buffer in combination with non-corroding waste containers." This case is envisioned as an idealized EA backfill-waste configuration in which the principal attribute of the backfill is the reduction of brine flow. Other enhancements, such as pH control, and reduction of the potential for cuttings releases are also considered feasible. While a backfill material or materials satisfying these specifications has not yet been identified, the properties assumed for this case are considered reasonable for clay-like materials, and a basis for material selection.

## Clay-like Backfill

Recommended properties for EA Case 2:

<u>property</u>	<u>range</u>	<u>expected value</u>	<u>comments</u>
porosity	0.1 - 0.4	0.25	Assume 100% saturation
permeability	$10^{-19}$ - $10^{-15}$ m <sup>2</sup>	$10^{-17}$ m <sup>2</sup>	
compressibility	$10^{-8}$ - $10^{-6}$ Pa	$10^{-7}$ Pa	
spalling release factor	0.001 - 0.1	0.1	Expected to be comparable to grouted waste
"puddle factor" (brine wetting phase saturation limit)			Ignore the 0.5 value used for the baseline and use the same residual saturations wetting phase values used in the SPM-2 baseline

## Comments on Case 2

Use of a clay-like backfill is subject to several common concerns that need to be resolved. The first is in regard to the effect of gas generation on a clay barrier. The clay is expected to be emplaced in a fully or partially saturated state, in effect constituting an additional source

of water for gas generation. The concern has been expressed that this additional water will adversely increase the rate of gas production, causing gas to penetrate the backfill barrier and destroy it. Instead, generation of some gas may be beneficial. In the best scenario, a gas pocket would surround the waste, isolating it from further contact with water or brine, self-limiting further gas production. In a less desirable scenario, the pressure of the gas would increase to the point where a leakage path through the barrier would form, excess gas would vent, and the clay would be sufficiently plastic (a design requirement) to "reheal". Periodic gas venting followed by re-establishment of the barrier after a drop in pore pressure could occur. Both of these gas generation scenarios are likely to support rather than contradict the barrier concept by preventing, or severely limiting flow of brine flow through and away from the waste: gas can get out, but brine can't easily contact the waste. Additional support for the use of clay as a barrier, comes, in fact, from archeologic analogues where long-term preservation probably occurred probably because the clay kept water away from the site.

The recommendation is made that backfill cells surround the waste cells in the BRAGFLO model geometry, to preserve the barrier concept.

The second common concern is in regard to the long-term stability of the clay, and the fact that a material that would adversely influence other system parameters would not be desirable. Alteration to another material would not be considered adverse, if changes in plasticity and permeability were minimal. However, any change that would increase the solubility of contaminants in brine, colloid production would be unacceptable, or adversely influence any other parameters is unacceptable.

#### pH Buffer Volume

The second topic of this memo is in regard to the volume occupied by a  $\text{Ca}^{++}$  ion buffer material, in this case something like  $\text{CaCO}_3$ , and if this might constitute a major component of the backfill volume. The conclusion of this calculation is that the buffer volume/room would be  $25 \text{ m}^3$ , or 2.5% of the total volume of  $2000 \text{ m}^3$  available for backfilling, and thus negligible. Assumptions were that 100 grams/(liter of brine) buffer material would be required, for a brine volume in the room of the order of  $500 \text{ m}^3$ , and that the buffer material has an order of magnitude density of  $2 \text{ grams/cm}^3$ .

Copies to:

MS 1335 Steve A. Goldstein (6705)  
MS 1335 Deidre Boak (6705)  
MS 1335 Fred T. Mendenhall (6705)  
MS 1335 David Rudeen (6705)  
MS 1335 Walt Beyeler (6705) MS 1335  
MS 1335 Nancy Hetrick  
MS 1341 John Theis  
MS 1341 Elaine Baker  
MS 1341 B. M. Butcher (day file) (6348)  
MS 1341 J. T. Holmes (6348)  
MS 1330 SWCF(DRM) (WBS 1.1.1.2.3) (6352)  
MS 1330 SWCF 1.1.7.2-A, CO/SPM-2 (Engineered Alternatives)  
MS 1328 D. R. Anderson (6749)  
MS 1328 M Marietta (6749)  
MS 1328 P Vaughn (6749)  
T. W. Thompson (WTAC)

Intentionally Left Blank

**Drez, January 3, 1995**

Date: 1/3/95  
To: File  
From: P. Drez  
Subject: Waste Material Parameter and Radionuclide Inventories for SPM-2 Calculations  
Derived from Draft WTWBIR Rev. 1 and IDB Rev. 10 Databases.

Intentionally Left Blank

Date: January 3, 1995  
From: Paul E. Drez *PEO*  
To: File  
Subject: Waste material parameter and radionuclide inventories for SPM2 calculations derived from DRAFT WTWBIR Rev. 1 and IDB Rev. 10 databases

---

#### Waste Material Parameter Data

The waste material parameter data for CH-TRU and RH-TRU wastes are reported in the attached Tables 1 and 2. These tables replace Tables 6-2 and 6-3 of Rev. 0 of the WTWBIR and subsequent internal revisions supplied to Sandia/NM on September 27, 1994 and November 29, 1994. Sandia/NM should assume for the attached tables the design basis volumes for CH-TRU ( $1.75E+05 \text{ m}^3 \approx 6.2E+06 \text{ ft}^3$ ) and RH-TRU ( $7080 \text{ m}^3 \approx 7955 \text{ canisters} \times 0.89 \text{ m}^3/\text{canister}$ ) wastes. Estimates of waste container materials have been provided at the bottom of the tables.

The stored and projected CH-TRU volumes for WIPP CH-TRU wastes from the Rev. 1 WTWBIR (due out 1/31/95) database has now increased to approximately  $1.6E+05 \text{ m}^3$  (from  $1.27E+05 \text{ m}^3$  in WTWBIR Rev. 0), requiring only a small amount of scaling to the WIPP design volume. One of the main reasons for this is the large projected volume of CH-TRU waste from the Savannah River Site (SRS).

#### Radionuclide Inventory Data

The WTWBIR effort has been aimed at deriving an inventory on a waste stream basis, rather than reporting "upper level" waste volumes as published in the IDB. For the Rev. 1 data submitted by the TRU waste generator/storage sites, we still do not have closure between the volume data in the IDB and the WTWBIR, that is, the volumes for the waste streams at some sites do not add up to the "total" volumes in the IDB. This closure should be achieved with the Rev. 2 WTWBIR data call due out by March 1995. Therefore, we have used the volume data from the DRAFT Rev. 10 IDB database to make the estimates of stored and projected volumes used in deriving the radionuclide information. By using the volume and radionuclide data from the IDB database, we have one internally consistent set of data for estimating the radionuclide inventory.

Table 3 represents the total radionuclide inventory for CH-TRU and RH-TRU wastes as derived from the Rev. 10 IDB database (to be published in the Spring of 1995). Sandia should use these numbers for the total design inventory for CH-TRU and RH-TRU as earlier defined in this memo. No calculations are necessary.

A few points of note about the inventory are included below:

- The total radionuclide inventory for CH-TRU waste is much higher than that included in the Rev. 0 of the WTWBIR. This is primarily due to two changes:

- The SRS has reported a large volume of CH-TRU projected waste in the IDB ( $\sim 5.1E+04$  m<sup>3</sup>), which was previously reported as "unknown." With the historically high Pu-238 content, this considerably raises the total curies in the CH-TRU inventory.
- During the calculations for the Rev. 0 inventory, the "projected" part (1993-2022) of the CH-TRU radionuclide inventory was accidentally left out of the totals reported, causing the inventory numbers to be low ( $\sim 25\%$ ). This has been corrected in this inventory definition.
- The total radionuclide inventory for RH-TRU waste is also much higher than that included in the Rev. 0 of the WTWBIR. During calculation of the RH-TRU inventory the volume defined by the sites included more waste than the repository could hold. I did not realize that the IDB radionuclide numbers only covered the "stored" part of the inventory. This made the WTWBIR reported RH-TRU inventory low by a factor of approximately 3-4. This has been corrected in this inventory definition.
- Considerably more RH-TRU waste has been reported in the Rev. 1 data submittals from the TRU waste generator/storage sites than the design capacity of WIPP. This is due to a very large submittal of RH-TRU waste from Hanford and a much smaller amount from SRS. The two sites were unable to define a radionuclide inventory for these waste streams. Therefore, these projected waste streams have been "set aside" and the calculations included in this memo use only those stored RH-TRU waste streams for which radionuclide data was submitted in the IDB. These stored volumes of RH-TRU waste, and the associated radionuclide inventories, have been use to correct for projected volumes and then scaling (as defined in Rev. 0 of the WTWBIR) of the RH-TRU volumes and radionuclide inventories to the design basis for WIPP (7955 canisters).
- Oak Ridge National Laboratory (ORNL) has not revised their ultra conservative estimate for U-235 in RH-TRU waste. Therefore, the U-235 number included in this data package is the same calculated number that was reported in the memo to file dated September 27, 1994, previously provided to Sandia.

The number is derived from the anticipated initial transportation limit in the RH-TRU cask of 325 grams of Pu-239 fissile gram equivalent (FGE). Assuming a 1:1 equivalence of U-235 FGE (as required by the TRUPACT-II SARP) to Pu-239, this provides a bounding limit of 325 grams of U-235/canister X 7955 canisters x  $2.19E-06$  curies/gram = 5.66 curies of U-235 in RH-TRU waste inventory. This number has been substituted in Table 3 to replace the overly conservative data reported by ORNL.

cc: Jimmy Dyke, DOE-CAO  
 John Suermann, DOE-CAO  
 J. Williams, DOE-EM-30  
 R. Lincoln, SNL/NM  
 D. Schafer, SNL/NM  
 F. Mendenhall, SNL/NM

# D

Table 1. CH-TRU WIPP Matrix Waste Parameter Profile Data for SPM-2

	Materials	(Kg/m <sup>3</sup> )		
		Maximum	Average	Minimum
Inorganics	Iron Based	2.5E+03	1.4E+02	0.0E+00
	Aluminum Based	1.3E+03	2.1E+01	0.0E+00
	Other Metals	1.4E+03	4.7E+01	0.0E+00
	Other Inorganics	2.1E+03	2.7E+01	0.0E+00
Organics	Cellulose	9.6E+02	1.3E+02	0.0E+00
	Rubber	6.8E+02	1.6E+01	0.0E+00
	Plastics	8.9E+02	5.1E+01	0.0E+00
Solidified Materials	Inorganic	2.2E+03	2.1E+02	0.0E+00
	Organic	1.4E+03	4.0E+00	0.0E+00
Soils		1.6E+03	7.9E+00	0.0E+00
Container Materials	Steel		1.4E+02	
	Plastic/Liners		3.2E+01	

# F

# T

D

Table 2. RH-TRU WIPP Matrix Waste Parameter Profile Data for SPM-2

	Materials	(Kg/m3)		
		Maximum	Average	Minimum
Inorganics	Iron Based	2.5E+03	1.3E+02	0.0E+00
	Aluminum Based	6.1E+02	3.1E+01	0.0E+00
	Other Metals	9.1E+02	4.9E+00	0.0E+00
	Other Inorganics	2.0E+03	3.3E+00	0.0E+00
Organics	Cellulose	4.8E+02	1.1E+01	0.0E+00
	Rubber	1.9E+02	3.1E+00	0.0E+00
	Plastics	5.5E+02	1.9E+01	0.0E+00
Solidified Materials	Inorganic	1.1E+03	1.3E+01	0.0E+00
	Organic	3.0E+00	6.4E-04	0.0E+00
Soils		1.9E+02	1.9E+00	0.0E+00
Container Materials	Steel		4.5E+02	
	Plastic/Liners		1.0E+00	
	Lead		4.7E+02	
	Steel Plug		2.2E+03	

F

T

Table 3. CH-TRU and RH-TRU Radionuclide Inventory for SPM 2 Calculations

Radionuclide	CH Curies	RH Curies
Ac-227	1.17E+00	3.35E-03
Am-240	1.61E-02	0.00E+00
Am-241	2.40E+05	2.21E+02
Am-243	3.57E+01	3.90E-03
Ba-137M	1.59E+04	3.77E+05
Bi-214	4.80E-02	0.00E+00
Bk-249	5.88E+02	6.70E-04
C-14	5.42E-04	7.91E+01
Cd-109	6.68E+03	0.00E+00
Ce-144	1.42E+04	3.58E+05
Cf-249	5.33E-02	4.52E-02
Cf-250	5.40E-01	6.09E-01
Cf-251	4.03E-03	0.00E+00
Cf-252	2.96E+03	2.01E+02
Cm-242	6.73E+01	0.00E+00
Cm-243	1.59E+00	1.22E+03
Cm-244	1.38E+04	7.73E+03
Cm-245	4.25E+01	0.00E+00
Cm-246	1.08E-01	0.00E+00
Cm-248	2.46E-02	00.0E+00
Co-58	2.04E+03	2.58E+05
Co-60	3.02E+02	1.61E+04
Cr-51	1.84E+02	2.30E+04
Cs-134	3.69E+02	1.48E+04
Cs-137	2.07E+04	5.53E+05
Es-253	1.02E+01	0.00E+00
Es-254	1.99E-02	0.00E+00
Es-254M	1.40E+01	0.00E+00
Eu-150	4.50E-05	0.00E+00
Eu-152	8.96E+01	3.76E+04
Eu-154	8.86E+01	2.29E+04
Eu-155	5.84E+01	6.71E+03
Fe-55	6.11E-04	1.99E+01
Fe-59	2.32E+01	2.31E+03
H-3	2.07E+00	4.66E+01
Kr-85	4.00E-01	4.83E+01
Mn-54	1.40E+03	1.78E+05
Nb-95	2.75E+03	6.52E+04
Ni-59	8.45E-03	0.00E+00
Ni-63	1.16E+00	1.90E+01
Np-237	6.67E+01	9.18E-03
Np-239	1.82E-02	0.00E+00
Pa-231	3.30E-03	0.00E+00
Pa-233	1.97E-03	0.00E+00
Pb-210	2.10E-02	0.00E+00

Table 3. CH-TRU and RH-TRU Radionuclide Inventory for SPM 2 Calculations (continued)

Radionuclide	CH Curies	RH Curies
Pb-214	4.80E-02	0.00E+00
Pm-147	5.25E+02	1.81E+03
Po-209	2.56E-06	0.00E+00
Po-210	2.52E-03	0.00E+00
Po-214	4.80E-02	0.00E+00
Po-218	4.80E-02	0.00E+00
Pr-144	1.42E+04	3.37E+05
Pu-236	5.76E-02	0.00E+00
Pu-238	4.24E+06	2.22E+03
Pu-239	3.92E+05	4.44E+03
Pu-240	6.93E+04	1.05E+03
Pu-241	1.93E+06	6.06E+04
Pu-242	4.91E+04	1.09E+01
Pu-244	1.00E-06	0.00E+00
Pu-245	0.00E+00	3.35E-03
Ra-226	5.57E+00	1.42E+01
Ra-228	2.75E-01	0.00E+00
Rh-106	6.20E+03	1.47E+05
Rn-222	4.80E-02	0.00E+00
Ru-106	6.20E+03	1.50E+05
Sb-125	2.84E+03	6.72E+04
Sb-126	1.56E-01	0.00E+00
Sm-151	1.07E+02	2.52E+03
Sr-90	9.85E+03	5.48E+05
Ta-182	0.00E+00	3.79E+00
Tc-99	4.22E+01	4.59E+02
Te-125M	7.09E+02	1.67E+04
Th-228	1.12E+00	1.34E-01
Th-230	2.08E-02	0.00E+00
Th-232	6.11E-01	1.51E-02
Th-234	9.50E-05	0.00E+00
U-232	3.02E+01	6.70E+00
U-233	1.31E+03	4.80E+02
U-234	1.75E+01	0.00E+00
U-235	1.15E+00	5.66E+00
U-236	2.98E-01	0.00E+00
U-238	2.01E-01	7.28E+00
Y-90	7.55E+03	1.79E+05
Zn-65	7.00E+00	8.83E+02
Zr-95	1.30E+03	3.25E+04

Radionuclide	CH Curies	RH Curies
Total	7.05E+06	3.47E+06

**Fewell and Sanchez, March 29, 1995**

Date: 3/29/95  
To: F. Mendenhall and N. Prindle  
From: M. Fewell and P. Sanchez  
Subject: Soil-Based VOC and Semi-VOC Concentration in the Gas Phase for SPM-2

Intentionally Left Blank

date: March 29, 1995

to: Fred Mendenhall, MS-1335 (6705)  
and Nancy Prindle, MS-1335 (6705)

from: Mert Fewell, MS-1328 (6749)  
and Paul Sanchez, MS-1395 (6700)

*Mert Fewell Mert Fewell for Paul Sanchez*

subject: Soil-based VOC and Semi-VOC Concentrations in the gas phase for SPM-2

The WID model for the VOC and semi-VOC source term is used to calculate upper bounds for the soil based concentrations of VOC's and semi-VOCs in the upper shaft seal and in the anhydrite layers at the land withdrawal boundary.

The soil-based concentration of hazardous constituent *i* in the gas phase is given by

$$c_{sb}^i = \frac{M_i}{M} = \frac{1000\rho_i\phi s_g V}{\bar{\rho}_{sd} V} = \frac{1000\rho_i\phi s_g}{\bar{\rho}_{sd}} \quad (1)$$

where

$$\bar{\rho}_{sd} = \left[ \rho_{gr}(1-\phi) + \rho_b(1-s_g)\phi + \overbrace{\rho_m\phi s_g}^{-0} \right], \quad (2)$$

$$\rho_i = \frac{P_i \hat{M}_i}{RT}, \text{ and} \quad (3)$$

$$s_g = 1 - s_b, \quad (4)$$

- $c_{sb}^i$   $\equiv$  the soil based concentration of hazardous constituent *i* in volume *V* (mg/kg),
- $M_i$   $\equiv$  the mass of hazardous constituent *i* contained in the gas phase in volume *V* (mg),
- $M$   $\equiv$  the combined mass of the solid, brine, and gas phases in volume *V* (kg),
- $\rho_i$   $\equiv$  the mass of hazardous constituent *i* per volume of the gas phase in volume *V* (g/m<sup>3</sup>),
- $\phi$   $\equiv$  the porosity of the solid (-),
- $s_g$   $\equiv$  the saturation of the gas phase(-),
- $V$   $\equiv$  the formation (rock) volume (m<sup>3</sup>),
- $\bar{\rho}_{sd}$   $\equiv$  the combined mass of the solid, brine, and gas phases in volume *V* (kg/m<sup>3</sup>),
- $\rho_{gr}$   $\equiv$  the grain density of the solid in volume *V* (kg/m<sup>3</sup>),
- $\rho_b$   $\equiv$  the brine density (kg/m<sup>3</sup>),
- $\rho_m$   $\equiv$  the density of the gas phase (kg/m<sup>3</sup>)

*Note: the density of the gas mixture is assumed to be negligible in comparison to the anhydrite and brine density,*

$P_i$   $\equiv$  the partial pressure of hazardous constituent  $i$  in the gas phase (Pa),

$\hat{M}_i$   $\equiv$  the molecular weight of hazardous constituent  $i$  (g),

$\mathcal{R}$   $\equiv$  the universal gas constant, (Nt-m/gmole/K),

$T$   $\equiv$  the temperature of the gas phase in volume  $V$  (K), and

$s_b$   $\equiv$  the brine saturation (-).

From Equations 1 through 4, soil-based concentrations of hazardous constituents increase with porosity, gas saturation, and the partial pressure of the hazardous constituents in the gas phase. Thus, substitution of upper bounded values for porosity, gas saturation, and partial pressure yields upper bounds for soil-based concentrations of hazardous constituents in the gas phase. Values for the parameters needed to calculate upper bounds for soil-based concentrations are displayed in Table 1.

### VOCs

The WID hazardous constituent source term for VOCs in the gas phase is based on the assumption that no post-closure release mechanisms will elevate concentrations of VOCs in the gas phase above those measured in drum headspaces. Using this assumption, the concentrations of VOCs in the gas phase at the regulatory boundaries are bounded by the headspace concentrations; these bounds can be calculated by transferring the headspace concentrations to the boundaries as depicted in Figure 1. In so doing, the maximum partial pressure is given by

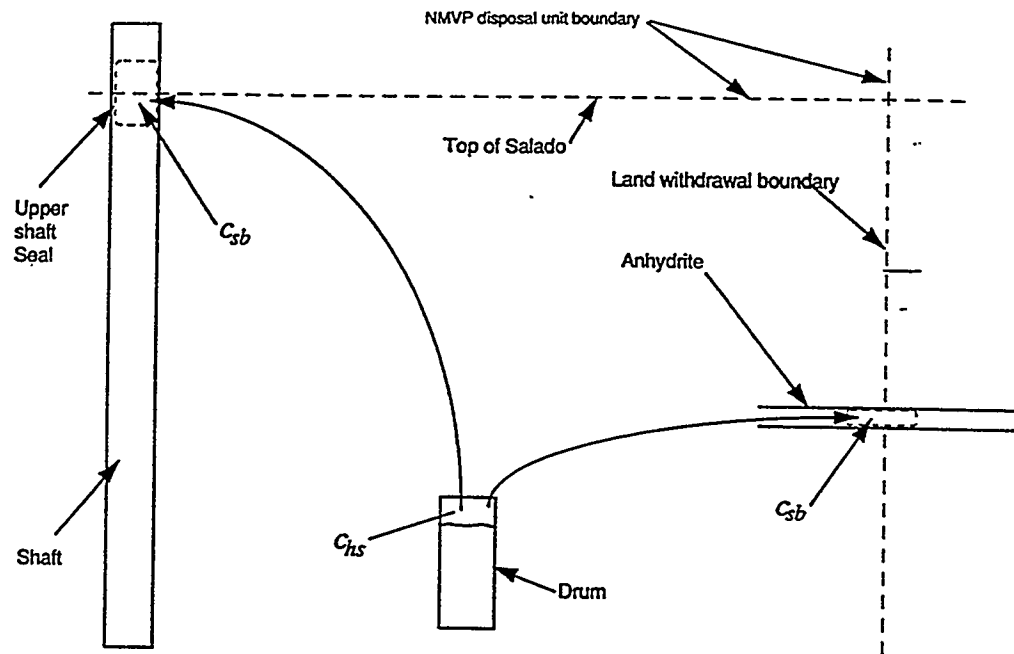
$$P_i = c_{hs}^i P, \quad (5)$$

where

$c_{hs}^i$   $\equiv$  the concentration of VOC  $i$  in drum headspaces (-), and

$P$   $\equiv$  the maximum pressure of the gas phase in the repository (PA).

*Note: The maximum pressure of the gas phase is assumed to be the lithostatic stress at the repository horizon.*



MEF01-30-65

Figure 1. Bounding soil-based VOC concentrations at the regulatory boundaries.

Upper bounds for soil-based concentrations of VOCs in the anhydrite at the land withdrawal boundary and in the upper shaft seals are compared to the health-based soil levels in Table 2 and 3. These values were calculated by substituting the bounding parameter values in Table 1b and the headspace concentration and molecular weight values from Tables 2 and 3 into Equations 1 through 5.

### Semi-VOCs

The WID hazardous constituent source term for semi-VOCs assumes that the concentrations are vapor pressure limited. This means that

$$P_i = P_i^* \quad (6)$$

where

$P_i^*$  = the vapor pressure of hazardous constituent  $i$  at the gas mixture temperature  $T$ .

The upper bounds for soil-based concentrations of semi-VOCs in the anhydrite at the land withdrawal boundary and in the upper shaft seals are compared to the health-based soil levels in Table 4 and 5. These values were calculated by substituting the bounding parameter values in Table 1b, the vapor pressure and molecular weight values from Tables 4 and 5, and Equation (6) into Equations 1 through 4.

Conclusions

Based on the WID source term model, upper-bounds of soil-based concentrations in the gas phase are, with the exception of carbon tetrachloride, two orders or more below the health-based levels. The upper-bounds of the soil-based concentration of carbon tetrachloride is at the health-based level in anhydrite and is below, but of the same order of magnitude as, the health-based soil level in the upper shaft seals (Tables 2 through 5). The soil-based concentration of carbon tetrachloride is more than an order of magnitude less than the health-based soil level for the lower limit of porosity in the anhydrite.

While concentrations in the repository may exceed those calculated by the WID source term model during the 10,000 year post-closure period, the results presented here do not consider transport, dilution of waste generated gas, degradation, and other processes that could lower hazardous constituent concentrations.

Table 1. WIPP values for parameters required in the calculation of soil-based concentrations of hazardous constituents

## a. Parameters values

Parameter	Value	Source
Lithostatic pressure	14.8 (mPa)	SPM-2 database
Universal gas constant	8.317 (Nt-m/gmole K)	—
Repository temperature	300 (K)	-
Anhydrite porosity	0.1-3%	SPM-2 database
Residual brine saturation in the anhydrite	0-60%	SPM-2 database
Upper shaft seal porosity	5%	SPM-2 database
Residual brine saturation in the upper shaft seal	20%	SPM-2 database
Anhydrite grain density	2.96E+03 (kg/m <sup>3</sup> )	SPM-2 database
Brine density	1.23E+03 (kg/m <sup>3</sup> )	1992 PA
Upper shaft seal grain density	2.16E+03 (kg/m <sup>3</sup> )	SPM-2 database

## b. Bounding values.

Parameter	Value
Anhydrite porosity	3.00%
Maximum gas saturation in anhydrite	100.00% *
Local soil density of anhydrite	2.87E+03
Upper shaft seal porosity	5.00%
Maximum gas saturation in upper shaft seal	80.00% *
Local soil density of the upper shaft seal	2.10E+03

\* The maximum gas saturation corresponds to the minimum brine saturation, i.e. the residual brine saturation.

Table 2. Upper Bounded Headspace Concentration Limited Soil Based VOC Concentrations in Anhydrite

VOCs	$C_{hs}^i$ (ppmv)	$\hat{M}_i$ (g)	$C_{hbs}^i$ (mg/kg)	$C_{sb}^i$ (mg/kg)
Acetone	92.6	58.08	0.33	8,000.
Benzene	9.18	78.11	0.04	24.14
Bromoform	9.09	252.7	0.14	88.61
1-Butanol	101	74.12	0.46	8,000.
2-Butanone/Methyl ethyl ketone	76.2	72.1	0.34	4,800.
Carbon disulfide		76.13		8,000.
Carbon tetrachloride	560	153.8	5.33 *	5.38
Chlorobenzene	12.1	112.6	0.08	1,600.
Chloroform	15.5	119.4	0.11	114.75
Cyclohexane	15.4	84.15	0.08	Note 7.
Cyclohexanone		98.15		400,000.
1,1-Dichloroethane	9.26	98.96	0.06	Note 7.
1,2-Dichloroethane	9.07	98.96	0.06	7.69
1,1-Dichloroethylene (ene)	11.1	96.94	0.07	11.67
(Z)-1,2-Dichloroethylene (ene)	9.05	96.94	0.05	Note 7.
Ethyl acetate		88.11		72,000.
Ethyl benzene	10.1	106.2	0.07	8,000.
Diethyl ether	12.1	74.12	0.06	16,000.
2-Ethoxyethanol		90.12		Note 7.
Formaldehyde		30.03		16,000.
Hydrazine		32.05		0.23
Isobutanol		74.12		24,000.

\* = 0.18 mg/kg for .1% porosity (the lower limit from Table 1)

## Notes:

1. Blanks indicate that data are not available.
2. The list of VOCs were compiled from the union of the target compounds identified for waste characterization in *Resource Conservation and Recovery Act Part B Permit Application*. DOE/WIPP 91-005, Rev. 3 and the list of VOCs found in letter WD:95:0214 from L. R. Fitch, Manager, Environment, Safety, Health, and Regulatory Compliance, Westinghouse Isolation Division, Westinghouse Electric Corporation to Dr. J. A. Mewhinney dated January 25, 1995.
3.  $C_{hs}^i$  is the headspace concentration for constituent i found in letter WD:95:0214 from L. R. Fitch, Manager, Environment, Safety, Health, and Regulatory Compliance, Westinghouse Isolation Division, Westinghouse Electric Corporation to Dr. J. A. Mewhinney dated January 25, 1995.
4.  $\hat{M}_i$  is the molecular weight of constituent i.
5.  $C_{hbs}^i$  is the headspace limited health-based soil level for constituent i.
6.  $C_{sb}^i$  is the health-based soil level for constituent i. These levels represent the most stringent limits for either carcinogenic or systemic risk from oral exposure. See memorandum from Paul Sanchez to Peter Swift and Mert Fewell dated January 24, 1995.
7. No health-based standard in IRIS 2 database.

Table 2. Upper Bounded Headspace Concentration Limited Soil Based VOC Concentrations in Anhydrite (conc.)

VOCs	$C_{hs}^i$ (ppmv)	$\hat{M}_i$ (g)	$C_{hbs}^i$ (mg/kg)	$C_{sb}^i$ (mg/kg)
Methanol	261	32.04	0.52	40,000.
Methylene chloride	739	50.49	2.31	93.33
Methyl isobutyl ketone	97.9	100.2	0.61	4,000.
2-Nitropropane		105.1		Note 7.
1,1,2,2-Tetrachloroethane	9.11	167.9	0.09	35.
Tetrachloroethylene (ene)	9.09	165.8	0.09	13.73
Toluene	25.1	92.14	0.14	16,000.
1,1,2-Trichloroethane		133.4		122.81
1,1,1-Trichloroethane	492	133.4	4.06	7,200.
Trichloroethylene (ene)	21.2	131.4	0.17	63.64
Trichlorofluoromethane		137.4		24,000.
1,3,5-Trimethylbenzene	8.96	120.2	0.07	Note 7.
1,2,4-Trimethylbenzene	12.1	120.2	0.09	Note 7.
1,1,2-Trichloro-1,2,2-trifluoroethane	52.4	187.4	0.61	2,400,000.
Vinyl chloride		62.5		Note 7.
p/m-xylene	12.6	106.2	0.08	160,000.
O-Xylene	15.3	106.2	0.10	160,000.

## Notes:

- Blanks indicate that data are not available.
- The list of VOCs were compiled from the union of the target compounds identified for waste characterization in *Resource Conservation and Recovery Act Part B Permit Application*. DOE/WIPP 91-005, Rev. 3 and the list of VOCs found in letter WD:95:0214 from L. R. Fitch, Manager, Environment, Safety, Health, and Regulatory Compliance, Westinghouse Isolation Division, Westinghouse Electric Corporation to Dr. J. A. Mewhinney dated January 25, 1995.
- $C_{hs}^i$  is the headspace concentration for constituent i found in letter WD:95:0214 from L. R. Fitch, Manager, Environment, Safety, Health, and Regulatory Compliance, Westinghouse Isolation Division, Westinghouse Electric Corporation to Dr. J. A. Mewhinney dated January 25, 1995.
- $\hat{M}_i$  is the molecular weight of constituent i.
- $C_{hbs}^i$  is the headspace limited health-based soil level for constituent i.
- $C_{sb}^i$  is the health-based soil level for constituent i. These levels represent the most stringent limits for either carcinogenic or systemic risk from oral exposure. See memorandum from Paul Sanchez to Peter Swift and Mert Fewell dated January 24, 1995.
- No health-based standard in IRIS 2 database.

Table 3. Upper Bounded Headspace Concentration Limited Soil Based VOC Concentrations in the Upper Shaft Seals

VOCs	$C_{hs}^i$ (ppmv)	$\hat{M}_i$ (g)	$C_{hbs}^i$ (mg/kg)	$C_{sb}^i$ (mg/kg)
Acetone	92.6	58.08	0.15	8,000.
Benzene	9.18	78.11	0.02	24.14
Bromoform	9.09	252.7	0.06	88.61
1-Butanol	101	74.12	0.21	8,000.
2-Butanone/Methyl ethyl ketone	76.2	72.1	0.15	4,800.
Carbon disulfide		76.13		8,000.
Carbon tetrachloride	560	153.8	2.43	5.38
Chlorobenzene	12.1	112.6	0.04	1,600.
Chloroform	15.5	119.4	0.05	114.75
Cyclohexane	15.4	84.15	0.04	Note 7.
Cyclohexanone		98.15		400,000.
1,1-Dichloroethane	9.26	98.96	0.03	Note 7.
1,2-Dichloroethane	9.07	98.96	0.03	7.69
1,1-Dichloroethylene (ene)	11.1	96.94	0.03	11.67
(Z)-1,2-Dichloroethylene (ene)	9.05	96.94	0.02	Note 7.
Ethyl acetate		88.11		72,000.
Ethyl benzene	10.1	106.2	0.03	8,000.
Diethyl ether	12.1	74.12	0.03	16,000.
2-Ethoxyethanol		90.12		Note 7.
Formaldehyde		30.03		16,000.
Hydrazine		32.05		0.23
Isobutanol		74.12		24,000.

## Notes:

- Blanks indicate that data are not available.
- The list of VOCs were compiled from the union of the target compounds identified for waste characterization in *Resource Conservation and Recovery Act Part B Permit Application*. DOE/WIPP 91-005, Rev. 3 and the list of VOCs found in letter WD:95:0214 from L. R. Fitch, Manager, Environment, Safety, Health, and Regulatory Compliance, Westinghouse Isolation Division, Westinghouse Electric Corporation to Dr. J. A. Mewhinney dated January 25, 1995.
- $C_{hs}^i$  is the headspace concentration for constituent i found in letter WD:95:0214 from L. R. Fitch, Manager, Environment, Safety, Health, and Regulatory Compliance, Westinghouse Isolation Division, Westinghouse Electric Corporation to Dr. J. A. Mewhinney dated January 25, 1995.
- $\hat{M}_i$  is the molecular weight of constituent i.
- $C_{hbs}^i$  is the headspace limited health-based soil level for constituent i.
- $C_{sb}^i$  is the health-based soil level for constituent i. These levels represent the most stringent limits for either carcinogenic or systemic risk from oral exposure. See memorandum from Paul Sanchez to Peter Swift and Mert Fewell dated January 24, 1995.
- No health-based standard in IRIS 2 database.

Table 3. Upper Bounded Headspace Concentration Limited Soil Based VOC Concentrations in the Upper Shaft Seals (conc.)

VOCs	$C_{hs}^i$ (ppmv)	$\hat{M}_i$ (g)	$C_{hbs}^i$ (mg/kg)	$C_{sb}^i$ (mg/kg)
Methanol	261	32.04	0.24	40,000.
Methylene chloride	739	50.49	1.05	93.33
Methyl isobutyl ketone	97.9	100.2	0.28	4,000.
2-Nitropropane		105.1		Note 7.
1,1,2,2-Tetrachloroethane	9.11	167.9	0.04	35.
Tetrachloroethylene (ene)	9.09	165.8	0.04	13.73
Toluene	25.1	92.14	0.07	16,000.
1,1,2-Trichloroethane		133.4		122.81
1,1,1-Trichloroethane	492	133.4	1.85	7,200.
Trichloroethylene (ene)	21.2	131.4	0.08	63.64
Trichlorofluoromethane		137.4		24,000.
1,3,5-Trimethylbenzene	8.96	120.2	0.03	Note 7.
1,2,4-Trimethylbenzene	12.1	120.2	0.04	Note 7.
1,1,2-Trichloro-1,2,2-trifluoroethane	52.4	187.4	0.28	2,400,000.
Vinyl chloride		62.5		Note 7.
p/m-xylene	12.6	106.2	0.04	160,000.
o-Xylene	15.3	106.2	0.05	160,000.

## Notes:

- Blanks indicate that data are not available.
- The list of VOCs were compiled from the union of the target compounds identified for waste characterization in *Resource Conservation and Recovery Act Part B Permit Application*. DOE/WIPP 91-005, Rev. 3 and the list of VOCs found in letter WD:95:0214 from L. R. Fitch, Manager, Environment, Safety, Health, and Regulatory Compliance, Westinghouse Isolation Division, Westinghouse Electric Corporation to Dr. J. A. Mewhinney dated January 25, 1995.
- $C_{hs}^i$  is the headspace concentration for constituent i found in letter WD:95:0214 from L. R. Fitch, Manager, Environment, Safety, Health, and Regulatory Compliance, Westinghouse Isolation Division, Westinghouse Electric Corporation to Dr. J. A. Mewhinney dated January 25, 1995.
- $\hat{M}_i$  is the molecular weight of constituent i.
- $C_{hbs}^i$  is the headspace limited health-based soil level for constituent i.
- $C_{sb}^i$  is the health-based-soil level for constituent i. These levels represent the most stringent limits for either carcinogenic or systemic risk from oral exposure. See memorandum from Paul Sanchez to Peter Swift and Mert Fewell dated January 24, 1995.
- No health-based standard in IRIS 2 database.

Table 4. Saturation Pressure Limited Soil Based Semi-VOC Concentrations in Anhydrite

Semi-VOCs	$P_v^i$ (atm)	$\hat{M}_i$ (g)	$C_{vbs}^i$ (mg/kg)	$C_{sb}^i$ (mg/kg)
Cresols (o, m, p)	4.77E-04	108	0.02	Note 6.
ortho-Dichlorobenzene		146.9		7,200.
1,4-Dichlorobenzene		146.9		Note 6.
2,4-Dinitrotoluene	6.71E-06	182	0.00	1.03
Hexachloroethane	1.00E-03	236.7	0.10	80.
Nitrobenzene	4.03E-04	123	0.02	40.
Polychlorinated biphenyls (PCBs)	1.01E-07	291.8	0.00	0.09
Pyridine	3.04E-02	79	1.02	80.

## Notes:

1. Blanks indicate that data are not available.
2. The list of VOCs were compiled from the union of the target compounds identified for waste characterization in *Resource Conservation and Recovery Act Part B Permit Application*. DOE/WIPP 91-005, Rev. 3 and the list of VOCs found in letter WD:95:0214 from L. R. Fitch, Manager, Environment, Safety, Health, and Regulatory Compliance, Westinghouse Isolation Division, Westinghouse Electric Corporation to Dr. J. A. Mewhinney dated January 25, 1995.
3.  $\hat{M}_i$  is the molecular weight of constituent i.
4.  $C_{vbs}^i$  is the vapor pressure limited health-based soil level for constituent i.
5.  $C_{sb}^i$  is the health-based soil level for constituent i. These levels represent the most stringent limits for either carcinogenic or systemic risk from oral exposure. See memorandum from Paul Sanchez to Peter Swift and Mert Fewell dated January 24, 1995.
6. No health-based standard in IRIS 2 database.

Table 5. Saturation Pressure Limited Soil Based Semi-VOC Concentrations in Upper Shaft Seals

Semi-VOCs	$P_v^i$ (atm)	$\hat{M}_i$ (g)	$C_{vbs}^i$ (mg/kg)	$C_{sb}^i$ (mg/kg)
Cresols (o, m, p)	4.77E-04	108	0.01	Note 6.
ortho-Dichlorobenzene		146.9		7,200.
1,4-Dichlorobenzene		146.9		Note 6.
2,4-Dinitrotoluene	6.71E-06	182	0.00	1.03
Hexachloroethane	1.00E-03	236.7	0.05	80.
Nitrobenzene	4.03E-04	123	0.01	40.
Polychlorinated biphenyls (PCBs)	1.01E-07	291.8	0.00	0.09
Pyridine	3.04E-02	79	0.46	80.

## Notes:

1. Blanks indicate that data are not available.
2. The list of VOCs were compiled from the union of the target compounds identified for waste characterization in *Resource Conservation and Recovery Act Part B Permit Application*. DOE/WIPP 91-005, Rev. 3 and the list of VOCs found in letter WD:95:0214 from L. R. Fitch, Manager, Environment, Safety, Health, and Regulatory Compliance, Westinghouse Isolation Division, Westinghouse Electric Corporation to Dr. J. A. Mewhinney dated January 25, 1995.
3.  $\hat{M}_i$  is the molecular weight of constituent i.
4.  $C_{vbs}^i$  is the vapor pressure limited health-based soil level for constituent i.
5.  $C_{sb}^i$  is the health-based soil level for constituent i. These levels represent the most stringent limits for either carcinogenic or systemic risk from oral exposure. See memorandum from Paul Sanchez to Peter Swift and Mert Fewell dated January 24, 1995.
6. No health-based standard in IRIS 2 database.

Distribution:

All WIPP Managers

MS-1328, M. Marrietta (6749)

MS-1341, R. Weiner (6747)

MS-1395, P. Sanchez (6700)

MS-1328, M. Fewell (6749)

SWCF-A: 1.1.2.7;SPM; RCRA; NQ: SBSP2M1.DOC(2 cys)

**Fitch, March 21, 1995**

Date: 3/21/95  
To: M. McFadden  
From: Fitch  
Subject: Future Inadvertent Intrusion Rates

Intentionally Left Blank



Westinghouse  
Electric Corporation

Government Operations

WD:95:03113  
DA:95:11026  
Waste Isolation Division

Box 2078  
Carlsbad New Mexico 88221

March 21, 1995

Mr. M. H. McFadden, Assistant Manager  
Office of Regulatory Compliance  
Carlsbad Area Office  
U.S. Department of Energy  
P.O. Box 3090  
Carlsbad, NM 88221-3090

Subject: FUTURE INADVERTENT INTRUSION RATES

Dear Mr. McFadden:

Per your verbal request, we suggest that you use the following drilling rates for disturbed case, repository performance assessment calculations:

- o complete one set of calculations using a rate of 25 events/square kilometer
- o complete one set of calculations using a rate of 17.5 events/square kilometer
- o complete one set of calculations using a rate of 10 events/square kilometer
- o complete one set of calculations using a rate of 3 events/square kilometer
- o complete one set of calculations using a rate of 1 event/square kilometer

These calculations will result in the identification of an expected number of inadvertent intrusions into the repository over the 10,000 year performance assessment period at several assumed rates of future drilling. The resultant numbers of calculated, expected intrusions at each of these assumed future drilling rates coupled with an analysis of the consequences of these intrusions will be used to develop permanent marker system design goals. These system design goals will allow the WIPP project to develop a concept that is "effective enough" to deter future inadvertent human intrusion during the 10,000 year regulatory time frame based on the expected level of repository performance.

The justification for, and logic behind such an approach is as follows:

- The WID has initiated research of drilling activities in the Delaware Basin. This assessment is limited to those activities occurring during the last 50 years as recorded in a Petroleum Information Corporation database (received on February 1, 1995), and additional information from the State Engineer's office. We have identified some other potential sources of information that may be useful. We will acquire whatever information that is available to ensure that the resulting expected drilling rate is defensible and that the DOE has shown due diligence in an attempt to include all relevant information. Until we complete this drilling research activity we have no technical or statistical basis for any future inadvertent intrusion rate to be used in assessments of long-term repository performance.
- We are required to design a permanent markers system for compliance with 40 CFR 191. Our intent is to design the permanent marker system to be effective in rendering future inadvertent intrusion events unlikely for the 10,000 year regulatory period of interest. A permanent marker system must be designed to ensure that future generations are warned of the presence of the repository, the wastes, and the associated hazards posed. In the required 10,000 year predictive exercise embodied in repository performance assessment one must consider the affect of future inadvertent intrusions into the repository. These two requirements, when coupled in the same long term performance assessment, make it clear that the impacts of future inadvertent intrusion events can be extremely impactful. The logical conclusion we have reached is that the permanent marker system must be solid.

When the calculations of repository performance are completed and we have finished the consequence analysis we will be in a position to conclude one of two things. Either the markers must be effective to some degree demonstrate compliance, or that compliance can be demonstrated with a zero level of effectiveness from the markers system and they are therefore a part of fulfilling the assurance requirements. If we conclude that the markers must be effective to demonstrate compliance, we must bear in mind that it will be impossible to quantify with statistical certainty, exactly how effective such a marker system will be, and/or for exactly how long the system can be expected to remain effective. One could conduct a detailed, probabilistic assessment of effectiveness on such a marker system in an attempt to quantify such a probability for success. The results of such an assessment would undoubtedly have a substantive level of uncertainty associated with

the result. The applicable regulations require that the markers be effective enough. Exactly what mechanism is best suited for the task of bringing the ideas of "probability" for successful markers and "effective enough" together can be debated at length. However, since we will attack this problem in a regulatory arena, we have concluded that convincing the regulator that the markers are "effective enough" will require that we provide as much evidence as possible and allow him to make his decision judiciously. The use of expert panels and/or peer reviews may also add some value. In the final analysis, the regulator's decision relative to marker system effectiveness, should it be required, will be one based purely on judgement.

When our research of the drilling activity in the Delaware Basin is complete, we will provide you with an intrusion rate for use in future decision making. In the meantime, the approach we have recommended to you here is a sound, logical way to address this important information need. Should you have any questions, contact Mr. B. A. Howard at (505) 234-8380.

Sincerely,



L. R. Fitch, Manager  
Environment, Safety, Health, and Regulatory Compliance

BAH:kds

cc: R. A. Bills, CAO  
G. T. Basabilvazo, CAO  
J. H. Maes, CAO  
J. A. Mewhinney, CAO  
N. H. Prindle, SNL  
L. E. Shephard, SNL  
P. N. Swift, SNL

Mr. McFadden

March 21, 1995

WD:95:03113

bcc: WID Distribution

C. E. Conway  
J. A. Davis  
K. S. Donovan  
J. L. Epstein  
R. F. Kehrman

**Jow and Anderson, March 1, 1995**

Date: 3/1/95  
To: L. Shepard  
From: H. Jow and D. Anderson  
Subject: PA Computational Approach to SPM2

Intentionally Left Blank

date: March 1, 1995

to: Les E. Shephard, MS-1395 (6701)



from: Hong-Nian Jew, MS-1328 (6741) and D. R. (Rip) Anderson, MS-1328 (6749)

subject: PA Computational Approach to SPM2

As we move closer to the deliverable date of SPM, i.e., 3/31/95, the computational strategy of performance assessment (PA) is at the junction of choosing the best possible path to meet the deadline and deliverable. We weighed the following factors in planning our strategy: time constraint, customer expectation, manpower resource, and technical rationale. We believe that the best course of meeting the 3/31/95 milestone and delivering the SPM product to DOE/CAO as a decision aid tool is to go forward with the mean value approach which is different from our traditional Latin Hypercube Sampling (LHS) approach.

The following are reasons for choosing the mean value approach:

**Customer Expectation:**

As we all are aware, the SPM product is important to the DOE/CAO programmatic decision. We also must meet the 9/95 milestones of FEPs screening and QA of the PA codes. Therefore, we need to get SPM done and deliver the product on time, i.e., 3/31/95.

**Time and Resource Constraints:**

The time available for the SPM calculations is from now through 3/17, which is not much time for the very complex and large amount of calculations we need to do. The number of calculations would be much more if we would choose the LHS approach (i.e., a factor of LHS sample size more; e.g., 60). All personnel supporting the WIPP project in both PA calculations would be less and we would have a better chance to complete the work in time.

WIPP PA Departments are fully dedicated to the SPM calculations. By going with the mean value approach, the number **Technical Rationale:**

- (1) If one would look at the Taylor's series expansion of a function, the mean value approach would give the zero-th order of approximation of "the mean of the CCDFs" generated by using LHS. This zero-th order of approximation is a reasonable estimate of "the mean of the CCDFs" for the decision analysis. We have some examples of comparing the mean value and the LHS approaches.

In general, these examples show that the CCDFs produced by the mean value calculations are close to the means produced by the LHS approach. We will also compare the CCDFs produced by the mean value approach for the two DCCA cases with those of LHS approach.

- (2) For the finite difference analysis such as the PA codes, assigning the "best value" for a parameter of a heterogeneous material which is coarsely grided in space is to use the arithmetic average of, say N measurements of the material property. Note that the arithmetic average of N measurements is also an unbiased estimator of the mean value of the subject material property. Therefore, using the mean value to describe the parameter value of a given material property is the best estimate.
- (3) For certain parameter values, the elicited uncertainty distributions cover orders of magnitude; i.e., they were elicited in the logarithm space instead of the linear space. For these distributions, the arithmetic mean would be skewed to the higher value side of the distribution. Furthermore, in certain instances, the calculated arithmetic means would be higher than the baseline value. In order to provide a better resolution in evaluating different experimental outcomes using the SPM process, for those distributions elicited in the logarithm space, the mean value will be calculated as the mean of the logarithms instead of the arithmetic mean.

The shortcoming of the mean value approach is, of course, not being able to include the evaluation of the uncertainty distributions of the parameter values and capturing that uncertainty in the display of CCDFs, and, in certain cases, not having a good resolution among different outcomes of a given activity.

Copy to:

MS-1328 Staff in 6741 and 6749  
MS-1328 Amy Johnson (6741)  
MS-1335 Deirdre Boak (6705)  
MS-1335 Steve Goldstein (6705)  
MS-1335 Fred Mendenhall (6705)  
MS-1335 Nancy Prindle (6705)  
MS-1328 Rip Anderson (6749)  
MS-1328 Hong-Nian Jow (6741)

**McFadden, December 19, 1994**

Date: 12/19/94  
To: R. Lincoln  
From: M. McFadden  
Subject: Systems Prioritization Method Information Needs and Product Requirements

Intentionally Left Blank

United States Government

Department of Energy

**memorandum**Carlsbad Area Office  
Carlsbad, New Mexico 88221

DATE: DEC 19 1994

REPLY TO  
ATTN OF: CAO:EPB:RAB: 94-2936

SUBJECT: Systems Prioritization Method Information Needs And Product Requirements

TO: Richard Lincoln, MS #1341, SNL/NM

The Systems Prioritization Method (SPM) Steering Committee has reviewed your memorandums of December 2 and 7, 1994, explaining your information requirements and product requirements. An important point is that the SPM Steering Committee will be responsible for abridging or eliminating any activities or activity sets. Please address, in writing, any request to consider eliminating activities to the committee.

The answers to the questions asked in the memorandum of December 2, 1994 are:

- Average the soil concentrations over the thickness of the marker beds and the cross sectional area of the shaft at the top of the Salado,  
  
Use the Resource Conservation and Recovery Act (RCRA) source term in the "White Paper",  
  
Assume no hazardous constituents other than waste will be in the underground, and  
  
R. Kehrman of Westinghouse will supply soil-based standards information prior to February 1995
- R. Bills will obtain this information from the National Transuranic Program Office as soon as he receives the detailed request from you
- Assume no addition to metals or cellulose will be made in the waste panels,  
  
Assume that all underground areas other than panels are rockbolted,  
  
Information will be provided shortly,  
  
Assume that there are 6.2 million cubic feet of waste,  
  
Assume no backfill for the baseline.

DEC 19 1994

Richard Lincoln

- 2 -

Information will be provided shortly, and

Assume for the Remote-Handled Waste that a steel cased salt plug will be used. (Contact R. Kehrman for location of design information). A concrete plug should be an activity.

Use the drilling frequency and time of drilling (random in time and space) to determine if E1E2 occurs or not,

Use 25 boreholes per square kilometer per 10,000 years. All other parameters will be as from 40 CFR 191. R. Kehrman will supply data regarding efficacy of passive markers for an activity, and

Assess current modelling capability to analyze shallow wells with the assumption that the wells do not affect the hydraulic gradient (i.e., they exist only as a zone of reduced permeability).

In response to the memorandum of December 7, 1994, your assumptions are essentially correct except that George Dials stated at the December 12, 1994, meeting that there would only be one CD-ROM and that the stakeholders would get the exact same material as the Carlsbad Area Office (CAO). It was also decided during this meeting that it may be appropriate to address certain side issues (e.g., criticality) in side bar calculations/studies, but that all issues to be addressed in this fashion are to be agreed to by the SPM Steering Committee. We additionally request that you also provide, on the CD-ROM, a copy of the second iteration SPM paper reports.



Michael H. McFadden  
Branch Chief  
Experimental Programs Manager

cc:

B. Bills, CAO  
J. Mewhinney, CAO  
B. Kehrman, WID

## DISTRIBUTION LIST

9 May 1996

### Federal Agencies

US Department of Energy (4)  
Office of Civilian Radioactive Waste Mgmt.  
Attn: Deputy Director, RW-2  
Acting Director, RW-10  
Office of Human Resources & Admin.  
Director, RW-30  
Office of Program Mgmt. & Integ.  
Director RW-40  
Office of Waste Accept., Stor., & Tran.  
Forrestal Building  
Washington, DC 20585

Attn: Project Director  
Yucca Mountain Site Characterization Office  
Director, RW-3  
Office of Quality Assurance  
101 Convention Center Drive, Suite #P-110  
Las Vegas, NM 89109

US Department of Energy  
Albuquerque Operations Office  
Attn: National Atomic Museum Library  
P.O. Box 5400  
Albuquerque, NM 87185-5400

US Department of Energy  
Research & Waste Management Division  
Attn: Director  
P.O. Box E  
Oak Ridge, TN 37831

US Department of Energy (6)  
Carlsbad Area Office  
Attn: G. Basabilvazo  
G. Dials  
D. Galbraith  
M. McFadden  
R. Lark  
J. A. Mewhinney  
P.O. Box 3090  
Carlsbad, NM 88221-3090

US Department of Energy  
Office of Environmental Restoration and  
Waste Management  
Attn: J. Lytle, EM-30  
Forrestal Building  
Washington, DC 20585-0002

US Department of Energy (3)  
Office of Environmental Restoration  
and Waste Management  
Attn: M. Frei, EM-34, Trevion II  
Washington, DC 20585-0002

US Department of Energy  
Office of Environmental Restoration  
and Waste Management  
Attn: S. Schneider, EM-342, Trevion II  
Washington, DC 20585-0002

US Department of Energy (2)  
Office of Environment, Safety & Health  
Attn: C. Borgstrom, EH-25  
R. Pelletier, EH-231  
Washington, DC 20585

US Department of Energy (2)  
Idaho Operations Office  
Fuel Processing & Waste Mgmt. Division  
785 DOE Place  
Idaho Falls, ID 83402

US Environmental Protection Agency (2)  
Radiation Protection Programs  
Attn: M. Oge  
ANR-460  
Washington, DC 20460

US Department of Energy  
Attn: E. Young  
Room E-178  
GAO/RCED/GTN  
Washington, DC 20545

Agnes Ortiz  
U.S. EPA, Mail Code 6602-J  
Office of Radiation  
402 N. Stuet, SW  
Washington, DC 20460

Cesar Clavell, Special Assistant  
for Research & Development  
Office of the Assistant Secretary of the Navy  
(Installations and Environment)  
CP-5 Rm 236  
Washington, DC 20360-5000

Stephen Hoffman  
Chief, Mining Section  
Office of Solid Waste  
U.S. Environmental Protection Agency  
401 M. Street, S.W. (OS-323W)  
Washington, DC 20480

Melvin W. Shupe, Director  
Environmental Remediation R&D Division  
EM-541 DAS Technology Development  
U.S. Department of Energy  
1000 Independence Ave., SW  
Washington, DC 20585

Edward P. Regnier  
Chief, Waste Management Unit  
U.S. Department of Energy  
Office of Environment, Safety, and Health  
1000 Independence Avenue, S.W.  
Washington, DC 20585

Thomas M. Crandall, Program Manager  
Office of Environmental Restoration and Waste  
Management  
U.S. Department of Energy, EM-451  
Washington, DC 20585-0002

Stephen W. Warren, Program Manager  
U.S. Department of Energy  
Office of Northwestern Area Programs  
Environmental Restoration  
Washington, DC 20585-0002

David S. Shafer  
Office of Southwestern Area Program  
Environmental Restoration  
U.S. Department of Energy  
EM-452, Trevion II  
Washington, DC 20585-0002

Scott R. Grace  
Environmental Restoration Division  
Department of Energy  
P.O. Box 928, Building 116  
Golden, CO 80402-0928

Jeffrey M. Lenhart  
U.S. Department of Energy  
Albuquerque Operations Office  
Technology Transfer & Commercialization Staff  
P.O. Box 5400  
Albuquerque, NM 87116

Abraham E. Van Luik  
Yucca Mountain Project Office  
U.S. Department of Energy  
P.O. Box 98608  
Las Vegas, NV 89193-8608

Ed Lopez, Regional Director  
U.S.A.F. Center for Environmental Excellence  
525 S. Griffin  
Dallas, Texas 75202

Michael L. Mastracci, PE  
Environmental Protection Agency  
Office of Research and Development, RD6B1  
Washington, DC 20460

U.S. Environmental Protection Agency (2)  
Attn: Russell F. Rhoades, Director  
Herbert R. Sherrow, Jr.  
1445 Ross Avenue, Suite 1200  
Dallas, TX 75202-2733

#### Boards

Defense Nuclear Facilities Safety Board  
Attn: D. Winters  
625 Indiana Ave. NW, Suite 700  
Washington, DC 20004

Nuclear Waste Technical Review Board (2)  
Attn: Chairman  
1100 Wilson Blvd., Suite 910  
Arlington, VA 22209-2297

Attorney General of New Mexico  
P.O. Drawer 1508  
Santa Fe, NM 87504-1508

Environmental Evaluation Group (3)  
Attn: Library  
7007 Wyoming NE  
Suite F-2  
Albuquerque, NM 87109

James T. Firkins, MBA  
Special Projects Coordinator  
State of New Mexico  
Energy, Minerals, and Natural Resources Dept.  
2040 South Pacheco  
Santa Fe, NM 87505

NM Energy, Minerals, and Natural  
Resources Department  
Attn: Library  
2040 S. Pacheco  
Santa Fe, NM 87505

NM Environment Department (3)  
Secretary of the Environment  
Attn: Mark Weidler  
1190 St. Francis Drive  
Santa Fe, NM 87503-0968

NM Bureau of Mines & Mineral Resources  
Socorro, NM 87801

NM Environment Department  
WIPP Project Site  
Attn: P. McCasland  
P.O. Box 3090  
Carlsbad, NM 88221

#### State Agencies

James M. Turner, Ph.D.  
Deputy Manager, Oakland Operations Office  
Oakland Federal Building  
1301 Clay St., 700N  
Oakland, CA 94612

Margaret C. Felts, Deputy Director  
California Environmental Protection Agency  
Department of Toxic Substances Control  
Site Mitigation Program  
400 P. Street, 4th Floor, P.O. Box 806  
Sacramento, CA 95812-0806

Jonathan P. Carter, Special Assistant  
Office of the Governor  
Statehouse  
Boise, ID 83720

Leland L. Mink, Director  
Idaho Water Resources  
Research Institute  
Morrill Hall, Room 106  
University of Idaho  
Moscow, ID 83843

James M. Souby, Executive Director  
Western Governor's Association  
Suite 1705, South Tower  
600 17th Street  
Denver, CO 80202

P.E. Verne Rosse, Deputy Administrator  
Bureau of Chemical Hazards  
Waste and Federal Facilities Management  
State of Nevada, Capitol Complex  
333 W. Nye Lane  
Carson City, NV 89710

Tom Leshendok, Deputy State Director  
Mineral Resources, Nevada State Office  
850 Harvard Way  
P.O. Box 12000  
Reno, NV 89520-0006

#### Laboratories and Corporations

Steve Frankiewicz  
Vice President  
Advanced Sciences, Inc.  
6739 Academy Rd. NE  
Albuquerque, NM 87109

Ann C. Marshall, Dept. Mgr.  
Community Relations  
Advanced Sciences, Inc.  
101 E. Mermod  
Carlsbad, NM 88220

Alan K. Kuhn, Ph.D., P.E.  
President, AK GeoConsult Inc.  
1312 Manitoba Drive, NE  
Albuquerque, NM 87111-29556

Lee Meerkhofer  
Applied Decision Analysis, Inc.  
2710 Sand Hill Road  
Menlo Park, CA 94025

Steve Stein  
Battelle Seattle  
4000 NE 41st St.  
Seattle, WA 98105

Evaristo J. Bonano, Ph.D.  
President, Beta Corporation International  
6613 Esther NE  
Albuquerque, NM 87109

Dr. William E. Schuler  
Sr. Vice President, Business Development  
BDM Federal, Inc.  
1801 Randolph Road S.E.  
Albuquerque, NM 87106

Bob Bills  
7001 Utica Ave #307  
Lubbock, TX 79424

Benjamin Ross, President  
Disposal Safety Incorporated  
1660 L. Street NW, Suite 510  
Washington, DC 20036

J. Willis  
Duke Engineering Services  
101 Convention Center Drive, Suite P110  
Las Vegas, NV 89109

Patricia J. Robinson, Manager  
Advanced Waste Technology  
Advanced Reactors Development  
Electric Power Research Institute  
3412 Hillview Ave  
Palo Alto, CA 94304-1395

Anthony B. Muller, Ph.D.  
Senior Scientist/Assistant Vice President  
Energy and Technology Management  
Corporation  
20201 Century Boulevard, Third Floor  
Germantown, MD 20874

Vernon Daub  
FERMCO  
P.O. Box 398704  
Cincinnati, OH 45239-8704

John A. Thies, Vice President  
Informatics Corporation  
8418 Zuni Road., #200  
Albuquerque, NM 87108

INTERA, Inc.  
Attn: G. A. Freeze  
1650 University Blvd. NE, Suite 300  
Albuquerque, NM 87102

INTERA, Inc. (2)  
Attn: S. B. Phawa, President  
J. F. Pickens  
6850 Austin Center Blvd., Suite 300  
Austin, TX 78731

INTERA, Inc.  
Attn: W. Stensrud  
P.O. Box 2123  
Carlsbad, NM 88221

Michael De Gruky  
Jet Propulsion Laboratory  
M.S. #525-3670  
4800 Oak Grove Dr.  
Pasadena, CA 91109-8099

Dr. Jeremy M. Boak  
Los Alamos National Laboratory  
P.O. Box 1663, MS J514  
Los Alamos, NM 87545

Julie Canepa  
Los Alamos National Laboratory  
P.O. Box 1663, MS J521  
Los Alamos, NM 87545

Ned Elkins  
Los Alamos National Laboratory  
101 Convention Center Drive, Suite 820  
Las Vegas, NV 89102

Gary Eller  
Los Alamos National Laboratory  
P.O. Box 1663, MS J514  
Los Alamos, NM 87545

Los Alamos National Laboratory  
Attn: B. Erdal, INC-12  
P.O. Box 1663  
Los Alamos, NM 87544

Dennis L. Hjeresen, Ph.D., Programs Manager  
Applied Environmental Technologies  
Mail Stop F641  
Los Alamos National Laboratory  
Los Alamos, NM 87545

David R. Janecky, Staff Geochemist  
Mail Stop J514  
Los Alamos National Laboratory  
Los Alamos, NM, 87545

C. Harris  
LATA, Suite 400  
2400 Louisiana NE  
Albuquerque, NM 87110

Al Schenker  
LATA, Suite 400  
2400 Louisiana NE  
Albuquerque, NM 87110

Dave Rudeen  
NMERI  
2201 Buena Vista Dr. SE  
Albuquerque, NM 87106

Jerry Kuhaida, Ph.D., P.G., Technical  
Coordinator  
Environmental Restoration Program  
Oak Ridge National Laboratory  
Martin Marietta Energy Systems, Inc.  
P.O. Box 2008  
Oak Ridge, TN 37831-6402

RE/SPEC, Inc  
Attn: J. L. Ratigan  
P.O. Box 725  
Rapid City, SD 57709

Walt Beyeler  
SAIC, Suite 400  
2201 Buena Vista Dr. SE  
Albuquerque, NM 87106

Richard M. Wheeler, Jr.  
Member of Technical Staff  
Systems Research Division  
Sandia National Laboratories  
Livermore, CA 94551-0969

M. Brady  
Sandia National Laboratories  
101 Convention Center Drive, Suite P110  
Las Vegas, NV 89109

Jim Cramer  
Science & Engineering Associates, Inc.  
SEA Plaza  
6100 Uptown Blvd  
Albuquerque, NM 87110

Southwest Research Institute (2)  
Center for Nuclear Waste Regulatory Analysis  
Attn: P. K. Nair, B. Sagar  
6220 Culebra Road  
San Antonio, TX 78228-0510

Jack B. Tillman, P.E.  
Southwest Regional Manager  
The S.M. Stoller Corporation  
314 West Mermod Street, Suite 102,  
Carlsbad, NM 88230

B. Brodfield, Vice President  
Stone & Webster Engineering Corporation  
245 Summer Street  
Boston, MA 02210

Alex Bangs  
Strategic Decision Group  
2440 Sand Hill Road  
Menlo Park, CA 94025-6900

Bruce Judd  
Strategic Decision  
2440 Sand Hill Road  
Menlo Park, CA 94025-6900

Tech Reps, Inc. (4)  
Attn: J. Chapman (2)  
T. Peterson (2)  
5000 Marble NE, Suite 222  
Albuquerque, NM 87110

TRW (4)  
Attn: R. Andrews, S. Bodnar  
L.D. Foust, J. Younker  
101 Convention Center Drive, Suite P110  
Las Vegas, NV 89109

Dr. Charles Metzger  
Project Management Organization  
101 Convention Center Drive, Suite P110  
Las Vegas, NV 89109

Westinghouse Electric Corporation (5)  
Attn: Library  
J. Epstein  
J. Lee  
B. A. Howard  
R. Kehrman  
P.O. Box 2078  
Carlsbad, NM 88221

John Steele  
Westinghouse Savannah River  
Savannah River Site  
Aiken, SC 29808

**National Academy of Sciences,  
WIPP Panel**

Howard Adler  
Oxyrase, Incorporated  
7327 Oak Ridge Highway  
Knoxville, TN 37931

Ina Alterman  
Board of Radioactive Waste Management  
GF456  
2101 Constitution Ave.  
Washington, DC 20418

Bob Andrews  
Board of Radioactive Waste Management  
GF456  
2101 Constitution Ave.  
Washington, DC 20418

Charles Fairhurst  
Department of Civil and Mineral Engineering  
University of Minnesota  
500 Pillsbury Dr. SE  
Minneapolis, MN 55455-0220

B. John Garrick  
PLG Incorporated  
4590 MacArthur Blvd., Suite 400  
Newport Beach, CA 92660-2027

Leonard F. Konikow  
US Geological Survey  
431 National Center  
Reston, VA 22092

Carl A. Anderson, Director  
Board of Radioactive Waste Management  
National Research Council  
HA 456  
2101 Constitution Ave. NW  
Washington, DC 20418

Christopher G. Whipple  
ICF Kaiser Engineers  
1800 Harrison St., 7th Floor  
Oakland, CA 94612-3430

John O. Blomeke  
720 Clubhouse Way  
Knoxville, TN 37909

Sue B. Clark  
University of Georgia  
Savannah River Ecology Lab  
P.O. Drawer E  
Aiken, SC 29802

Konrad B. Krauskopf  
Department of Geology  
Stanford University  
Stanford, CA 94305-2115

Della Roy  
Pennsylvania State University  
217 Materials Research Lab  
Hastings Road  
University Park, PA 16802

David A. Waite  
CH<sub>2</sub> M Hill  
P.O. Box 91500  
Bellevue, WA 98009-2050

Thomas A. Zordon  
Zordan Associates, Inc.  
3807 Edinburg Drive  
Murrysville, PA 15668

### Universities

J.C. Helton  
Department of Mathematics  
Arizona State University  
Tempe, AZ 85287

Dr. Ron K. Bhada, Associate Dean  
College of Engineering  
Waste-Mgmt. Educ. & Research Consortium  
Box 30001/Dept. WERC  
Las Cruces, NM 88003-0002

Lynn D. Tyler, P.E., Ph.D.  
Professor of Mechanical Engineering  
Oklahoma Christian University  
of Science and Arts  
Box 11000  
Oklahoma City, OK 73136-1100

Steve Hora  
University of Hawaii at Hilo  
Hilo, HI 96720

Sul Kassicieh  
Anderson School of Management  
1924 Las Lomas NE, Room 2106  
University of New Mexico  
Albuquerque, NM 87131-1221

Department of Geology  
Attn: Library  
141 Northrop Hall  
University of New Mexico  
Albuquerque, NM 87131

Rodney C. Ewing  
Department of Geology  
University of New Mexico  
Albuquerque, NM 87131

Yocov Y. Haimes, Center Director and  
Lawrence R. Quarles Professor of  
Systems Engineering and Civil Engineering  
University of Virginia, 103 Small Building  
Charlottesville, VA 22903

Barry W. Johnson, Professor  
School of Engineering & Applied Science  
Department of Electrical Engineering  
University of Virginia  
Charlottesville, VA 22903-2442

College of Ocean & Fishery Sciences  
Attn: G. R. Heath  
University of Washington  
583 Henderson Hall, HN-15  
Seattle, WA 98195

#### Libraries

Thomas Brannigan Library  
Attn: D. Dresp  
106 W. Hadley St.  
Las Cruces, NM 88001

Government Publications Department  
Zimmerman Library  
University of New Mexico  
Albuquerque, NM 87131

New Mexico Junior College  
Pannell Library  
Attn: R. Hill  
Lovington Highway  
Hobbs, NM 88240

New Mexico State Library  
Attn: N. McCallan  
325 Don Gaspar  
Santa Fe, NM 87503

New Mexico Tech  
Martin Speere Memorial Library  
Campus Street  
Socorro, NM 87810

WIPP Public Reading Room  
Carlsbad Public Library  
101 S. Halagueno St.  
Carlsbad, NM 88220

#### Foreign Addresses

Carlos Torres  
Waste Management Section  
International Atomic Energy Agency  
Wagramer Strasse 5, P.O. Box 100  
A-1400

Henning von Maravic  
Commission of the European Communities  
Directorate General XII/F/5  
T-61, E-S 4  
200, rue de la Loi  
B-1049 Brussels

Studiecentrum Voor Kernenergie (2)  
Attn: A. Bonne  
J. Marivoet  
Centre d'Etudes de l'Energie Nucleaire  
SCK/CEN Boeretang 200  
B-2400 Mol

Atomic Energy of Canada, Ltd. (2)  
Whiteshell Laboratories  
Attn: B. Goodwin  
A. Wikjord  
Pinawa, Manitoba, CANADA R0E 1L0

Doug Metcalfe, Assessment Specialist  
Wastes and Impacts Division  
Atomic Energy Control Board (AECB)  
P. O. Box 1046, Station B  
280 Slater Street  
Ottawa K1P 5S9, CANADA

Toellisuuden Voima Oy (TVO) (2)  
Attn: Timo Aikas  
Jukka-Pekka Salo  
Annankatu 42C  
FIN-00100 Helsinki

Kal Jakobsson, Engineering Geologist  
Nuclear Waste Mgmt., Nuclear Safety Dept.  
Finnish Centre for Radiation and Nuclear Safety  
P.O. Box 14  
FIN-00881 Helsinki

Timo Vieno  
VTT ENERGY  
P.O. Box 1604  
FIN-02044 VTT

Francois Chenevier (2)  
ANDRA  
Route de Panorama Robert Schumann  
B. P. 38  
F-92266 Fontenay-aux-Roses, Cedex

Commissariat a L'Energie Atomique  
Attn: D. Alexandre  
Centre d'Etudes de Cadarache  
F-13108 Saint Paul Lez Durance Cedex

Pierre Escalier des Orres  
Commissariat à l'Energie Atomique  
IPSN/DES/SESID  
BP N° 6  
F-92266 Fontenay-aux-Roses Cedex

Radiation Protection and Waste Mgmt. Div. (6)  
Attn: O. Ilari, P. Lalieux, Claes Nordborg,  
J. Olivier, C. Pescatore, B. Ruegger  
OECD Nuclear Energy Agency  
Le Seine Saint Germain, 12, boulevard des Iles  
F-92130 Issy-les-Moulineaux

Agence Nationale pour la Gestion  
des Déchets Radioactifs (ANDRA) (2)  
Attn: M. Menut, P. Raimbault  
Parc de la Croix Blanche  
1-7, rue Jean Monnet  
F-92298 Chatenay-Malabry Cedex

Claude Sombret  
Centre d'Etudes Nucleaires de la Vallee Rhone  
CEN/VALRHO  
S.D.H.A. B.P. 171  
F-30205 Bagnols-sur-Ceze

Bundesministerium fur Forschung und  
Technologie  
Postfach 200 706  
D-5300 Bonn 2

Bundesanstalt fur Geowissenschaften und  
Rohstoffe  
Attn: M. Langer  
Postfach 510 153  
D-30631 Hannover

Gesellschaft fur Anlagen  
und Reaktorsicherheit (GRS) mbH (2)  
Attn: B. Baltes  
P. Bogorinski  
Schwertnergasse 1  
D-50667 Koln

Institut fur Tief Lagerung  
Attn: K. Kuhn  
Theodor-Heuss-Strasse 4  
D-3300 Braunschweig

Ferruccio Gera  
Environmental & Geo Engineering Department  
ISMES S.P.A.  
Via Pastrengo 9  
24068 Seriate, BG

Richard Storck  
Gesellschaft Für Anlagen- und  
Reaktorsicherheit  
(GRS) mbH  
Theodor-Heuss-Strasse 4  
Postfach 2163  
D-38011 Braunschweig

Japan Atomic Energy Research Institute (2)  
Attn: Hideo Matsuzuri, Principal Scientist  
Shingo Tashiro  
Tokai-Mura, Ibaraki-Ken, 319-11  
JAPAN

Hiroyuki Umeki  
Isolation System Research Program  
Radioactive Waste Management Project  
Power Reactor and Nuclear Fuel  
Development Corporation, PNC  
1-9-13, Akasaka, Minato-ku, Tokyo 107  
JAPAN

Kwan Sik Chun, Director  
Radwaste Disposal Tech. Development  
Nuclear Environment Management Center  
Korea Atomic Energy Research Institute  
P.O. Box 105, Yusong, Taejon, 305-600  
KOREA

Netherlands Energy Research (ECN) (2)  
Attn: J. Pruk  
L. H. Vons  
P.O. Box 1  
NL-1755 ZG Petten

Pedro Carboneras  
ENRESA  
Emilio Vargas 7  
E-28043 Madrid

Johan Andersson  
Intera Information Technologies  
Vallvägen 22  
S-125 33 ÄLVSJÖ

Swedish Nuclear Fuel  
and Waste Management Co. (SKB) (2)  
Attn: T. Eng  
T. Papp  
Box 5864  
S-102 40 Stockholm

Svensk Karnbransleforsorjning AB  
Attn: F. Karlsson  
Project KBS (Karnbranslesakerhet)  
Box 5864  
S-102 48 Stockholm

Swedish Nuclear Power Inspectorate (SKI)  
Attn: Stig Wingefors  
Klarabergsviadukten 90  
S-106 58 Stockholm  
Jörg Hadermann  
Paul Scherrer Institute  
Waste Management Laboratory  
CH-5232 Villigen PSI

Nationale Genossenschaft fur die Lagerung  
Radioaktiver Abfalle (3)  
Attn: S. Vomvoris  
F. Von Dorp  
P. Zuidema (Chairman)  
Hardstrasse 73  
CH-5430 Wettingen

Johannes O. Vigfusson  
HSK - Swiss Nuclear Safety Inspectorate  
Federal Office of Energy  
CH-5232 Villigen HSK

AEA Technology  
Attn: J. H. Rees  
D5W/29 Culham Laboratory  
Abington, Oxfordshire OX14 3DB  
UNITED KINGDOM

AEA Technology  
Attn: W. R. Rodwell  
044/A31 Winfrith Technical Centre  
Dorchester, Dorset DT2 8DH  
UNITED KINGDOM

AEA Technology  
Attn: J. E. Tinson  
B4244 Harwell Laboratory  
Didcot, Oxfordshire OX11 0RA  
UNITED KINGDOM

Daniel A. Galson, Galson Sciences Ltd.  
5 Grosvenor House  
Melton Road, Oakham  
Rutland LE15 6AX  
UNITED KINGDOM

Z A Gralewski, RM Consultants Ltd.  
Suite 7, Hitching Court  
Abingdon Business Park  
Abingdon Oxon. OX11 1RA  
UNITED KINGDOM

P. Grindrod  
Intera Information Technologies  
Chiltern House, 45 Station Road  
Henley-on-Thames, Oxon. RG9 1AT  
UNITED KINGDOM

D. R. Knowles  
British Nuclear Fuels, plc  
Risley, Warrington, Cheshire WA3 6AS  
1002607 UNITED KINGDOM

Trevor Sumerling  
Safety Assessment Management  
Beech Tree House, Hardwick Road  
Whitchurch-on-Thames  
Reading RG8 7HW  
UNITED KINGDOM

B G J Thompson  
Her Majesty's Inspectorate of Pollution  
Romney House  
43 Marsham Street  
London SW1P 3PY  
UNITED KINGDOM

<b>Internal</b>					
<u>MS</u>	<u>Org.</u>				
0415	5411	G. Brown	1335	6801	N. H. Prindle (4)
0425	5415	R. Lincoln	1337	6000	W. Weart
0467	5337	C. Lazne	1341	6747	K. Trauth
0715	6652	R. E. Luna	1341	6747	R. Weiner
0727	6406	T. Sanders	1341	6748	J. T. Holmes
0728		D. Benz	1345	6331	D. Gallegos
0740	6200	W. Gauster	1345	6347	L. Hill
0746	6613	L. Painton	1345	6631	E. K. Webb
0746	6613	B. Cranwell	1345	6416	P. Kaplan
0755	6612	A. Verardo	1395	6700	P. Brewer
0815	6932	F. Mendenhall	1395	6707	M. Marietta
1320	6719	E. J. Nowak	1395	6800	L. Shephard
1320	6748	G. Perkins	1395	6841	V. H. Slaboszewicz
1322	6121	J. R. Tillerson	1395	6742	A. Orrell
1324	6115	P. B. Davies	0100	7613-2	Document Processing (2) for DOE/OSTI
1328	6741	H. N. Jow	0619	12615	Print Media
1328	6741	M. Tierney	0899	4414	Technical Library (5)
1328	6749	D. R. Anderson	1330	6752	NWM Library (20)
1328	6749	D. Boak (60)	9018	8523-2	Central Technical Files
1330	6752	C. B. Michaels (2)	9201	8112	W. L. Hsu
1335	6705	M. Chu	9201	8112	L. Brandt